UCLA
UCLA Electronic Theses and Dissertations

Title
Novel Repression Mechanisms for Metal Transport Genes in Saccharomyces cerevisiae

Permalink
https://escholarship.org/uc/item/34r7x122

Author
Nery, Camille Reyes

Publication Date
2013

Peer reviewed|Thesis/dissertation

eScholarship.org Powered by the California Digital Library
University of California

UNIVERISTY OF CALIFORNIA

Los Angeles

Novel Repression Mechanisms for Metal Transport Genes in *Saccharomyces cerevisiae*

A dissertation submitted in partial satisfaction of the

requirements for the Doctor of Philosophy

in Biochemistry and Molecular Biology

by

Camille Reyes Nery

2013

ABSTRACT OF THE DISSERTATION

Novel Repression Mechanisms for Metal Transport Genes

in *Saccharomyces cerevisiae*

by

Camille Reyes Nery

Doctor of Philosophy in Biochemistry and Molecular Biology

University of California, Los Angeles, 2013

Professor Guillaume F. Chanfreau, Chair

The transition metals iron and zinc are essential requirements for all living organisms. They participate in a variety of critical metabolic pathways, enzymatic activity, and provide structural support for countless proteins. Metal ion imbalance can be detrimental to organisms, as metal deficiency can alter many biological processes while metal excess can lead to toxicity. To alleviate these detrimental situations, the yeast *Saccharomyces cerevisiae* has developed tightly controlled regulatory mechanisms for the proper expression of proteins that control import, export, and storage of these essential metals. This regulation is required to ensure the efficient

uptake, transport, and storage of specific metal ions during periods of metal concentration fluctuations.

The work presented in the first chapter of this dissertation identifies the use of cryptic transcription as a means for regulatory control of the subtelomeric metal genes *ZRT1* and *FIT3.* These transcripts arise from promoter units upstream of the *ZRT1*/*FIT3* transcription unit and extend into the open reading frame (ORF). We show that these transcripts are degraded by the cytoplasmic Non-Sense Mediated Decay (NMD) Pathway and are only stabilized in the absence of the NMD Pathway; hence termed Cytoplasmically Degraded Cryptic Unstable Transcripts (CD-CUTs). We further show that these CD-CUTs act to prevent expression of *ZRT1* by interfering with RNA polymerase II binding and activator binding (Zap1p) to the *ZRT1* promoter unit.

As we identified the use of CD-CUTs to mediate the repression of *ZRT1*/*FIT3* during normal zinc/iron conditions, the mechanistic mode of action of these transcripts remained elusive. In an attempt to identify how a cytoplasmically degraded transcript can mediate transcription in the nucleus, we chose to study the cytoplasmic trafficking of these species. In chapter two, we show that the export of the *ZRT1*/*FIT3* CD-CUTs is likely mediated by the SR-type mRNA export factor Hrb1p and dependent on the essential mRNA export factor Mex67p.

Lastly, we identify an additional mode of regulation for the iron transport gene *FIT3* by the glucose repressor Mig1p. Mig1p has been extensively characterized as a repressor of glucose responsive genes and in chapter three, we show that this regulation can be applied to iron regulation. We believe that Mig1p regulates the repression of *FIT3* during conditions of normal iron and/or after switch back to normal iron conditions following iron starvation to prevent the deleterious expression of *FIT3*, thereby preventing the potentially harmful effects of iron toxicity.

The dissertation of Camille Reyes Nery is approved.

David A. Campbell

Catherine F. Clarke

Albert J. Courey

Steven E. Jacobsen

Guillaume F. Chanfreau, Committee Chair

University of California, Los Angeles

2013

TABLE OF CONTENTS

Section	Pages
List of Tables and Figures	vi
Acknowledgements	viii
Vita	ix
Chapter 1: *Cryptic Transcription Mediates Repression of Subtelomeric Metal Homeostasis Genes*	
Introduction	1
Article Reprint, *Cryptic Transcription Mediates Repression of Subtelomeric Metal Homeostasis Genes*	14
Supplementary Figures	28
References	34
Chapter 2: *Possible Mechanisms for the Cytoplasmic Trafficking of Cytoplasmically Degraded Cryptic Unstable Transcripts (CD-CUTS)*	
Introduction	40
Results	44
Discussion	51
Figures	55
References	66
Chapter 3: *A Novel Role for the Glucose Repressor Mig1p in the Repression of FIT3*	
Introduction	70
Results	73
Discussion	79
Figures	82
References	94

List of Tables and Figures

Figures (Chapter, Figure, Title)	Page
1A. Overview of Iron Regulon in *Saccharomyces cerevisiae*	12
1B. Overview of Zinc Regulon in *Saccharomyces cerevisiae*	13
1.1 Tiling arrays profiles of the *upf1Δ* mutant relative to the wild-type strain	16
1.2 Characterization of CD-CUT of zinc and iron responsive genes	17
1.3 The main ZRT1 CD-CUT is controlled by the histone deacetylase Rpd3p	19
1.4 Mutations of the upstream regions and insertion of transcription terminators result in a derepression of *ZRT1* and *FIT3*	20
1.5 Effects of transcription terminators upstream *ZRT1* on *ZRT1* induction and analysis of RNA Polymerase II and Zap1p occupancies by ChIP	21
1.6 CD-CUT mediated transcriptional repression can be rescued by over-expression or constitutive activation of transcriptional activators	23
1.7 Model of biogenesis, action, and degradation of CD-CUTs	25
S1 Tiling array profiles of *ZPS1* and *FLO11*	28
S2 Mapping of the CD-CUTs of *ZRT1* and *ADH4* genes by Northern blot analysis	29
S3 Analysis of zinc regulon genes induction in NMD mutants	30
S4 Kinetics of *FIT3* induction in strains lacking Xrn1p, Upf1p, or in the double mutant *xrn1Δrat1-1*	31
S5 Insertion of GFP cassettes upstream from *ZRT1* and *ADH4*	32
S6 Kinetics of *ZRT1* induction in wild-type, *hda2Δ*, *hda3Δ*, *upf1Δ*, *hda2Δupf1Δ*, and *hda3Δupf1Δ* strains	33
2.1 Decreased levels of *ZRT1* mRNA upon loss of Npl3p	55
2.2 Loss of Gbp2p does not affect stabilization of *ZRT1* CD-CUT	56
2.3 *ZRT1* CD-CUTs are stabilized by loss of Hrb1p	57
2.4 *FIT3* CD-CUTs are stabilized upon loss of Hrb1p	58
2.5 RNA pol II occupancy is decreased in NMD and SR-type mRNA export factor mutants	59

2.6 Non-Sense Mediated Decay Pathway targets are also substrates for Hrb1p mediated export 60

2.7A Inhibition of mRNA export results in higher fraction of *ZRT1* CD-CUTs degraded by the nuclear exosome 61

2.7B Inhibition of mRNA export results in higher fraction of *FIT3* CD-CUTs degraded by the nuclear exosome 62

2.8A Nup100p does not mediate export of *ZRT1* CD-CUT 63

2.8B Nup116p does not mediate export of *ZRT1* CD-CUT 64

2.9. ZRT1 and FIT3 CD-CUTs are likely exported by the SR-like protein Hrb1p and dependent on the essential export factor Mex67p. 65

3.1 *FIT3* derepression in wild-type strain grown in galactose 82

3.2 Migp mutants exhibit differential *FIT3* mRNA expression profiles 82

3.3 Migp mutants display differential *FIT*-family expression profiles 83

3.4 Mig1p mediated repression is not observed for other genes (ARN, *FRE)* in the Aft1p iron regulon 84

3.5 Mig1p mediates *FIT3* mRNA repression in normal iron conditions 85

3.6 Mig1p mediated repression is specific to *FIT3* 86

3.7 Mig1p mediated repression is specific to *FIT3* 87

3.8 Mig1p mediated repression is specific to *FIT3* 88

3.9A Mig1p mediates repression of *FIT3* after switch to normal iron conditions following iron starvation 89

3.9B Mig1p mediates repression of *FIT3* after switch to normal iron conditions following iron starvation 90

3.10A Deletion of upstream Mig1p-like binding site confers partial derepression of *FIT3* 91

3.10B Deletion of upstream Mig1p-like binding site increases *FIT3* mRNA expression after shift to normal iron conditions following iron starvation 92

3.11 Model for Mig1p mediated repression for FIT3 in normal iron conditions. 93

Acknowledgements

This work would not have been possible without the guidance and support of my advisor Dr. Guillaume F. Chanfreau. I would like to thank Guillaume for allowing me to be a part of his laboratory and fostering my scientific and analytical skills for all these years at UCLA. I am deeply indebted to his many ideas that have progressed the work presented in this dissertation. In addition, I would like to thank my committee members for their support and advice on the work presented in this dissertation. I would also like to thank Isabelle Toesca, Shakir Sayani, and Cesar Fernandez for their contributions to our publication *Cryptic Transcription Mediates Transcription of Metal Homeostasis Genes* (PloS Genetics, 2011). Many thanks to PloS Genetics for allowing reprint and public use of this article.

I also would like to thank a few of Guillaume's former graduate students: Chrissie Lee and Defne Egecioglu who first helped mentored me upon joining Guillaume's laboratory, I owe all my RNA/DNA methods to them; Cynthia Lee for all her advice and help with metal metabolism; and Tadashi Kawashima for all his technical assistance throughout the years. Our laboratory would not be functional without the gracious assistance of Ana Mariscal who catered to all our needs with media, dishware, and support.

Lastly I'd like to thank my amazing family and friends who have been nothing but supportive and patient throughout my graduate school career. Without their support, I would not have had the courage to pursue my interest in science.

VITA

Education
B.S. Biology, Loyola Marymount University, Los Angeles CA 2003.
Department of Biology

Educational Research Experience

- Graduate Student Researcher**:** Dr. Guillaume F. Chanfreau Laboratory, University of California Los Angeles Department of Chemistry and Biochemistry. Los Angeles, CA. March 2006 to Present.

- Undergraduate Student Researcher**:** Dr. Pippa Drennan Laboratory, Loyola Marymount University Department of Biology. Los Angeles, CA
  January 2001 to May 2003

Publications and Presentations

- Toesca, I., Nery CR., Fernandez, CF., Sayani, S., and Chanfreau, GF. Cryptic Transcription Mediates Repression of Subtelomeric Metal Homeostasis Genes, *PLoS Genetics* 7(6): e1002163. June 2011

- Regulation of Iron Import Facilitators in *Saccharomyces cerevisiae.* FASEB Summer Research Conferences: Trace Elements in Biology and Medicine. Snowmass Village, CO. June 2010. Poster Presentation.

- Regulation of an Iron Import Facilitator by Transcriptional Interference in *Saccharomyces cerevisiae.* Gordon Research Conference: Cell Biology of Metals. Newport, RI. August 2009. Poster Presentation.

Fellowships
Ruth L. Kirschstein National Research Service Award for Individual Predoctoral Fellowships to Promote Diversity in Health-Related Research, September 2008 to September 2012.

Research Supplement for Underrepresented Minorities to Guillaume F. Chanfreau, University of California Los Angeles. September 2006 to September 2008.

Graduate Teaching Experience
Teaching Assistant, University of Los Angeles, California
Department of Chemistry and Biochemistry

- CHEM 153L Biochemical Methods I: Winter 2006, Spring 2006.
- CHEM 153B: DNA, RNA, and Protein Synthesis.

Professional Experience and Skills

Gen-Probe Inc. March 2005 to September 2005
San Diego, CA
Research Associate II
Product Development, PROGENSA PCA3

GeneOhm Sciences Inc. September 2003 to March 2005
San Diego, CA
Research Associate I and II
Product Development

Chapter 1: Cryptic Transcription Mediates Transcription of Metal Homeostasis Genes

Transition metal ions are essential requirements for all living organisms. They participate in a variety of critical metabolic pathways, enzymatic activity, and structural support for countless proteins. Metal ion imbalance can be detrimental to organisms, as metal deficiency can alter many biological processes while metal excess can lead to toxicity. To alleviate these detrimental situations, organisms have developed tightly controlled regulatory mechanisms to maintain metal homeostasis. This regulation is required to ensure the efficient uptake, transport, and storage of specific metal ions during periods of metal concentration fluctuations.

Iron utilization in Saccharomyces cerevisiae

Iron is an element required by all organisms as it participates as a cofactor in many redox reactions. While it is the most abundant element in the earth's crust, it remains largely bio-unavailable to many organisms. Iron is primarily available in the insoluble ferric (Fe^{3+}) form (Van Ho et al., 2002) and organisms must employ ways to solubilize and internalize ferric iron. Organisms have developed tightly regulated mechanisms in order to control the expression of proteins that facilitate the import, export, and storage of iron. Without these proper regulatory mechanisms, the misregulation of iron homeostasis results in severe cellular consequences. Too little iron imported into the cell can lead to severe iron deficiency and alteration of metabolic pathways (Balci et al., 2007). On the other hand, high levels of iron can be toxic to the cell due to the generation of reactive oxygen species (ROS) by Fenton Chemistry. These ROS can then cause serious damage to nucleic acids, proteins, and lipids (Rouault and Klausner, 1997; Rouault and Klausner, 1996). Clearly, the regulation of intracellular iron is important for the healthy maintenance and survival of all organisms.

The budding yeast *Saccharomyces cerevisiae* has been utilized to extensively study the import and mobilization of iron (Philpott et al., 2002) due to the conservation of

some proteins involved in iron metabolism between yeast and mammalian cells (Van Ho et al., 2002). During iron deprivation, yeast respond by transcriptional activation of genes that express proteins involved in the acquisition of iron (Philpott et al., 2002). Iron import into *S. cerevisiae* is mediated by a multitude of proteins whose transcriptional activation in iron depletion is dependent on the activators Aft1p/Aft2p (Yamaguchi-Iwai et al., 1996). Aft1p/Aft2p stimulates transcription of genes encoding components of the iron regulon, comprising both the reductive and non-reductive system of iron uptake (Yamaguchi-Iwai et al., 1996).

In the reductive system of iron uptake, ferric iron is first reduced to ferrous iron by metalloreductases encoded by *FRE1* and *FRE2* (Georgatsou and Alexandraki, 1994). This ferrous iron is then available for transport by the high affinity transport system comprised of proteins encoded by *FET3* and *FTR1* (Askwith et al., 1994; Stearman et al., 1996). The high affinity transport system is activated during limiting iron conditions and has a Km of 0.15 uM (Eide et al., 1992). Fet3p is a multi-copper ferroxidase that oxidizes the Fe^{2+} substrate to Fe^{3+}. This Fe^{3+} is then transported into the cell by the Ftr1p permease. The high affinity Fet3p/Ftr1p transport system is responsible for the majority of iron uptake in cells during conditions of iron starvation (Eide et al., 1992).

The reduction and uptake of ferric iron is not the only method employed by yeast to internalize iron. Yeast can also employ strategies to import and extract iron bound to siderophores. Siderophores are low molecular mass organic compounds secreted by other mirco-organisms. Siderophores can then bind ferric iron with high affinity and solubilize this iron (Philpott et al., 2002). While *S. cerevisiae* do not secrete siderophores, they have developed systems to utilize siderophore bound iron. One such system is the *FIT* family of proteins. Fit1p, Fit2p, and Fit3p are cell wall mannoproteins that facilitate the uptake of siderophore-bound iron (Philpott et al., 2002; Protchenko et al., 2001). They trap siderophore-bound iron in the cell wall and facilitate the uptake

through the cell wall. In addition, siderophore-bound iron can be transported across the plasma membrane by the *ARN* (Arn1p-Arn4p) family of transporters (Heymann et al., 2000; Yun et al., 2000a; Yun et al., 2000b). Lastly, siderophore-bound iron that reaches the plasma membrane can be reduced from the ferric bound form to the ferrous free form by the *FRE* (Fre1p-Fre6p) family of metalloreductases (Yun et al., 2001).

In conditions of excess iron, yeast utilize the low affinity transporter Fet4p for bulk uptake of iron. While ferrous iron is a substrate for Fet4p, this transport system is not specific to iron and can transport other transition metals such as zinc and copper (Dix et al., 1997; Dix et al., 1994). Fet4p is responsible for iron uptake under anaerobic conditions when the high affinity transport system of Fet3p/Ftr1p is not functional (Hassett et al., 2000).

As mentioned above, the genes encoding the protein members of the iron regulon are controlled by the iron transcription factor Aft1p (Yamaguchi-Iwai et al., 1996). Aft1p is constitutively expressed as a cytosolic protein. Under conditions of iron starvation, Aft1p undergoes a nuclear translocation where it binds to specific iron responsive elements (FeREs) upstream of the target genes (Yamaguchi-Iwai et al., 1996; Yamaguchi-Iwai et al., 2002) to activate transcription. Aft2p, a paralog of Aft1p, has been shown to have overlapping functions and targets of Aft1p. It has been shown to also bind to iron responsive elements (FeREs) in conditions of iron limitation and can activate the entire iron regulon in the absence of Aft1p (Rutherford and Bird, 2004; Rutherford et al., 2001). While Aft2p has overlapping functions as Aft1p, it is believed that Aft2p plays a role in mobilizing internal iron stores and resistance to oxidative stress (Blaiseau et al., 2001; Rutherford et al., 2001)

Zinc utilization in Saccharomyces cerevisiae

Similar to iron, zinc is another essential metal important for the enzymatic and structural activity of many proteins. Zinc is a key component to many transcription factors that regulate transcription. It is not a redox reactive metal, however misregulation of zinc can also be deleterious to the cell. Zinc uptake in *Saccharomyces cerevisiae* is transporter mediated and is time, temperature, and concentration dependent (Zhao and Eide, 1996a). Similar to iron uptake in yeast, zinc uptake is mediated by two separate uptake systems: the high affinity and low affinity transport systems (Zhao and Eide, 1996a, b). The zinc regulated transporter Zrt1p, is the main component of the high affinity transport system and is induced during periods of zinc limitation. It is responsible for the majority of zinc uptake during zinc starvation. Conversely, the low affinity system comprised of Zrt2p is induced during zinc replete conditions (Zhao and Eide, 1996b; Zhao and Eide, 1997) and is the major pathway for uptake in zinc replete conditions. Both uptake systems are specific to the transport of zinc and are regulated by the transcription factor Zap1p (Frey et al., 2011; Zhao et al., 1998; Zhao and Eide, 1996a).

The metalloprotein Zap1p regulates transcription of zinc uptake genes (*ZRT1*, *ZRT2*, *ZRT3*) by binding to zinc responsive elements (ZREs) in the promoter regions of its target genes (Zhao et al., 1998). Within Zap1p are two activation domains, AD1 and AD2, which are required for the proper activation of the target genes (Bird et al., 2000a; Bird et al., 2000b). Zap1p can also regulate its own transcription through a positive autoregulatory mechanism, increasing synthesis during limited zinc and therefore increasing transcription of its target genes. During zinc repletion, the formation of low affinity zinc finger domains within Zap1p results in Zap1p binding to other sites in the genome and away from its target genes (Zhao and Eide, 1997). Zap1p plays a dual role in zinc regulation, acting as a zinc sensor and as a transcriptional activator. As a zinc

sensor, the zinc ion binds directly to Zap1p, resulting in the inhibition of transcriptional activation of Zap1p target genes (Zhao and Eide, 1997).

Excess zinc can be stored in the vacuole, which is a major storage site for zinc. Stored zinc in the vacuole can also be utilized by cells through the action of Zrt3p. This vacuolar zinc transporter is also activated by Zap1p and increases zinc export from the vacuole to the cytosol during zinc limitation (MacDiarmid et al., 2000). The vacuolar zinc importers Zrc1p and Cot1p transport zinc from the cytosol to the vacuole for storage when cytosolic zinc levels are high (Kamizono et al., 1989; MacDiarmid et al., 2000).

While the mechanism of induction and transcriptional targets of both the iron and zinc regulon are well characterized, the mechanisms that repress the expression of these targets in normal metal conditions remains poorly understood. Elucidating these mechanisms of transcriptional control is important because the abnormal expression of these genes may result in metal deficiency or toxicity in metal deplete and replete conditions respectively. It has been shown that non-coding RNAs (ncRNAs) transcribed near protein coding genes can be used as a means of transcriptional control (Jacquier, 2009). A large portion of the eukaryotic genome is transcribed, the majority of which is non-coding (Marquardt et al., 2011). The purpose of these non-coding RNAs has long been debated, whether side effects of transcription known as “transcriptional noise” or having distinct regulatory roles for transcriptional control of neighboring genes.

Non-coding RNAs (ncRNAs) and their degradation pathways in Saccharomyces cerevisiae

Non-coding transcripts are not restricted to defined annotated features in the genome and can vary in length from 20 nucleotides (small ncRNAs) to as long as several kbs (long ncRNAs) (Jacquier, 2009; Neil et al., 2009). They have been shown to regulate protein-coding genes at both the transcriptional and post transcriptional level.

Transcriptional control can occur by directly affecting RNA polymerase II activity through transcriptional interference of RNA pol II and chromatin modifier proteins, or enhancing promoter activity (Kornienko et al., 2013), (Martens et al., 2004). Post-transcriptional regulation by ncRNAs could occur by acting as competing RNAs to regulate RNA levels and by modulating mRNA stability (Kornienko et al., 2013).

In *S. cerevisiae*, transcriptional regulation by non-coding RNAs has been demonstrated through a number of hallmark examples. The *SRG1* sense ncRNA was shown to regulate the transcription of *SER3* (Martens et al., 2004) through a transcriptional interference mechanism, where transcription of *SRG1* inhibits activator binding necessary for the activation of *SER3*. *PHO84* antisense RNA stabilization is accompanied by the recruitment of histone deacetylases, which in turn results in downstream *PHO84* transcriptional repression (Camblong et al., 2007). Finally, antisense transcription at the *IME4* locus determines cell fate according to cell type (Hongay et al., 2006). By all means, the listed examples are not the only cases of ncRNA regulation in *S. cerevisiae*, but clearly show that ncRNA regulation is a widespread mechanism of transcriptional control applicable to different biosynthetic pathways.

As mentioned above, these ncRNAs arise from areas of un-annotated regions of the genome (Jacquier, 2009; Neil et al., 2009). These transcripts are transcribed by RNA polymerase II (Houseley and Tollervey, 2009) and are only stable in the absence of nuclear and cytoplasmic RNA degradation systems (Carneiro et al., 2007; Davis and Ares, 2006; Thompson and Parker, 2007; van Dijk et al., 2011; van Hoof et al., 2000; Wyers et al., 2005). In the presence of a functional nuclear RNA degradation pathway, these transcripts are rapidly degraded. Because of this rapid turnover, these transcripts have been termed as CUTs, Cryptic Unstable Transcripts (Neil et al., 2009). CUTs range

in size from 200 to 600 nucleotides in length, contain a 5' cap, and are promoter associated RNAs (Davis and Ares, 2006; Jacquier, 2009). Conversely, another class of non-coding transcripts have been identified and are known as SUTs Stable Unannotated Transcripts. SUTs are generally more stable than CUTs and average in length of ~700 nucleotides (Xu et al., 2009). Like CUTs, SUTs are also promoter-associated transcripts. Both CUTs and SUTs have been shown to arise from nucleosome free regions (NFRs); intergenic regions close to the 5' end of genes (Lee et al., 2007). A third class of ncRNAs termed as XUTs, Xrn1-sensitive Unstable Transcripts, have been shown to be bona fide regulatory ncRNAs destabilized by Xrn1p, the 5' to 3' RNA exonuclease (van Dijk et al., 2011).

In *S. cerevisiae*, CUTs can be subjected to degradation through the nuclear or cytoplasmic degradation system. In the nuclear RNA degradation system, these transcripts are polyadenylated by the TRAMP complex, which targets these transcripts for degradation by the nuclear exosome (Wyers et al., 2005). The TRAMP complex is composed of the poly(A) polymerase Trf4p/Trf5p, the nucleocytoplasmic mRNA transport proteins Air1p/Air2p, and the RNA helicase Mtr4p. Together this complex polyadenylates cryptic transcripts marking them for degradation by the nuclear exosome (Wyers et al., 2005). The exosome is a large complex of 3' to 5' nucleases implicated in nuclear RNA processing and degradation events of pre-mRNAs (Houseley and Tollervey, 2009; van Hoof et al., 2000). In addition, aberrant and cryptic transcripts may also be degraded through the activity of Rat1p, the nuclear 5' to 3' exonuclease (Johnson, 1997).

RNAs that escape degradation by the nuclear degradation system can be degraded by the cytoplasmic degradation system. Cytoplasmic turnover of mRNAs can occur in two ways; first by deadenylation followed by 3' to 5' degradation by the

cytoplasmic exosome, and second through decapping followed by 5' to 3' degradation by Xrn1p (Parker, 2012). Deadenylation is predominately catalyzed by the Ccr4p/Pop2/NOTp Complex which shortens the poly(A) tail from ~90 residues to ~65 residues (Daugeron et al., 2001; Tucker et al., 2001). Deadenylated mRNAs can then undergo 3' to 5' exonucleolytic decay by the exosome (Anderson and Parker, 1998). mRNA decapping is carried out by the Dcp1p/Dcp2p protein complex which cleaves the 5' cap structure from the mRNA (Steiger et al., 2003). Following decapping, mRNAs are degraded by Xrn1p, the major 5' to 3' cytoplasmic exonuclease (Hsu and Stevens, 1993).

Additionally, mRNAs can undergo cytoplasmic degradation through specialized decay pathways. These specialized pathways are responsible for the turnover of mRNAs containing premature translation termination codons, truncated mRNAs, and mRNAs that contain sequence features which render a stalled ribosome (Parker, 2012; Shoemaker and Green, 2012). These mRNAs must be eliminated as aberrant translation can result in deleterious consequences for the cell including truncated proteins, which may have dominant and toxic effects. Transcripts that lack stop codons are degraded by the Non Stop Decay (NSD) pathway. (Frischmeyer et al., 2002) These transcripts include truncated mRNAs and mRNAs that do not contain a stop codon but contain a poly(A) tail. The No Go Decay (NGD) is responsible for eliminating transcripts that contain a sequence feature that stall a translating ribosome. These sequence features include stable stem loops, pseudoknots, and damaged RNA bases (Doma and Parker, 2006; Passos et al., 2009).

Transcripts containing premature translation termination codons (PTCs) are eliminated through the Non-sense Mediated Decay (NMD) (Chang et al., 2007; Shoemaker and Green, 2012). The NMD system requires three key factors Upf1p,

Upf2p, and Upf3p (Upframe Shift Factors). Upf1p contains ATPase and helicase activities and interacts with both Upf2p and Upf3p (Leeds et al., 1991; Leeds et al., 1992; Peltz et al., 1993; Peltz et al., 1994). It is thought that Upf1p is recruited to the mRNA after recognition of the PTC. Upon interaction of Upf1p with both Upf2p and Upf3p as well as components of the Exon Junction Complex (EJC), rapid decay of this PTC containing mRNA occurs (Chang et al., 2007).

Cryptic Transcription and Metal Homeostasis Gene Regulation in Saccharomyces cerevisiae

Previous work from our laboratory has shown that yeast deficient in the exoribonucleases Xrn1p and Rat1p, as well as cells deficient in the double stranded RNA endonuclease Rnt1p exhibit the presence of 5' extended species of *FIT3* mRNA in normal iron conditions. The 5' start site of these extended species found in these ribonuclease mutants was found to originate ~3.3kb upstream of the *FIT3* translation initiation codon (Lee et al., 2005). While *FIT3* is a known target for the iron transcription factor Aft1p, the repression of *FIT3* in normal iron conditions must be mediated by a separate regulatory mechanism. In this regulatory mechanism, upstream cryptic transcription results in transcriptional read through of the *FIT3* transcription unit, therefore repressing transcription of the normal *FIT3* mRNA through promoter occlusion. Using tiling microarrays generated for a previous study (Sayani et al., 2008), careful analysis of intergenic regions of the yeast genome revealed many subtelomeric gene regions accumulated RNAs upstream and outside of annotated gene regions in NMD and exonuclease mutants. Interestingly, these intergenic regions lie upstream of many subtelomeric genes involved in metal homeostasis; namely *FIT3*, *ZRT1*, and *ADH4*.

This observation lead us to believe that cryptic transcription could be used as a mechanism for regulatory control of genes involved in metal homeostasis and not just as

“transcriptional noise” that intergenic transcription has been perceived to be. Characterization of this novel regulatory mechanism in metal metabolism of *S. cerevisiae* would allow us to better understand the complex mechanisms of regulation that are important in the essential homeostatic balance of essential metals.

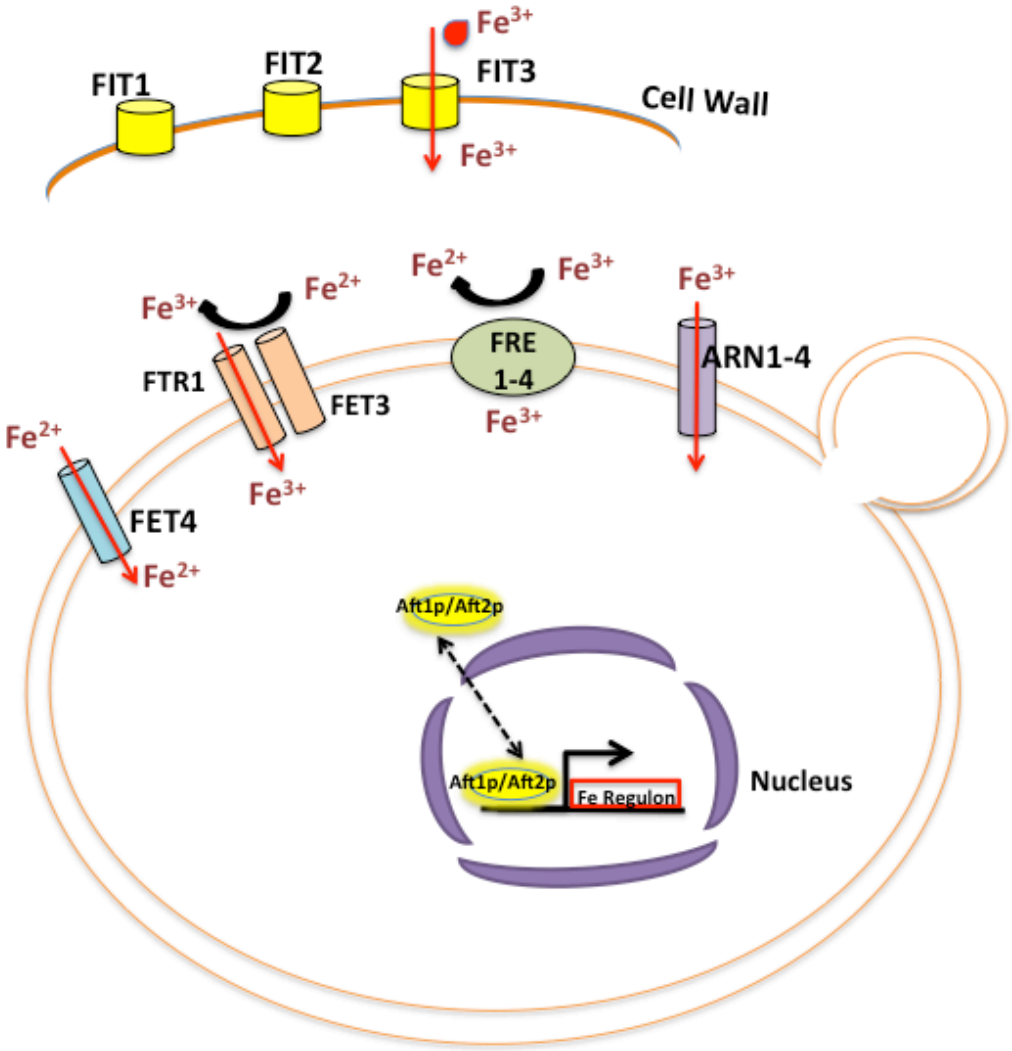


Figure 1A. Overview of Iron Regulon in *Saccharomyces cerevisiae.*

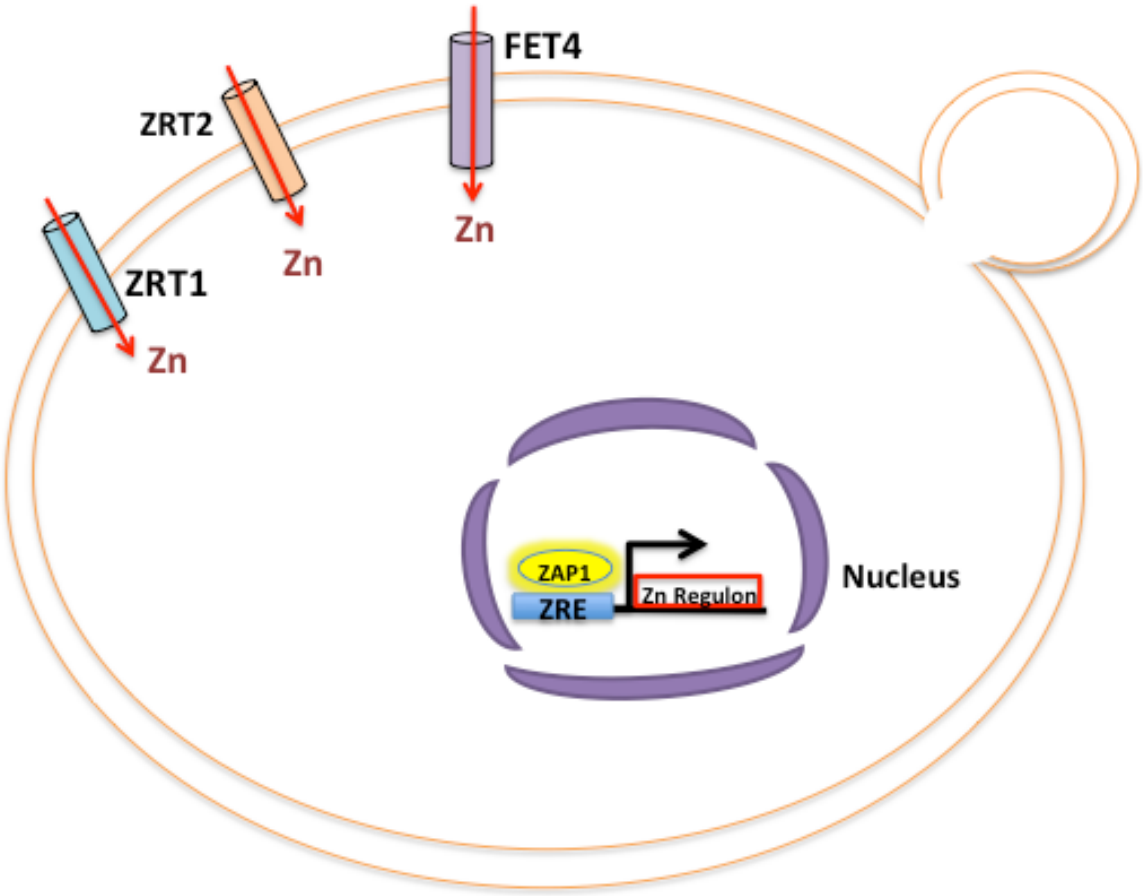


Figure 1B. Overview of Zinc Regulon in *Saccharomyces cerevisiae.*

My contributions to this publication are illustrated in Figures 1E, 1G, 4B, 4C, 5A, 5B, 6B, 6C, 6D, and supplementary figure S4.

OPEN ACCESS Freely available online PLoS GENETICS

Cryptic Transcription Mediates Repression of Subtelomeric Metal Homeostasis Genes

Isabelle Toesca[¤], **Camille R. Nery**[◔], **Cesar F. Fernandez, Shakir Sayani, Guillaume F. Chanfreau***

Department of Chemistry and Biochemistry and the Molecular Biology Institute, University of California Los Angeles, Los Angeles, California, United States of America

Abstract

Nonsense-mediated mRNA decay (NMD) prevents the accumulation of transcripts bearing premature termination codons. Here we show that *Saccharomyces cerevisiae* NMD mutants accumulate 5′–extended RNAs (CD-CUTs) of many subtelomeric genes. Using the subtelomeric *ZRT1* and *FIT3* genes activated in response to zinc and iron deficiency, respectively, we show that transcription of these CD-CUTs mediates repression at the *bona fide* promoters, by preventing premature binding of RNA polymerase II in conditions of metal repletion. Expression of the main *ZRT1* CD-CUT is controlled by the histone deacetylase Rpd3p, showing that histone deacetylases can regulate expression of genes through modulation of the level of CD-CUTs. Analysis of binding of the transcriptional activator Zap1p and insertion of transcriptional terminators upstream from the Zap1p binding sites show that CD-CUT transcription or accumulation also interferes with binding of the transcriptional activator Zap1p. Consistent with this model, overexpressing Zap1p or using a constitutively active version of the Aft1p transcriptional activator rescues the induction defect of *ZRT1* and *FIT3* in NMD mutants. These results show that cryptic upstream sense transcription resulting in unstable transcripts degraded by NMD controls repression of a large number of genes located in subtelomeric regions, and in particular of many metal homeostasis genes.

Citation: Toesca I, Nery CR, Fernandez CF, Sayani S, Chanfreau GF (2011) Cryptic Transcription Mediates Repression of Subtelomeric Metal Homeostasis Genes. PLoS Genet 7(6): e1002163. doi:10.1371/journal.pgen.1002163

Editor: Hiten D. Madhani, University of California San Francisco, United States of America

Received April 12, 2011; **Accepted** May 14, 2011; **Published** June 30, 2011

Copyright: © 2011 Toesca et al. This is an open-access article distributed under the terms of the Creative Commons Attribution License, which permits unrestricted use, distribution, and reproduction in any medium, provided the original author and source are credited.

Funding: This work is supported by grants GM61518 from NIH and RSG 06-040 from the American Cancer Society to GFC and by NRSA F31 GM084678 from the National Institute from General Medical Sciences to CRN. The funders had no role in study design, data collection and analysis, decision to publish, or preparation of the manuscript.

Competing Interests: The authors have declared that no competing interests exist.

* E-mail: guillom@chem.ucla.edu

◔ These authors contributed equally to this work.

¤ Current address: Department of Microbiology, Immunology, and Molecular Genetics, University of California Los Angeles, Los Angeles, California, United States of America

Introduction

A large fraction of eukaryotic genomes is transcribed, even in the non-coding regions (reviewed in [1]). One of the major questions that arise from these observations is to understand whether the RNAs expressed from these regions serve any functional purpose or whether they correspond to genomic noise that is ultimately routed for degradation. Transcription of non-coding (nc) RNAs nearby protein-coding genes has emerged as a means of transcriptional control (reviewed in [1,2]). In the yeast *S.cerevisiae*, the first and best-documented example is the *SRG1* ncRNA, which regulates transcription of the *SER3* gene involved in serine metabolism through transcriptional interference [3]. While the *SRG1* ncRNA is transcribed in the sense direction upstream of its target gene, most ncRNAs found to regulate *S.cerevisiae* transcription are antisense transcripts, such as the ones described for the *PHO84*, *Ty-1* and *GAL10* loci [4–7], which control chromatin modification marks at these genes. However, upstream sense transcription resulting in the *ICR1* ncRNA has been found to regulate the *FLO11* gene [8].

Cryptic transcripts can also be generated through the transcription of elements that control the expression of *bona fide* protein coding genes. There is ample evidence that promoter regions are associated with bidirectional transcription in *S.cerevisiae* [2,9]. In addition, it has been shown that enhancers are transcribed by RNA polymerase II [10]. In *S.cerevisiae*, many transcripts associated with intergenic or promoter transcription are unstable under normal conditions. They are hardly detectable in wild-type strains because of their rapid degradation by nuclear RNA turnover. Indeed, many transcripts associated with cryptic transcription are detectable only when the activity of the nuclear exosome, or that of the TRAMP-complex, which stimulates exosome activity, is inhibited [2,11,12]. Therefore, these transcripts have been labeled "CUTs" for Cryptic Unstable Transcripts. Most of the degradative activities targeting CUTs seem to be concentrated in the nucleus. However, the cytoplasmic exonuclease Xrn1p can degrade the antisense RNAs that regulate the *Ty-1* gene [5]. In addition, several CUTs can be degraded by the cytoplasmic degradation machinery [12–13], showing that the degradation of RNAs arising from transcription in non-coding regions can result from both nuclear and cytoplasmic RNA degradation pathways.

Nonsense mediated decay is an RNA surveillance mechanism that recognizes transcripts containing premature translation termination codons (PTCs; [14,15]). This degradation system is used to prevent accumulation of aberrant mRNAs that would encode potentially toxic proteins [16,17], but is also used for gene expression control. For example, NMD degrades alternatively or inefficiently spliced mRNAs that contain PTCs [18–21], and transcripts containing long 3′-UTRs [22]. In *S.cerevisiae*, NMD also controls Mg^{++} uptake by degrading the transcript encoding the

Author Summary

Precise expression of genes relies on their accurate and timely transcription and on turning off these genes when production of the proteins is not required. Our study describes that in the baker's yeast, *S. cerevisiae*, repression of many genes relies on transcription of long extended RNAs upstream from where transcription normally initiates. These long extended RNAs are degraded by a machinery that recognizes that these RNAs do not encode any functional proteins. Using genes involved in controlling the uptake of the essential elements zinc and iron, we find that transcription of these long extended non-coding RNAs represses transcription by preventing the binding of the transcriptional machinery to the normal transcriptional control elements. Our findings show that repression of transcription of many genes relies on the transcription of unstable long RNAs and that this mechanism of control is particularly prevalent for genes involved in controlling the level of metals inside cells.

major Mg^{++} transporter [23]. Previous studies using microarray analysis of *S.cerevisiae* NMD mutants have shown that NMD influences directly or indirectly the expression of many genes, including some that do not exhibit PTCs [24–26]. The identification of RNAs that associate with the NMD factor Upf1p by RNA pull-down has proved to be an efficient way to discriminate direct and indirect NMD targets [27]. However, many NMD targets do not accumulate to high levels in the presence of a functional NMD system, which renders this approach difficult for low expression transcripts. In this study, using tiling microarrays, we show that NMD degrades 5′-extended transcripts generated by cryptic transcription upstream from *bona fide* promoters, and that upstream transcription is responsible for the repression of metals homeostasis genes in conditions of metal repletion. These results show that NMD controls the expression of a large number of genes by modulating the expression of 5′-extended RNAs that control transcription.

Results

Accumulation of 5′-extended unstable RNAs of subtelomeric genes in NMD mutants

We previously used tiling microarrays to show that NMD controls the degradation of inefficiently spliced *S.cerevisiae* pre-mRNAs [21]. Further analysis of these microarrays in intergenic areas revealed that many subtelomeric regions accumulated RNA signal outside and upstream from the open-reading frames (ORF) in the *upf1Δ* and *xrn1Δ* mutants. Examples shown in Figure 1 include the subtelomeric *ZRT1* gene encoding the primary zinc transporter [28], the *FIT3* gene involved in siderophore-iron transport facilitation [29], and the *FLO5* gene encoding a cell wall protein (Figure 1). Many genes located in subtelomeric regions are involved in the response to adverse growth conditions [30]. In the case of the *FIT3* and *FLO5* genes, the array profiles suggested that these species originate 5′-to the normal transcriptional start site and extend in the open-reading frame (which was confirmed by northern analysis, see below). In the case of *ADH4* and *ZRT1*, increase of signal in the upstream regions correlated with a decrease of signal in the downstream regions (Figure 1). Northern blot analysis using antisense riboprobes confirmed that these species correspond to 5′-extended transcripts originating upstream from the *bona fide* promoters and partially or completely overlapping the open-reading frame (Figure 2 and see below). Based on the array profiles, some of these species were very long, containing 5′-extensions up to several kb for *ZRT1* (Figure 1, Figure S2). In the case of *FIT3*, a previous study had mapped in detail the 5′-extended species that extends into the ORF [31]. Thus, these species are different from the short antisense CUTs transcribed divergently from the promoters [2,9]. Accumulation of 5′-extended transcripts in NMD mutants has been reported for a few transcripts, but was interpreted as the result of transcriptional noise [27]. We hypothesized that some of these 5′-extended unstable transcripts might be used for regulatory purposes, as shown in other systems [3,32,33]. Because the accumulation of 5′-extended transcripts relied on the inactivation of cytoplasmic degradation pathways, we named these 5′-extended species CD-CUTs (Cytoplasmically Degraded Cryptic Unstable Transcripts).

NMD mutants show a delay in the induction of subtelomeric metal homeostasis genes

In the case of subtelomeric genes involved in zinc metabolism (*ZRT1*, *ADH4*, *VEL1*, *YOR387C*, Figure 1; ZPS1, Figure S1), the accumulation of CD-CUTs was correlated with a decreased signal in the ORF regions, suggesting that they might play a negative role in the expression of the *bona fide* mRNAs. Interestingly, zinc regulon genes not located in subtelomeric areas, such as the one encoding the low affinity zinc transporter *ZRT2* [34] did not exhibit CD-CUTs (data not shown). We found that the growth conditions used for the microarrays (synthetic complete minimal medium) corresponded to mild zinc deficiency conditions, in which some of the zinc regulon genes were partially induced (data not shown). Therefore the decrease of signal observed in the ORF regions for *ZRT1* and *ADH4* (Figure 1) might be due to a defect in the partial induction of these genes in minimal medium. We further analyzed the expression of zinc responsive mRNAs and their corresponding CD-CUTs in wild-type and *upf1Δ* strains grown in the presence or absence of zinc, using northern blots and antisense riboprobes covering the open-reading frames (ORFs) or the upstream (UP) regions (Figure 2A). This analysis confirmed the accumulation of CD-CUTs of *ZRT1*, *ADH4* and *ZPS1* in the *upf1Δ* mutant strain. For *ZPS1*, CD-CUTs were readily detectable in the wild-type as well as in the *upf1Δ* strain, explaining why only a modest increase in upstream signal was observed for this gene on the arrays, which compare the transcripts levels of the *upf1Δ* mutant to the wild-type (Figure S1). Some CD-CUTs were detected only with the upstream riboprobes, demonstrating that they are independent from the ORFs (Figure 2A). However, most CD-CUTs were also detected using the ORF riboprobes (Figure 2A and see below), indicating that they extend through the ORFs. A detailed characterization of the *ZRT1* and *ADH4* CD-CUTs using various upstream probes and ORF probes is shown in Figure S2 and described below. ORF riboprobes detected the induction of the normal *ZPS1*, *ADH4*, and *ZRT1* mRNAs in wild-type cells grown in a medium lacking zinc (Figure 2A). However, these mRNAs were less abundant in the *upf1Δ* mutant (Figure 2A). This observation suggested that the accumulation of CD-CUTs due to NMD inactivation was deleterious to the expression of the *bona fide* mRNAs. We further characterized the expression of these genes in the *upf1Δ* mutant by monitoring their kinetics of induction (Figure 2B). This experiment showed that the *upf1Δ* mutant exhibited a delay in the induction of the subtelomeric *ZPS1*, *ZRT1*, *ADH4* (Figure 2B) and *VEL1/YOR387C* genes (Figure S3A). The induction defect was also observed in the *upf2Δ* and *upf3Δ* strains (Figure S3A), indicating that it is a general feature of NMD mutants. In contrast, the induction of other zinc regulon genes such as *ZRT2*, *GPG1* (*YGL121C*) and *PHM7* (*YOL084W*), which are not localized in subtelomeric regions and do not exhibit CD-CUTs (data not shown) was unaffected by

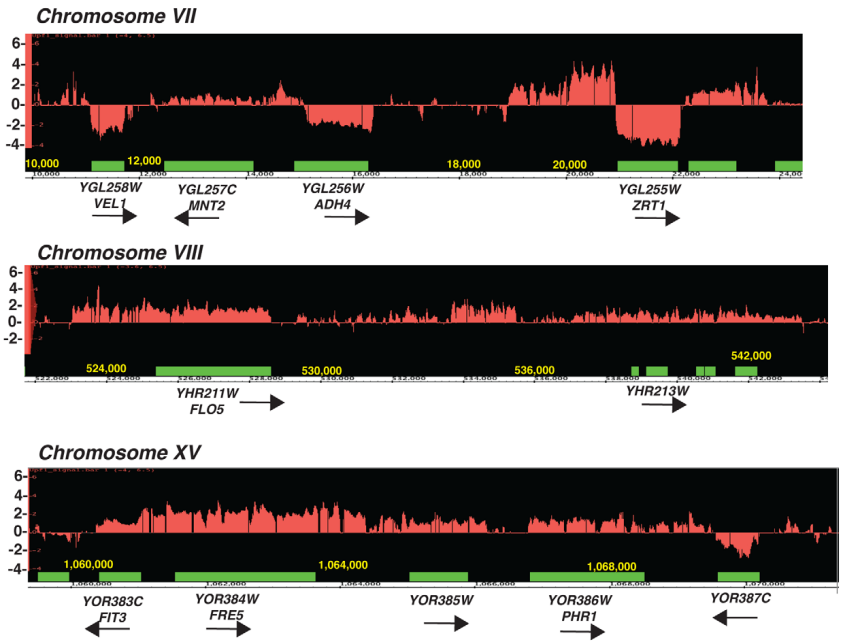


Figure 1. Tiling arrays profiles of the *upf1Δ* mutant relative to the wild-type strain. Green boxes represent the boundaries of open-reading frames, red the $\log_2$ ratio of the RNA signals detected in the *upf1Δ* mutant relative to wild-type. Arrows indicate the direction of transcription of the ORFs. Shown are three segments of three chromosomes.
doi:10.1371/journal.pgen.1002163.g001

Upf1p absence (Figure 2B). A previous study found that NMD can influence gene expression by controlling the level of transcriptional activators [35]. We found that the mRNA levels of the Zap1p activator (which activates zinc regulon genes) were similar in wild-type and *upf1Δ* mutants (Figure S3B), suggesting that the delay of induction in the absence of Upf1p was not due to reduced Zap1p levels. Overall these results show that the defective induction of subtelomeric zinc-responsive genes in the *upf1Δ* mutant is not due to a global deficiency in zinc sensing in this mutant, but is specific to genes that exhibit CD-CUTs. Defective induction was also observed for the *FIT3* iron depletion-responsive gene in a strain lacking Xrn1p or Upf1p activity (Figure S4). Overall these observations suggest that the presence or transcription of CD-CUTs represses the expression of many subtelomeric genes, some of which are involved in zinc or iron homeostasis.

Long 5′-extended transcripts of subtelomeric genes are primarily targeted by NMD, while short 5′-extended transcripts are degraded by NMD and nuclear RNA degradation pathways

To further investigate the mechanisms of turnover of CD-CUTs by the different RNA degradation machineries, we analyzed the accumulation of CD-CUTs of *ZRT1* and *ADH4* in strains lacking Upf1p, the nuclear exosome component Rrp6p, or both. These two genes were chosen because the 5′-extensions found in the CD-CUTs of *ZRT1* and *ADH4* are very different in size (extension of 2 kb for *ZRT1* vs. a few hundred nucleotides for *ADH4*). This analysis showed that the major *ZRT1* CD-CUT (CD-CUT1, Figure 2C) accumulated dramatically in the *upf1Δ* strain, and to a much lesser extent in the *rrp6Δ* mutant. Accumulation of the *ZRT1* main CD-CUT-1 was not increased in the *upf1Δrrp6Δ* double mutant compared to the *upf1Δ* single mutant (Figure 2C). These observations suggest that the degradation of the longer CD-CUT of *ZRT1* relies mostly on NMD, consistent with the long upstream region lacking any extended ORF. In contrast, the short *ADH4* CD-CUT accumulated to similar levels in the *upf1Δ* and *rrp6Δ* strains (Figure 2D). Strikingly, the accumulation of this CD-CUT was dramatically increased in the *upf1Δrrp6Δ* double mutant (Figure 2D, time zero), suggesting that this CD-CUT is degraded by the cooperative action of the nuclear exosome and of NMD. Interestingly the induction of the *bona fide ADH4* mRNA was completely defective in this double mutant strain, while the single mutants were only partially delayed. The correlation between the strong accumulation of the *ADH4* CD-CUT in the *upf1Δrrp6Δ* double mutant and the severe induction defect of the *bona fide ADH4* mRNA provides further evidence for the repression of this subtelomeric gene by its CD-CUT.

The CD-CUT of the subtelomeric iron responsive gene *FIT3* was previously shown to accumulate in the *xrn1Δrat1-1* double mutant [31], raising the question of which exonuclease was primarily responsible for its degradation. We analyzed the

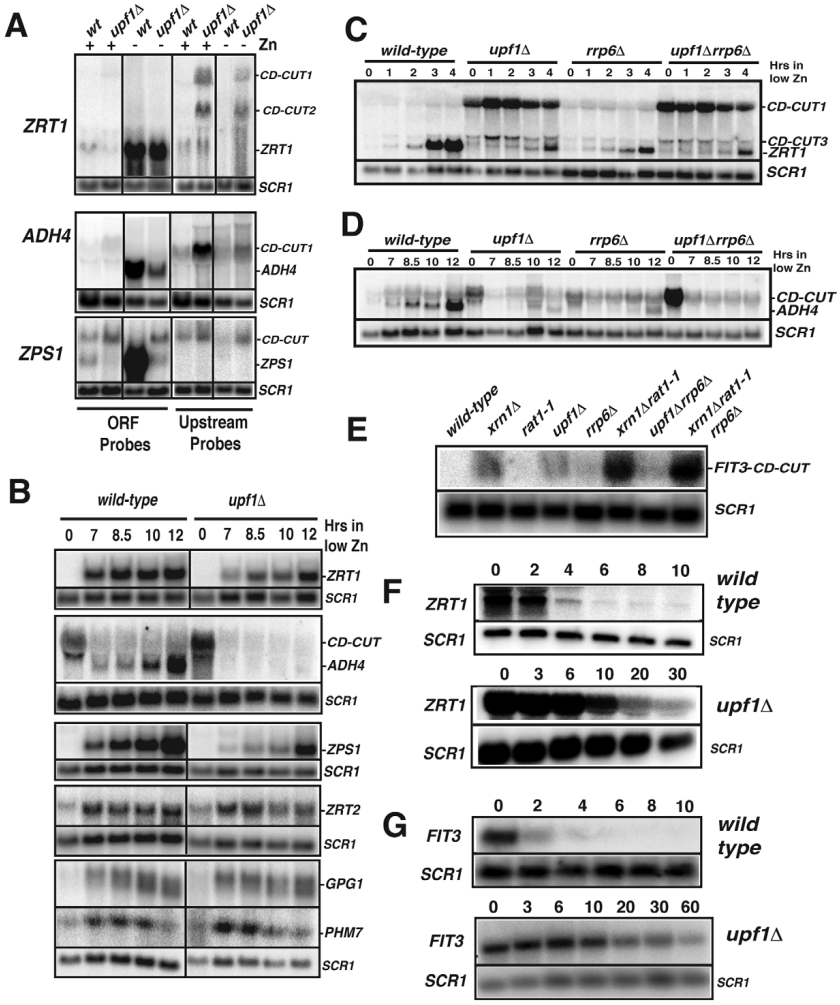


Figure 2. Characterization of CD-CUT of zinc and iron responsive genes. A. Northern blots of indicated genes in wild-type and *upf1Δ* strains grown in the presence (+) or absence (−) of zinc. Extended species are marked as CD-CUT1 and 2. *SCR1* was used as a loading control. B. Kinetics of induction of zinc regulon genes in wild-type and *upf1Δ* strains after a shift to a medium lacking zinc. C–E. Analysis of *ZRT1*, *ADH4* and *FIT3* CD-CUT and mRNA expression in ribonuclease mutants. C. Northern analysis of *ZRT1* induction in wild-type, *upf1Δ*, *rrp6Δ* and *upf1Δrrp6Δ* prior to and after a shift into low zinc medium. D, as in A for *ADH4*. E, northern analysis of the *FIT3* CD-CUT in iron-replete conditions in the indicated strains. F–G. Analysis of *ZRT1* (F) and *FIT3* (G) CD-CUT turnover in wild-type and *upf1Δ* strains. The GAL promoter was inserted upstream from the major site of transcription initiation of the *ZRT1* or *FIT3* CD-CUTs. After growth in galactose containing medium, cells were switched to glucose-containing medium and cell aliquots were harvested at the indicated times after the switch. CD-CUT levels were analyzed by northern blots using upstream riboprobes.
doi:10.1371/journal.pgen.1002163.g002

expression of this CD-CUT in strains lacking Xrn1p, Upf1p, Rrp6p, in the *xrn1Δrat1-1* mutant strain and in other double mutant strains. This analysis revealed that the long CD-CUT of *FIT3* accumulated to the highest level in the strain lacking Xrn1p and to a lesser extent Upf1p (Figure 2E), and its accumulation was not dramatically increased by Rrp6p inactivation, in contrast to

what was found for *ADH4*. Thus, based on this steady-state analysis, the long CD-CUT of *FIT3* is also primarily targeted by cytoplasmic turnover pathways that include Xrn1p and Upf1p.

The turnover of the *ZRT1* and *FIT3* CD-CUTs is dependent on NMD

Because CD-CUTs exhibit a lack of extended ORFs, we interpreted their accumulation in the *upf1Δ* and *xrn1Δ* mutant strains as the result of a lack of degradation by NMD. Alternatively, we could not rule out that transcription of these upstream regions might be indirectly up-regulated in these mutants. To test this hypothesis, *GFP-HIS3* cassettes [36] were inserted upstream from the normal *ZRT1* or *ADH4* promoters in wild-type and *upf1Δ* strains, such that the expression of the *GFP* mRNA was under the control of the upstream regions (Figure S5A). Northern blot analysis of *GFP* inserted upstream from *ZRT1* or *ADH4* showed that this reporter transcript was expressed at similar levels in the wild-type and *upf1Δ* strains (Figure S5B). These results suggested that the accumulation of CD-CUTs in NMD mutants is not due to an increased transcription of these upstream regions, but to the absence of ORF in the 5′- extension of the CD-CUTs.

To gain further evidence that the turnover of CD-CUTs is directly dependent on NMD, we replaced the region upstream from the site of transcription initiation of the *ZRT1* and *FIT3* CD-CUTs with a galactose inducible promoter. This allowed us to measure the rate of decay of these CD-CUTs in the presence or absence of functional NMD. The kinetics of turnover of the *ZRT1* CD-CUT (Figure 2F) or of the *FIT3* CD-CUT (Figure 2G) showed that these species are much more unstable in the presence of functional NMD ($t_{1/2}$ = 2–3 min.) than in the absence of Upf1p ($t_{1/2}$ = 20–30 min.). Because the turnover rate of these species is strongly decreased when NMD is inactivated, we conclude that these CD-CUTs are directly targeted by NMD for their degradation.

The main CD-CUT of *ZRT1* is activated by the histone deacetylase Rpd3p

Previous microarray analysis of a strain inactivated for the histone deacetylase Rpd3p showed that *ZRT1* is derepressed in the *rpd3Δ* strain and that Sir2p played a role antagonistic to Rpd3p in *ZRT1* expression [37]. To investigate whether Rpd3p or Sir2p control *ZRT1* by modulating the expression of its CD-CUT, we inactivated Upf1p in *rpd3Δ* or *sir2Δ* backgrounds and studied the induction of *ZRT1* in these strains. *ZRT1* was strongly derepressed in the *rpd3Δ* strain (Figure 3A, time zero), in agreement with previous data [37]. Strikingly, inactivation of Rpd3p in the *upf1Δ* strain completely rescued the induction defect of this NMD mutant, and resulted in a strong derepression of *ZRT1* in normal zinc conditions (Figure 3A). Inactivation of Rpd3p also resulted in the almost complete disappearance of the *ZRT1* CD-CUT observed in the *upf1Δ* strain. These results show that Rpd3p positively controls the expression of CD-CUT of *ZRT1*, and suggest that the derepression of *ZRT1* in the *rpd3Δ* mutant [37] is due to the absence of the CD-CUT. In contrast, Sir2p inactivation reduced *ZRT1* levels (Figure 3A), in agreement with the previous results [37]. Combining the *sir2Δ* deletion to the *upf1Δ* deletion exacerbated the *ZRT1* induction delay when compared to the *upf1Δ* mutant (Figure 4A), but the *sir2Δupf1Δ* mutant did not exhibit higher levels of CD-CUT than the *upf1Δ* single mutant (Figure 4A). Therefore, the negative effects of Sir2p inactivation on *ZRT1* expression are unlikely to be directly linked to its effect on the *ZRT1* CD-CUT.

To investigate the specificity of the effect observed with Rpd3p on the *ZRT1* CD-CUT levels, we performed the same genetic analysis with the Hos1p, Hda1p, Hda2p and Hda3p deacetylases. The *hos1Δ* strain showed a slight delay in the induction of *ZRT1*, correlated with an increase of CD-CUT levels, but the *hos1Δupf1Δ* double mutant showed no additive effect when combined with the *upf1Δ* deletion (Figure 3B). Neither Hda1p (Figure 3C), nor Hda2p or Hda3p (Figure S6) were found to affect *ZRT1* induction or repression. These results show that the major effect observed with Rpd3p on the *ZRT1* CD-CUT is specific to this deacetylase. We tried to corroborate these results by monitoring the presence of Rpd3p in the region 5′ to *ZRT1* but could not obtain reproducible evidence for enrichment by ChIP (data not shown). However the genetic data shown above strongly suggest that Rpd3p mediates the repression of *ZRT1* through the modulation of the transcription of the CD-CUT.

Inactivation of the transcription of the CD-CUTs by deletion or transcriptional termination relieves *ZRT1* and *FIT3* repression and can rescue the induction defect of the *upf1Δ* mutant

If CD-CUTs are involved in the repression of the *ZRT1* gene, we predicted that the replacement of its upstream region by the *GFP-HIS3* coding cassette (Figure S5A) might alleviate its repression. Northern blot analysis of the strain carrying one of the insertions upstream from *ZRT1* (*zrt1-up1*; inserted 1978 to 578 nucleotides upstream from the *ZRT1* ATG; Figure S5A) showed a four-fold derepression of *ZRT1* in zinc repletion conditions, both in the wild-type and *upf1Δ* backgrounds (Figure 4A). Insertion of this cassette eliminated the detection of the main CD-CUT of *ZRT1*, with the exception of the short CD-CUT3 (Figure 4A). This insertion also partially suppressed the induction defect of the *upf1Δ* strain during zinc deficiency (Figure S5C). The kinetics of disappearance of *ZRT1* upon shifting back to zinc-containing medium was also monitored in these strains after 4 hours of induction, but we found no difference in the rate of *ZRT1* shutoff in the presence or absence of its main CD-CUT (Figure S5C). A similar derepression was observed for *FIT3* in a strain carrying a 3 Kb deletion of the region upstream of the *FIT3* gene (from −4 kb to −1 kb upstream *FIT3*; *fit3-upΔ*, Figure 4B). Analysis of the *fit3-upΔxrn1Δ* double mutant strain showed that the CD-CUTs of *FIT3* were eliminated in this double mutant, which confirmed that the derepression was due to the absence of the CD-CUT. Thus, deleting the regions encoding the CD-CUTs is sufficient to trigger derepression of the *bona fide* mRNAs, even in a wild-type context.

To provide more direct evidence that transcription of CD-CUTs is responsible for repression of the downstream promoters, we inserted the *ADH1* transcription terminator (*ADH1t*) at 3 positions upstream from *ZRT1* (*tA*: −1839, *tB*: −771 and *tC*: −184 bp; Figure 4C, 4D). If CD-CUT transcription or accumulation prevents the binding of RNA polymerase or of the transcriptional activator Zap1p, we hypothesized that terminating transcription of the CD-CUTs prior to the *ZRT1* transcriptional control elements could derepress *ZRT1* and/or rescue of the induction defect of NMD mutants. We first assessed *ZRT1* mRNA and CD-CUTs levels in these strains in normal zinc conditions (Figure 4C). A sample from a strain grown in low zinc conditions was included as a control for the *ZRT1* mRNA. Insertion of *ADH1t* at position A did not result in major *ZRT1* derepression, probably because terminating transcription at this site results in activation of an alternative CD-CUT downstream from that site (labeled CD-CUT1′. Figure 4C). However insertion of this terminator resulted in a much shorter transcript that was now insensitive to a *upf1* deletion, further showing that the sensitivity of

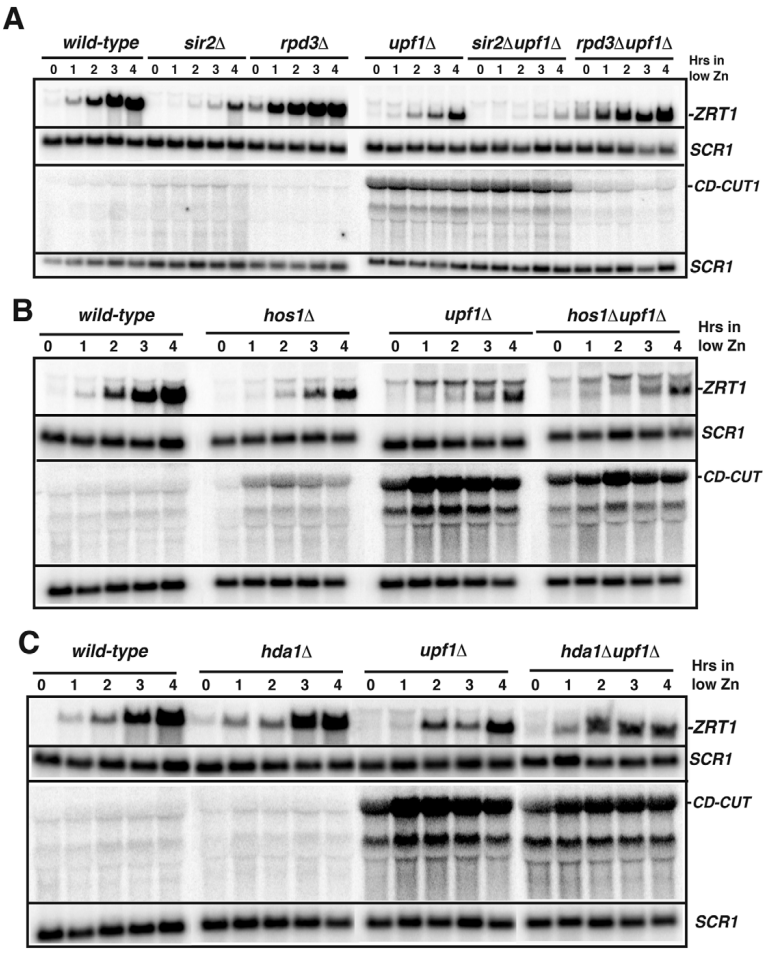


Figure 3. The main *ZRT1* CD-CUT is controlled by the histone deacetylase Rpd3p. A. Northern blot analysis of *ZRT1* mRNA and CD-CUTs in wild-type, *sir2Δ*, *rpd3Δ*, *upf1Δ* and *sir2Δupf1Δ* and *rpd3Δupf1Δ* deletion strains. B. Northern blot analysis of *ZRT1* mRNA and CD-CUTs in wild-type, *hos1Δ*, *upf1Δ* and *hos1Δupf1Δ* strains. C. Northern blot analysis of *ZRT1* mRNA and CD-CUTs in wild-type, *hda1Δ*, *upf1Δ* and *hda1Δupf1Δ* strains.
doi:10.1371/journal.pgen.1002163.g003

CD-CUTs to NMD is dependent on their long size, and potentially on the lack of extended ORF in the 5′-extension. Strikingly, insertion of the *ADH1t* at positions −771 (B) or −184 (C) resulted in a derepression of *ZRT1* (Figure 4C). The strongest effect was observed for *ADH1t-C*, possibly because this terminator stops all CD-CUT transcription immediately before the *ZRT1* TATA box. In the *ADH1t-B* strain, an increased accumulation of the CD-CUT3 is observed, while this species disappears in the *ADH1t-C* strain. These results show that terminating transcription of the CD-CUTs upstream from the *ZRT1* promoter is sufficient to derepress *ZRT1* in conditions of non-induction. Additionally, insertion of these terminators allowed us to map in further detail the CD-CUTs upstream from *ZRT1*. Based on the hybridization pattern with the different probes (Figure S2A), the effect of the various terminators on their mobility in northern blots (Figure 4C), the approximate architecture of these CD-CUTs is shown in Figure 4D.

Transcription of the zinc regulon genes is activated by binding of the transcriptional activator Zap1p to their promoters during zinc deficiency [28,38]. The terminator sequence inserted at position 771 is located upstream from the three major Zap1 binding sites (ZRE; [38]), while the terminator sequence inserted

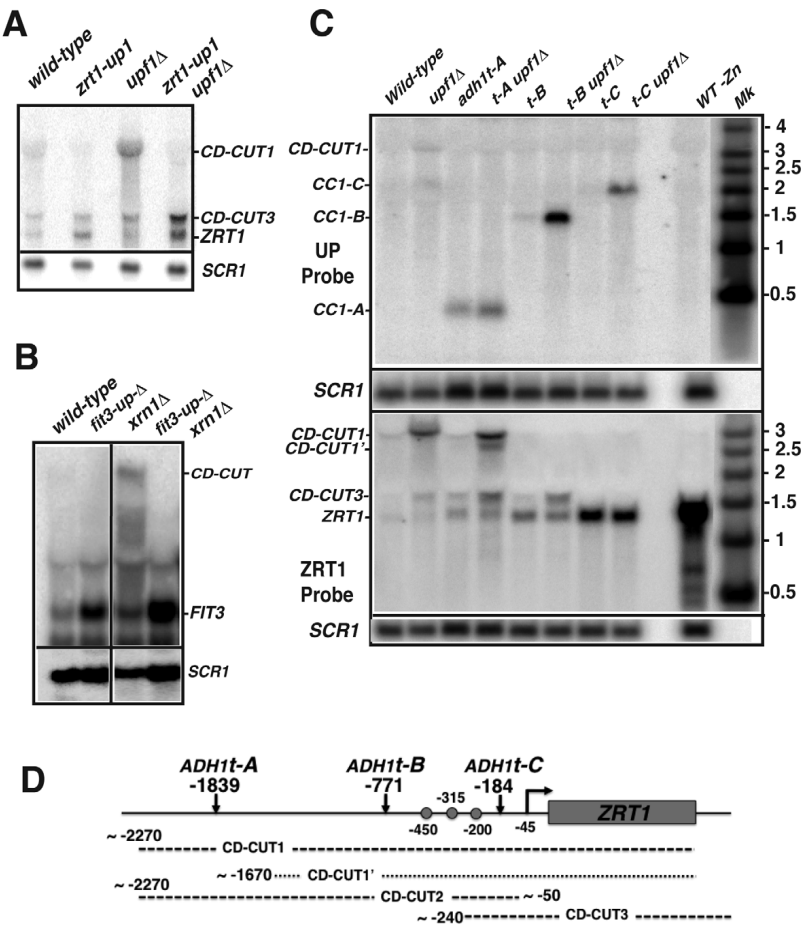


Figure 4. Mutations of the upstream regions and insertion of transcription terminators result in a derepression of *ZRT1* and *FIT3*. A. Effects of the insertion of a *GFP-HIS3* cassette upstream *ZRT1* (*zrt1-up1*) on *ZRT1* mRNA levels in zinc repletion conditions in wild-type and *upf1Δ* strains. *ZRT1* RNAs were assessed by northern blot using an ORF probe. B. Effects of the deletion of the region upstream *FIT3* (*fit3-upΔ*) on *FIT3* levels in iron repletion conditions in wild-type and *xrn1Δ* strains. *FIT3* RNAs were assessed by northern blot using an ORF probe. C. Effects of the insertion of *ADH1t* transcriptional terminators at various sites upstream *ZRT1* on *ZRT1* mRNA and CD-CUT levels in zinc repletion conditions in wild-type and *upf1Δ* strains. Mk is a size marker. The upper membrane was hybridized with a probe upstream from the *ZRT1* ORF, while the lower membrane was hybridized with a probe corresponding to the *ZRT1* ORF. D. *ADH1t* terminator insertion sites and schematic maps of *ZRT1* CD-CUT species. Dots represent the three major Zap1p binding sites.
doi:10.1371/journal.pgen.1002163.g004

at position 184 is inserted downstream from them (Figure 4D). Based on this, we hypothesized that if transcription of the CD-CUTs prevents binding of Zap1p, the two strains containing terminators at the two positions might behave differently during a shift into low zinc conditions. Indeed, insertion of the *ADH1t* at position B derepressed *ZRT1*, and also fully rescued the induction defect of the *upf1Δ* strain (Figure 5A). However strains carrying an insertion of the *ADH1t* at position C failed to induce *ZRT1* in conditions of induction, even in a context of active NMD. This result suggests that the region located between positions B and C, which contains most of the Zap1p binding sites must be accessible for *ZRT1* induction. It is unclear why the strain containing the *ADH1t* at position C failed to induce *ZRT1*, even when NMD is active. It is possible that the higher levels of expression of the

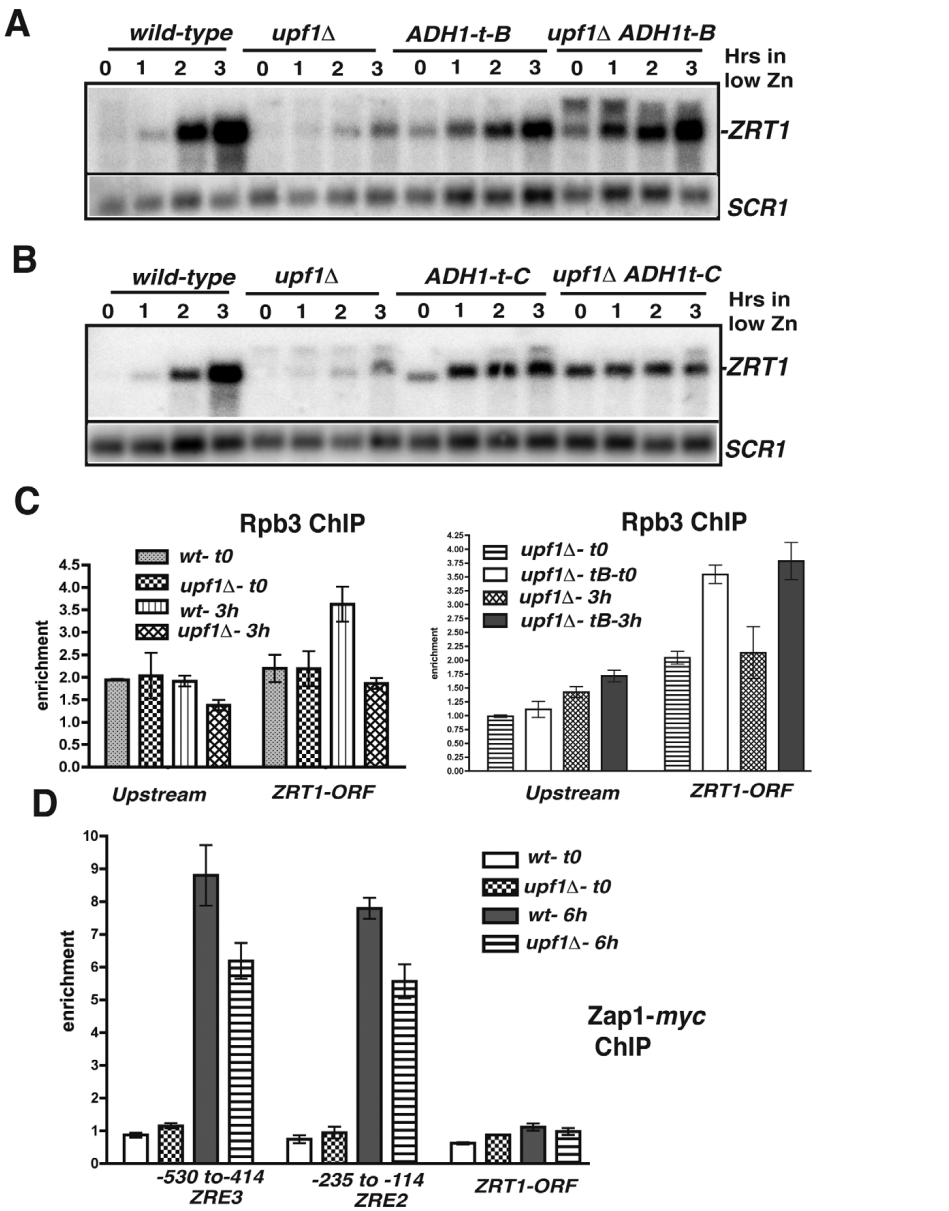

A
wild-type
upf1Δ
ADH1-t-B
upf1Δ ADH1t-B
0 1 2 3 0 1 2 3 0 1 2 3 0 1 2 3
Hrs in low Zn
-ZRT1
SCR1
B
wild-type
upf1Δ
ADH1-t-C
upf1Δ ADH1t-C
0 1 2 3 0 1 2 3 0 1 2 3 0 1 2 3
Hrs in low Zn
-ZRT1
SCR1
C
Rpb3 ChIP
wt- t0
upf1Δ- t0
wt- 3h
upf1Δ- 3h
enrichment
Upstream
ZRT1-ORF
Rpb3 ChIP
upf1Δ- t0
upf1Δ- tB-t0
upf1Δ- 3h
upf1Δ- tB-3h
enrichment
Upstream
ZRT1-ORF
D
wt- t0
upf1Δ- t0
wt- 6h
upf1Δ- 6h
enrichment
Zap1-myc ChIP
-530 to-414 ZRE3
-235 to -114 ZRE2
ZRT1-ORF

Figure 5. Effects of transcription terminators upstream *ZRT1* on *ZRT1* induction and analysis of RNA Polymerase II and Zap1p occupancies by ChIP. A and B. Effects of the insertion of ADH1 transcriptional terminators at various sites upstream *ZRT1* on *ZRT1* mRNA during zinc depletion in wild-type and *upf1Δ* strains. C. Analysis of RNA polymerase II occupancy in wild-type, *upf1Δ* and *upf1Δ ADH1t*-B strains grown in normal zinc medium (t0) or after a 3 hours shift in low zinc. Shown are normalized qPCR analysis of the different regions from ChIP samples obtained using anti-Rpb3p antibodies normalized to input DNA and to a qPCR product for a control non-transcribed region. D. Analysis of Zap1p occupancy at different sites of the *ZRT1* gene. Legends as in 5C except that a myc-tagged version of Zap1p was used.
doi:10.1371/journal.pgen.1002163.g005

ZRT1 transporter in non-induction conditions resulted in higher cellular zinc levels prior to induction, thus delaying the response. Additionally we cannot rule out that inserting the *ADH1t* at site C might have changed the chromatin structure, and thus perturbed the induction of *ZRT1*.

Binding of RNA Polymerase II and of the transcriptional activator Zap1p is defective in the NMD mutant *upf1Δ*

To corroborate these results, we studied RNA Polymerase II occupancy in two regions, upstream from *ZRT1* (−1223 to −1123), and within the *ZRT1* ORF (+905 to +1021), using chromatin immunoprecipitation (ChIP) of the Rpb3p subunit. We found slightly above background levels of occupancy of the polymerase in conditions of zinc repletion in both regions in wild-type and *upf1Δ* strains (Figure 5C). Interestingly, Rpb3p occupancy was similar for both strains in the upstream region, indicative of a similar level of transcription of the CD-CUTs. This result further indicates that accumulation of the CD-CUTs in the *upf1Δ* strain is due to a lack of degradation rather than increased transcription. Upon a shift to low zinc medium, Rpb3p occupancy increased for the wild-type strain in the *ZRT1* ORF, but not in the upstream region, reflecting the induction of the *ZRT1* gene. However this increase was not observed in the *upf1Δ* strain, corroborating the results observed by northern analysis. To show that the insertion of the terminator upstream from *ZRT1* rescues the induction defect of the *upf1Δ* strain by allowing polymerase binding, we performed the same analysis by comparing Rpb3p occupancy in the *upf1Δ* and *upf1Δ-ADH1t-B* strains. Strikingly, Rpb3p levels were increased upon insertion of *ADH1t* at position B in the *upf1Δ* strain, both in normal zinc medium and after 3 hrs of induction, showing that the derepression of *ZRT1* and the rescue of the induction defects are due to increased RNA Polymerase occupancy.

We also analyzed binding of the transcriptional activator Zap1p by ChIP in wild-type and *upf1Δ* strains using a *myc*-tagged version of Zap1p inserted at the chromosomal locus. We found background levels of Zap1p occupancy to its binding sites (ZREs) in conditions of repression in both strains (Figure 5D). However increased occupancy was observed in the wild-type strain upon a shift to low zinc (Figure 5D). Binding was reduced in the *upf1Δ* mutant, further showing that the accumulation of CD-CUTs perturbs Zap1p binding during *ZRT1* induction. Zap1p enrichment was highly specific, as it was not observed in the *ZRT1* coding region (Figure 5D). Overall the differences in RNA polymerase II and Zap1p occupancies in the *ZRT1* gene are consistent with the results described above by Northern blot, showing that the effects observed in NMD mutants upon accumulation of CD-CUTs are indicative of transcriptional defects of the *ZRT1* gene.

Overexpression or constitutive activation of transcriptional activators of subtelomeric genes suppresses their induction defect in the *upf1Δ* and *xrn1Δ* strains

The previous result showed that binding of the Zap1p activator is deficient in the NMD mutant *upf1Δ* during the low zinc response. If so, we predicted that overexpressing Zap1p might suppress the induction delay in this strain. Indeed, overexpressing Zap1p in the *upf1Δ* mutant was sufficient to rescue *ZRT1* induction to levels comparable to those observed in the wild-type strain (Figure 6A). This result shows that defective binding of Zap1p to the ZREs in the *upf1Δ* mutant can be overcome by overexpressing this activator. To extend these results to another gene induced in different conditions and controlled by a different activator, we monitored the expression of *FIT3* in wild-type and *xrn1Δ* strains expressing *aft1-up*, a constitutively active version of Aft1p (kindly provided by J.Kaplan; [39,40]. Aft1p is one of the two major transcriptional activators involved in the low iron response [39]. As expected, expression of the *aft1-up* allele resulted in derepression of the *FIT3* mRNA in normal iron conditions in the wild-type strain (Figure 6B). However, similar levels of the mature *FIT3* transcript were observed in an *xrn1Δ* background when the *aft1-up* allele was expressed, showing that the presence of a constitutively activated form of Aft1p can overcome CD-CUT-mediated repression. The accumulation of the *FIT3* CD-CUT was not affected by expression of the *aft1-up* construct (Figure 6B), showing that this effect was not due to a decrease of expression of CD-CUT. We also monitored *FIT3* induction in these strains upon a shift to low iron conditions (Figure 6C). Interestingly, *FIT3* levels did not increase in the *aft1-up* strain upon a shift to low iron conditions (Figure 6C). However *FIT3* accumulation was higher in the *xrn1Δ aft1-up* double mutant, possibly because of a reduced degradation of the *FIT3* mRNA in the absence of Xrn1p.

Accumulation of CD-CUTs abolishes the derepression of *FIT3* induced by a Mediator component mutation

To investigate the specificity of the effects described above, we searched for conditions in which the induction of *ZRT1* or *FIT3* was uncoupled from activation by their transcriptional activators. Mutation of the Med2p tail component of the Mediator complex into a non-phosphorylated isoform (*med2-S208A*) was shown to result in a constitutive expression of *FIT3* [41]. This observation led us to investigate the effect of the accumulation of the *FIT3* CD-CUT on the derepression of *FIT3* induced by this Mediator component mutation. We inactivated Xrn1p in a strain carrying the *med2-S208A* mutation (kind gift of F.Holstege) and analyzed the expression of *FIT3*. *FIT3* derepression was observed in the *med2-S208A* mutant grown in normal medium (Figure 6D; time zero), in agreement with previous findings [41], but this mutant did not exhibit any further induction in low iron until 3 hours after the shift. Strikingly, inactivating Xrn1p in the *med2-S208A* strain abolished the derepression of *FIT3* observed in the *med2-S208A* strain (Figure 6D). However the *xrn1Δmed2-S208A* mutant strain was not as defective for induction as the *xrn1Δ* strain, since the double mutant showed kinetics of *FIT3* induction comparable to the wild-type strain. The result obtained in normal iron conditions (time zero, Figure 6D) shows that the accumulation of the *FIT3* CD-CUT can inhibit the activation of *FIT3* that results from a mediator component mutation. These results contrast with the result observed previously with the *aft1-up* mutation, which can activate expression of *FIT3* even when CD-CUTs accumulate due to the inactivation of Xrn1p. Taken together, these results suggest

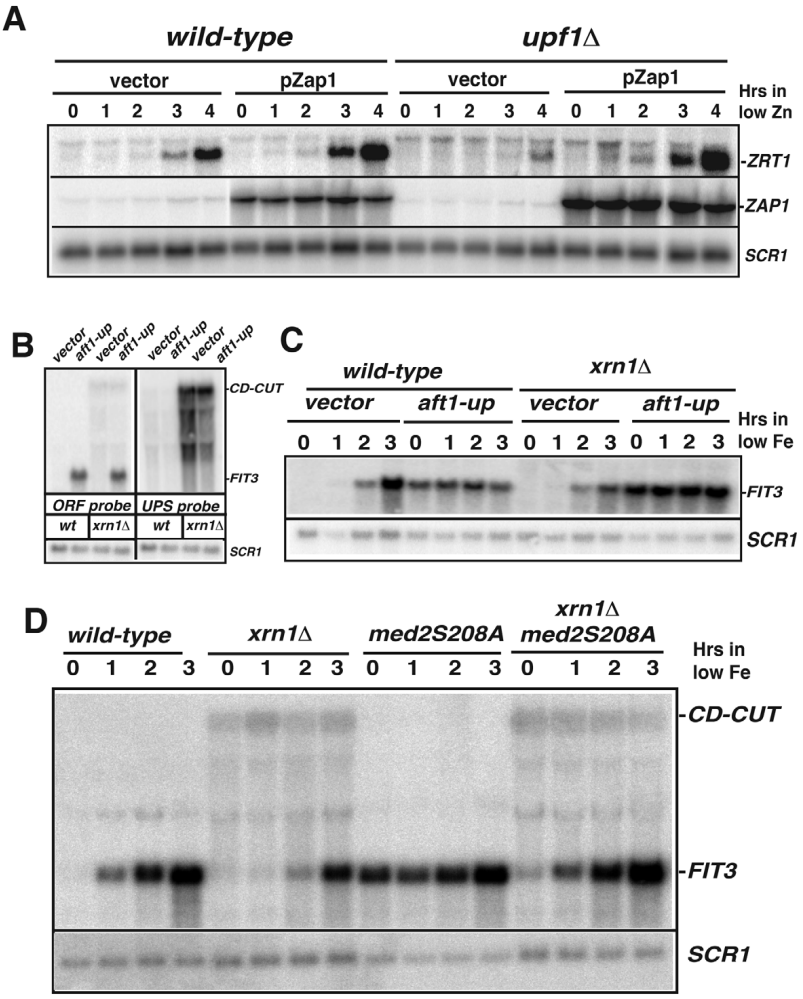


Figure 6. CD-CUT mediated transcriptional repression can be rescued by overexpression or constitutive activation of transcriptional activators. A. Overexpression of Zap1 rescues the *ZRT1* induction defect observed in the *upf1Δ* mutant. Induction of *ZRT1* in wild-type and *upf1Δ* mutant containing an empty vector or a vector overexpressing Zap1p (pZap1) under the control of a *MET25* promoter. The WT or *upf1Δ* stains containing the vector pUG35 or pIT31 were grown in normal zinc conditions (time zero) or after overexpression of Zap1 and shift into low zinc medium. B and C. Expression of the *aft1-up* allele induces *FIT3* expression even in the presence of the *FIT3* CD-CUT. A plasmid expressing the *aft1-up* allele or a control vector were transformed into wild-type and *xrn1Δ* strain, and the levels of *FIT3* mature mRNA or those of the CD-CUT were assessed by northern analysis using an ORF or an upstream (UP) probe, respectively. In panel C, the level of the *FIT3* mRNA was assessed in these strains prior to and after a shift to low iron conditions. D. Analysis of *FIT3* induction in wild-type, *xrn1Δ*, *med2S208A* and double mutant strains.
doi:10.1371/journal.pgen.1002163.g006

that the function of the *FIT3* and *ZRT1* CD-CUTs is to prevent the premature binding of the RNA polymerase or of transcriptional activators such as Zap1 and Aft1p when these genes are transcriptionally repressed.

Discussion

Stable non-coding RNAs that can be detected without perturbations of the RNA degradation machinery have been shown to accumulate near many genes [42–44]. Here we show that strains defective for NMD accumulate 5′-extended forms (CD-CUTs) of many subtelomeric genes, some of which are involved in zinc and iron uptake and homeostasis. The accumulation of CD-CUTs is observed for a large number of genes located in subtelomeric regions in NMD mutants (Figure 1; Table S1). NMD also degrades the upstream sense ncRNA *ICR1* that regulates the *FLO11* gene ([8]; Figure S1B). Therefore CD-CUTs degraded by NMD are not exclusively involved in regulating metal homeostasis genes. Given the number of transcripts for which we detected a potential accumulation of CD-CUTs in NMD mutants by tiling arrays (Table S1), and the fact that extended forms of *SRG1*, which regulate *SER3* transcription can be degraded by NMD [13], we speculate that cryptic upstream sense transcription might be used more widely than previously thought. However most of these transcripts are normally undetectable or present at very low levels because of active NMD.

CD-CUTs are clearly degraded by NMD, as shown by their extended half-life in the absence of Upf1p (Figure 2F, 2G) and because they are no longer stabilized by a *upf1* deletion when a long ORF is inserted in their place (Figure S5B). CD-CUTs are likely recognized as NMD substrates because of the lack of extended ORFs in the 5′-regions upstream from the natural ORF. This might result in random translation initiation in the 5′-region, followed shortly by a stop codon, resulting in recognition of a *faux*/extended 3′-UTR [45], thus targeting them to NMD. In support of this model, terminating transcription of the main *ZRT1* CD-CUT in a manner that results in a shorter transcript renders it insensitive to a *upf1* deletion (Figure 4C, *adh1t-A* strain). CD-CUTs accumulating in NMD-deficient strains are different from the CUTs accumulating in nuclear exosome or TRAMP complex mutants [11,46,47]. CD-CUTs are much larger than CUTs, and most of them extend within the open-reading frames to terminate at or near the site of normal 3′ processing of the ORF mRNAs (Figure 1 and Figure 2, Figure S2, Figure 4D). Thus, both the nuclear exosome and cytoplasmic NMD degradation machineries are used to regulate gene expression but act on different sets of promoter-associated unstable RNAs. However, the two pathways can sometimes intersect, for example, in the case of the *ADH4* CD-CUT, which is efficiently degraded only when both NMD and the nuclear exosome is inactivated (Figure 2; Figure 7).

How do CD-CUTs mediate transcriptional repression?

The precise mechanism by which CD-CUTs mediate transcriptional repression is not fully understood. Accumulation of CD-CUTs in NMD mutants negatively interferes with production of the normal transcripts and with RNA polymerase II and transcriptional activator binding (Figure 5, Figure 6, Figure 7). We do not know whether acting in *cis* is strictly required, which would be consistent with an *SRG1*-like transcriptional interference model [3]. We tried to express the *ZRT1* CD-CUTs from a plasmid to test for the possibility of a *trans* effect, but could not detect any reproducible effect on *ZRT1* induction (data not shown). A recent study showed that transcription of the sense upstream ncRNA *ICR1* mediates transcriptional control of the subtelomeric *FLO11* gene [8]. We found that the region upstream from the *FLO11* gene encoding *ICR1* shows elevated RNA levels in the *upf1Δ* strain (Figure S6). Like *ICR1*, expression of the *ZRT1* CD-CUT is under the control of the histone deacetylase Rpd3p (Figure 4 and [8]). Based on these similarities, it is possible that the mechanisms of transcriptional control of the *FLO11* gene mediated by *ICR1* described in [8] may be applicable to the action of the CD-CUTs that control other subtelomeric regions.

The experiments in which we inserted transcription terminators upstream from *ZRT1* do not allow us to differentiate between the *cis* and *trans*-acting models for CD-CUTs. Insertion of the terminator at position B relieves repression and allows the *upf1Δ* strain to induce *ZRT1* in low zinc conditions (Figure 5). However in this strain, the CD-CUTs terminate before the Zap1 binding sites, so the results could be interpreted either way (transcriptional interference or *trans*-acting). Insertion of the terminator at position C relieves repression, but also inhibits *ZRT1* induction even when NMD is active (Figure 5). Thus, we cannot conclude whether the CD-CUTs act in *trans* or are only the product of transcription that generates transcriptional interference. Because NMD mutants show higher CD-CUTs levels without a higher level of RNA Polymerase in the CD-CUT transcribed region (Figure 5C) and also result in stronger repression, we favor the hypothesis that these RNAs act in *trans*. However, further work is required to fully prove this point. Another unanswered question is to understand how the transcriptional machinery overcomes CD-CUT mediated repression in conditions of induction. It is possible that CD-CUT transcription is decreased in these conditions, but neither northern analysis nor the ChIP data seem to indicate that this is the case. Another alternative is that activation of the transcriptional activators is so potent during induction that it can overcome CD-CUTs mediated repression, even if the level of transcription of CD-CUTs does not change. The results obtained with the Zap1p overexpression or the constitutive Aft1p allele strains (Figure 6) are consistent with this model.

How does a cytoplasmic degradation pathway influence nuclear transcription?

One of the paradoxes raised by our observations is that 5′-extended species of subtelomeric genes are degraded by NMD, which is a cytoplasmic degradation pathway (Figure 7), yet, these CD-CUTs mediate transcriptional repression, and must therefore be localized to the nucleus if they mediate repression. Interestingly, many subtelomeric genes exhibit a perinuclear localization in *S.cerevisiae* [48]. In addition, connections have been made between nuclear activation of genes and localization at the periphery of the nuclear envelope near the nuclear pores (reviewed in [49]). Finally, Upf1p has been shown to interact with two nucleoporins localized on the outer side of the nuclear envelope, Nup100p and Nup116p ([50]; Figure 7), suggesting that at least part of the NMD process might occur at the vicinity of the nuclear envelope (Figure 7). Therefore if both subtelomeric genes and NMD components are localized close to the nuclear envelope but on opposite sides of the nuclear pores, the physical distance between the sites of transcription and action of CD-CUTs, and their site of degradation might be closer than thought from just considering the nuclear/cytoplasmic distribution (Figure 7). This would possibly allow retrograde transport of these CD-CUTs from their site of degradation to their site of action, and would allow a regulation of transcription by ncRNAs primarily degraded in the cytoplasm (Figure 7). It is also possible that CD-CUTs might be

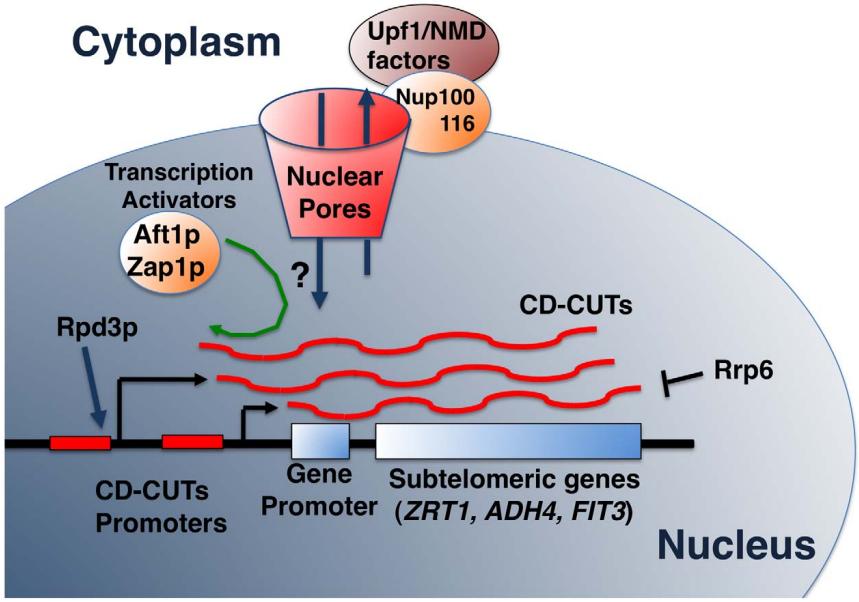


Figure 7. Model of biogenesis, action, and degradation of CD-CUTs. The model shows the degradation of CD-CUTs by the NMD pathway, potentially localized at the vicinity of the nuclear pore due to the anchoring by the Nup100/116 nucleoporins [50]. Hypothetical retrograde transport of CD-CUTs is shown by a question mark but would explain the increased repression of subtelomeric genes in the absence of cytoplasmic degradation in NMD mutants.
doi:10.1371/journal.pgen.1002163.g007

degraded when they emerge out of the nuclear pore complex, and that failure to degrade induces an increase of their nuclear localization, explaining a higher level of repression in NMD mutants. A better analysis of the mechanisms of nuclear/cytoplasmic trafficking of these CD-CUTs will ultimately allow a full understanding of their mechanisms of action.

Conserved functions for ncRNAs and NMD in the control of the expression of metal homeostasis genes

Despite these unanswered questions, our results have uncovered a novel function for NMD in controlling the accumulation of transcripts that negatively interfere with transcription of genes involved in zinc and iron homeostasis. Previous work has shown that upstream ncRNAs are involved in controlling gene expression related to metals homeostasis. It was shown that Zap1p activates the transcription of ncRNAs which mediate the repression of zinc-dependent alcohol dehydrogenases by transcriptional interference during zinc deficiency [51]. However it is unclear whether or not these ncRNAs are targeted by NMD, in a manner similar to CD-CUTs that regulate *ZRT1*, *ADH4* and *FIT3*. A potential transcriptional interference mechanism involving long unstable upstream sense ncRNA has also been described in *Chlamydomonas* during copper deficiency [52], suggesting that this mechanism has been conserved during evolution to contribute generally to metal homeostasis genes regulation. Thus, there seems to be prevalent use of ncRNA transcription to control gene expression during metals homeostasis in different organisms. In addition to the potential crosstalk with transcription described here, NMD was also recently shown to regulate Mg^{++} cellular levels [23] by degrading the transcript encoding the main Mg^{++} transporter. The fact that this RNA surveillance system is so intimately implicated in the regulation of metals homeostasis in general might be linked to the prevalence of these metals in the ribosome and in their function of translation and in its fidelity [23], possibly revealing another layer of co-evolution between NMD and translation.

Materials and Methods

Yeast strains and media

Most strains were derived from BY4741 or 4742 (Open Biosystems). Strains in which the *GFP-HIS* cassette in the upstream region of *ZRT1* or *ADH4* gene were obtained by homologous recombination [36]. The strain carrying the deletion of the region upstream *FIT3* and the strains containing the terminator insertions were obtained by *delitto perfetto* [53]. Double mutants in which the *UPF1* or *XRN1* genes were knocked out were obtained by direct disruption of these genes in other mutant strains, as described [21]. Insertion of the myc-tag for Zap1p was performed as described [36].

Strains were grown in conditions of non-induction in either YPD or Synthetic Complete medium (SC) supplemented with 2 mM $ZnCl_2$. Growth in condition of low zinc gene induction was performed in either a Chelex-treated synthetic complete medium (CSC) or a SC medium containing 1 mM EDTA, pH adjusted to

4.4 with 20 mM citrate. CSC was prepared as described [28] except that all amino acid required were added and pH adjusted to 4.4. Growth in conditions of low iron gene induction was performed by adding BPS chelator as described [31]. Strains were grown in YPD (pre-low iron shifts) or SC+2 mM Zn (pre-low zinc shifts) until $OD_{600} = 0.5$, washed twice in sterile water, and shifted into YPD medium with BPS (low iron shift) or SC+EDTA medium (low zinc shift) for the indicated times. For the experiments including overexpression of Zap1p, WT or *upf1Δ* strains containing the vector pUG35 or pIT31 (see below) were grown in SC medium without Uracil (SC-URA) supplemented with 2 mM Zn. At $OD_{600} = 0.45$, cells were washed twice in sterile water and shifted in SC-URA without methionine (SC-URA-MET) supplemented with 2 mM Zn for 2 hours to overexpress Zap1p prior to zinc starvation. After 2 h, cells were washed twice in sterile water and maintained in log phase in SC-URA-MET medium containing 1 mM EDTA. Kinetics of induction were performed as described above.

Plasmids

A PCR product corresponding to the *ZAP1* gene was generated from genomic DNA with primers containing the restriction sites *ClaI* and *SalI* and inserted in the vector pUG35 digested by the same restriction enzymes. After transformation and amplification in *E. coli*, the plasmid (pIT31) was confirmed by sequencing. The *aft1-up* expression plasmid was obtained from J.Kaplan (U.of Utah).

RNA analysis

Tiling Arrays used in this study were described previously [21,31] and are accessible in the GEO database (accession number GSE11621). Northern blot hybridization analysis was performed as previously described [21,31]. All riboprobes were synthesized with the T3 MAXIscript kit (Ambion). Riboprobes were hybridized at 67°C except for the *ADH4* ORF probe (65°C).

Chromatin Immunoprecipitation (ChIP)

ChIPs using anti-Rpb3 RNA polymerase II subunit and a myc-tagged version of Zap1p inserted at the chromosomal locus were performed as described [54,55].

Supporting Information

Figure S1 Tiling array profiles of *ZPS1* and *FLO11*. A. Tiling array profile in the region of the *ZPS1* gene. Shown is the $\log_2$ ratio of signal detected for the *upf1Δ* strain divided by the signal for the wild-type strain. B. Tiling Array profile of the *upf1Δ* mutant compared to the wild-type strain in the right subtelomeric region of Chr IX containing the *FLO11* gene. The *FLO11* gene is localized on the Crick strand (transcribed right to left) from positions 393,672 to 389,569. The increase of signal in the *upf1Δ* mutant upstream from the *FLO11* gene is indicative of higher levels of the *ICR1* ncRNA controlling *FLO11*. Note that the neighbor genes *MRS1* and *SEC11* located in region 397,000–399,000 are not affected by the *upf1Δ* deletion.
(TIF)

Figure S2 Mapping of the CD-CUTs of *ZRT1* (A) and *ADH4* (B) genes by northern blot analysis. The *ZRT1* probes cover the following nucleotides: Probe 1: −2410 to −2089; Probe 2: −800 to −211; Probe 3: −257 to −84; Probe 4: +931 to +1131; Probe 5: +1141 to +1341 (downstream from the ORF).
(TIF)

Figure S3 Analysis of zinc regulon genes induction in NMD mutants. A. Kinetics of induction of zinc regulon genes in wild-type, *upf2Δ* and *upf3Δ* strains after a shift to a medium lacking zinc. Gene induction was monitored by northern blot using probes hybridizing to the corresponding genes. *SCR1* was used as a loading control. B. Analysis of *ZAP1* mRNAs levels in wild-type and *upf1Δ* strains. *ZAP1* mRNA levels were analyzed by northern blot from cells grown in SC+2 mM Zn (time zero), or after a shift to SC+EDTA (low Zn). An RNA sample from a *zap1Δ* strain was included as a negative control for the detection of the ZAP1 mRNA.
(TIF)

Figure S4 Kinetics of *FIT3* induction in strains lacking Xrn1p, Upf1p or in the double mutant *xrn1Δrat1-1*. Shown is a northern blot analysis of *FIT3* expression in the indicated strains using a probe complementary to *FIT3*.
(TIF)

Figure S5 Insertion of GFP cassettes upstream from *ZRT1* and *ADH4*. A. Schematic representation of the *ZRT1* and *ADH4* genes and location of the *GFP-HIS3* cassettes deletions/insertions (UP1 and UP2, UP). The dashed lines represent the regions replaced by the cassettes. B. GFP mRNA levels analyzed by northern blot in the different insertion strains. Levels were normalized to *SCR1*. A strain without GFP insertion was included as negative control. C. Effects of the deletion of the upstream region and of the insertion of a *GFP-HIS3* cassette on the kinetics of induction and shutoff of *ZRT1*. Insertion of the *GFP-HIS3* cassette upstream from *ZRT1* (*zrt1-up1*) results in a three-fold increase in the *ZRT1* mRNA peak in the *upf1Δ* strain during zinc deficiency. *ZRT1* induction was faster in the strain carrying this insertion compared to the wild-type, as shown by the amount of the *ZRT1* mRNA expressed after 30 to 120 minutes. After 4 hours of induction, the kinetics of disappearance of *ZRT1* upon shifting back to zinc-containing medium was also monitored in these strains (+zinc), and samples were harvested at the indicated times after addition of zinc to the medium. RNAs extracted from all four strains were loaded on the same gel and analyzed on the same membranes exposed to the same times, but each strain is shown as a separate panel for clarity and space purposes.
(TIF)

Figure S6 Kinetics of *ZRT1* induction in wild-type, *hda2Δ hda3Δ*, *upf1Δ*, *hda2Δupf1Δ* and *hda3Δupf1Δ* strains.
(TIF)

Table S1 List of *S.cerevisiae* ORFs for which 5′ extended species were observed by tiling microarrays in the *upf1Δ* and/or *xrn1Δ*strains.
(XLS)

Acknowledgments

We thank Cynthia Lee, Sabeeha Merchant, Michael Grunstein, and Siavash Kurdistani for helpful discussions; F. Holstege and S. Kurdistani for yeast strains; J.Kaplan for the *aft1-up* plasmid; Kevin Roy for critical reading of the manuscript; and one anonymous reviewer of a grant proposal for helpful suggestions.

Author Contributions

Conceived and designed the experiments: IT CRN GFC. Performed the experiments: IT CRN CFF SS. Analyzed the data: IT CRN CFF SS GFC. Wrote the paper: GFC.

References

1. Jacquier A (2009) The complex eukaryotic transcriptome: unexpected pervasive transcription and novel small RNAs. Nat Rev Genet 10: 833–844.
2. Neil H, Malabat C, d'Aubenton-Carafa Y, Xu Z, Steinmetz LM, et al. (2009) Widespread bidirectional promoters are the major source of cryptic transcripts in yeast. Nature 457: 1038–1042.
3. Martens JA, Laprade L, Winston F (2004) Intergenic transcription is required to repress the Saccharomyces cerevisiae SER3 gene. Nature 429: 571–574.
4. Camblong J, Iglesias N, Fickentscher C, Dieppois G, Stutz F (2007) Antisense RNA stabilization induces transcriptional gene silencing via histone deacetylation in S. cerevisiae. Cell 131: 706–717.
5. Berretta J, Pinskaya M, Morillon A (2008) A cryptic unstable transcript mediates transcriptional trans-silencing of the Ty1 retrotransposon in S. cerevisiae. Genes Dev 22: 615–626.
6. Houseley J, Rubbi L, Grunstein M, Tollervey D, Vogelauer M (2008) A ncRNA modulates histone modification and mRNA induction in the yeast GAL gene cluster. Mol Cell 32: 685–695.
7. Camblong J, Beyrouthy N, Guffanti E, Schlaepfer G, Steinmetz LM, et al. (2009) Trans-acting antisense RNAs mediate transcriptional gene cosuppression in S. cerevisiae. Genes Dev 23: 1534–1545.
8. Bumgarner SL, Dowell RD, Grisafi P, Gifford DK, Fink GR (2009) Toggle involving cis-interfering noncoding RNAs controls variegated gene expression in yeast. Proc Natl Acad Sci U S A 106: 18321–18326.
9. Xu Z, Wei W, Gagneur J, Perocchi F, Clauder-Munster S, et al. (2009) Bidirectional promoters generate pervasive transcription in yeast. Nature 457: 1033–1037.
10. Kim TK, Hemberg M, Gray JM, Costa AM, Bear DM, et al. (2010) Widespread transcription at neuronal activity-regulated enhancers. Nature 465: 182–187.
11. Wyers F, Rougemaille M, Badis G, Rousselle JC, Dufour ME, et al. (2005) Cryptic pol II transcripts are degraded by a nuclear quality control pathway involving a new poly(A) polymerase. Cell 121: 725–737.
12. Lee A, Hansen KD, Bullard J, Dudoit S, Sherlock G (2008) Novel low abundance and transient RNAs in yeast revealed by tiling microarrays and ultra high-throughput sequencing are not conserved across closely related yeast species. PLoS Genet 4: e1000299. doi:10.1371/journal.pgen.1000299.
13. Thompson DM, Parker R (2007) Cytoplasmic decay of intergenic transcripts in Saccharomyces cerevisiae. Mol Cell Biol 27: 92–101.
14. Chang YF, Imam JS, Wilkinson MF (2007) The Nonsense-Mediated Decay RNA Surveillance Pathway. Annu Rev Biochem 76: 51–74.
15. Isken O, Maquat LE (2007) Quality control of eukaryotic mRNA: safeguarding cells from abnormal mRNA function. Genes Dev 21: 1833–1856.
16. Frischmeyer PA, Dietz HC (1999) Nonsense-mediated mRNA decay in health and disease. Hum Mol Genet 8: 1893–1900.
17. Kuzmiak HA, Maquat LE (2006) Applying nonsense-mediated mRNA decay research to the clinic: progress and challenges. Trends Mol Med 12: 306–316.
18. Mitrovich QM, Anderson P (2000) Unproductively spliced ribosomal protein mRNAs are natural targets of mRNA surveillance in C. elegans. Genes Dev 14: 2173–2184.
19. Lareau LF, Inada M, Green RE, Wengrod JC, Brenner SE (2007) Unproductive splicing of SR genes associated with highly conserved and ultraconserved DNA elements. Nature 446: 926–929.
20. Ni JZ, Grate L, Donohue JP, Preston C, Nobida N, et al. (2007) Ultraconserved elements are associated with homeostatic control of splicing regulators by alternative splicing and nonsense-mediated decay. Genes Dev 21: 708–718.
21. Sayani S, Janis M, Lee CY, Toesca I, Chanfreau GF (2008) Widespread impact of nonsense-mediated mRNA decay on the yeast intronome. Mol Cell 31: 360–370.
22. Kebaara BW, Atkin AL (2009) Long 3′-UTRs target wild-type mRNAs for nonsense-mediated mRNA decay in Saccharomyces cerevisiae. Nucleic Acids Res 37: 2771–2778.
23. Johansson MJ, Jacobson A (2010) Nonsense-mediated mRNA decay maintains translational fidelity by limiting magnesium uptake. Genes Dev 24: 1491–1495.
24. Lelivelt MJ, Culbertson MR (1999) Yeast Upf proteins required for RNA surveillance affect global expression of the yeast transcriptome. Mol Cell Biol 19: 6710–6719.
25. He F, Li X, Spatrick P, Casillo R, Dong S, et al. (2003) Genome-wide analysis of mRNAs regulated by the nonsense-mediated and 5′ to 3′ mRNA decay pathways in yeast. Mol Cell 12: 1439–1452.
26. Guan Q, Zheng W, Tang S, Liu X, Zinkel RA, et al. (2006) Impact of nonsense-mediated mRNA decay on the global expression profile of budding yeast. PLoS Genet 2: e203. doi:10.1371/journal.pgen.0020203.
27. Johansson MJ, He F, Spatrick P, Li C, Jacobson A (2007) Association of yeast Upf1p with direct substrates of the NMD pathway. Proc Natl Acad Sci U S A 104: 20872–20877.
28. Lyons TJ, Gasch AP, Gaither LA, Botstein D, Brown PO, et al. (2000) Genome-wide characterization of the Zap1p zinc-responsive regulon in yeast. Proc Natl Acad Sci U S A 97: 7957–7962.
29. Protchenko O, Ferea T, Rashford J, Tiedeman J, Brown PO, et al. (2001) Three cell wall mannoproteins facilitate the uptake of iron in Saccharomyces cerevisiae. J Biol Chem 276: 49244–49250.
30. Robyr D, Suka Y, Xenarios I, Kurdistani SK, Wang A, et al. (2002) Microarray deacetylation maps determine genome-wide functions for yeast histone deacetylases. Cell 109: 437–446.
31. Lee A, Henras AK, Chanfreau G (2005) Multiple RNA surveillance pathways limit aberrant expression of iron uptake mRNAs and prevent iron toxicity in S. cerevisiae. Mol Cell 19: 39–51.
32. Martianov I, Ramadass A, Serra Barros A, Chow N, Akoulitchev A (2007) Repression of the human dihydrofolate reductase gene by a non-coding interfering transcript. Nature 445: 666–670.
33. Wang X, Arai S, Song X, Reichart D, Du K, et al. (2008) Induced ncRNAs allosterically modify RNA-binding proteins in cis to inhibit transcription. Nature.
34. Zhao H, Eide D (1996) The ZRT2 gene encodes the low affinity zinc transporter in Saccharomyces cerevisiae. J Biol Chem 271: 23203–23210.
35. Taylor R, Kebaara BW, Nazarenus T, Jones A, Yamanaka R, et al. (2005) Gene set coregulated by the Saccharomyces cerevisiae nonsense-mediated mRNA decay pathway. Eukaryot Cell 4: 2066–2077.
36. Longtine MS, McKenzie A, 3rd, Demarini DJ, Shah NG, Wach A, et al. (1998) Additional modules for versatile and economical PCR-based gene deletion and modification in Saccharomyces cerevisiae. Yeast 14: 953–961.
37. Bernstein BE, Tong JK, Schreiber SL (2000) Genomewide studies of histone deacetylase function in yeast. Proc Natl Acad Sci U S A 97: 13708–13713.
38. Zhao H, Butler E, Rodgers J, Spizzo T, Duesterhoeft S, et al. (1998) Regulation of zinc homeostasis in yeast by binding of the ZAP1 transcriptional activator to zinc-responsive promoter elements. J Biol Chem 273: 28713–28720.
39. Yamaguchi-Iwai Y, Dancis A, Klausner RD (1995) AFT1: a mediator of iron regulated transcriptional control in Saccharomyces cerevisiae. EMBO J 14: 1231–1239.
40. Philpott CC, Rashford J, Yamaguchi-Iwai Y, Rouault TA, Dancis A, et al. (1998) Cell-cycle arrest and inhibition of G1 cyclin translation by iron in AFT1-1(up) yeast. EMBO J 17: 5026–5036.
41. van de Peppel J, Kettelarij N, van Bakel H, Kockelkorn TT, van Leenen D, et al. (2005) Mediator expression profiling epistasis reveals a signal transduction pathway with antagonistic submodules and highly specific downstream targets. Mol Cell 19: 511–522.
42. Bertone P, Stolc V, Royce TE, Rozowsky JS, Urban AE, et al. (2004) Global identification of human transcribed sequences with genome tiling arrays. Science 306: 2242–2246.
43. Kapranov P, Cheng J, Dike S, Nix DA, Duttagupta R, et al. (2007) RNA maps reveal new RNA classes and a possible function for pervasive transcription. Science 316: 1484–1488.
44. Nagalakshmi U, Wang Z, Waern K, Shou C, Raha D, et al. (2008) The transcriptional landscape of the yeast genome defined by RNA sequencing. Science 320: 1344–1349.
45. Amrani N, Dong S, He F, Ganesan R, Ghosh S, et al. (2006) Aberrant termination triggers nonsense-mediated mRNA decay. Biochem Soc Trans 34: 39–42.
46. Davis CA, Ares M, Jr. (2006) Accumulation of unstable promoter-associated transcripts upon loss of the nuclear exosome subunit Rrp6p in Saccharomyces cerevisiae. Proc Natl Acad Sci U S A 103: 3262–3267.
47. Chekanova JA, Gregory BD, Reverdatto SV, Chen H, Kumar R, et al. (2007) Genome-wide high-resolution mapping of exosome substrates reveals hidden features in the Arabidopsis transcriptome. Cell 131: 1340–1353.
48. Grund SE, Fischer T, Cabal GG, Antunez O, Perez-Ortin JE, et al. (2008) The inner nuclear membrane protein Src1 associates with subtelomeric genes and alters their regulated gene expression. J Cell Biol 182: 897–910.
49. Dieppois G, Stutz F (2010) Connecting the transcription site to the nuclear pore: a multi-tether process that regulates gene expression. J Cell Sci 123: 1989–1999.
50. Nazarenus T, Cedarberg R, Bell R, Cheatle J, Forch A, et al. (2005) Upf1p, a highly conserved protein required for nonsense-mediated mRNA decay, interacts with the nuclear pore proteins Nup100p and Nup116p. Gene 345: 199–212.
51. Bird AJ, Gordon M, Eide DJ, Winge DR (2006) Repression of ADH1 and ADH3 during zinc deficiency by Zap1-induced intergenic RNA transcripts. EMBO J 25: 5726–5734.
52. Moseley JL, Page MD, Alder NP, Eriksson M, Quinn J, et al. (2002) Reciprocal expression of two candidate di-iron enzymes affecting photosystem I and light-harvesting complex accumulation. Plant Cell 14: 673–688.
53. Storici F, Lewis LK, Resnick MA (2001) In vivo site-directed mutagenesis using oligonucleotides. Nat Biotechnol 19: 773–776.
54. Yang PK, Hoareau C, Froment C, Monsarrat B, Henry Y, et al. (2005) Cotranscriptional recruitment of the pseudouridylsynthetase Cbf5p and of the RNA binding protein Naf1p during H/ACA snoRNP assembly. Mol Cell Biol 25: 3295–3304.
55. Steinmetz EJ, Warren CL, Kuehner JN, Panbehi B, Ansari AZ, et al. (2006) Genome-wide distribution of yeast RNA polymerase II and its control by Sen1 helicase. Mol Cell 24: 735–746.

Supplemental Information

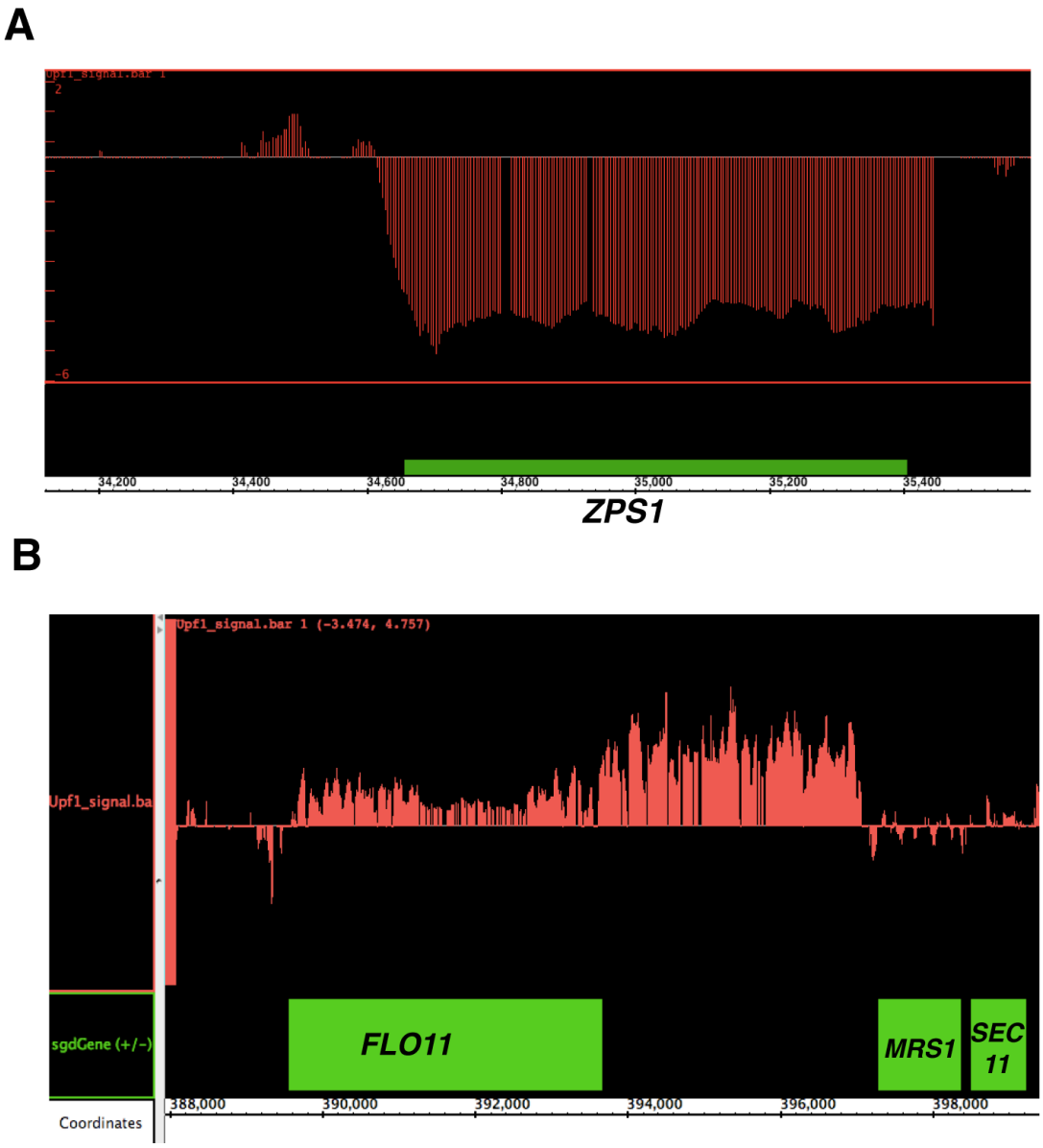


Figure S1. Tiling array profiles of *ZPS1* and *FLO11*. A. Tiling array profile in the region of the *ZPS1* gene. Shown is the $\log_2$ ratio of signal detected for the *upf1Δ* strain divided by the signal for the wild-type strain. B. Tiling Array profile of the *upf1Δ* mutant compared to the wild-type strain in the right subtelomeric region of Chr IX containing the *FLO11* gene. The *FLO11* gene is localized on the Crick strand (transcribed right to left) from positions 393,672 to 389,569. The increase of signal in the *upf1Δ* mutant upstream from the *FLO11* gene is indicative of higher levels of the *ICR1* ncRNA controlling *FLO11*. Note that the neighbor genes *MRS1* and *SEC11* located in region 397,000–399,000 are not affected by the *upf1Δ* deletion.

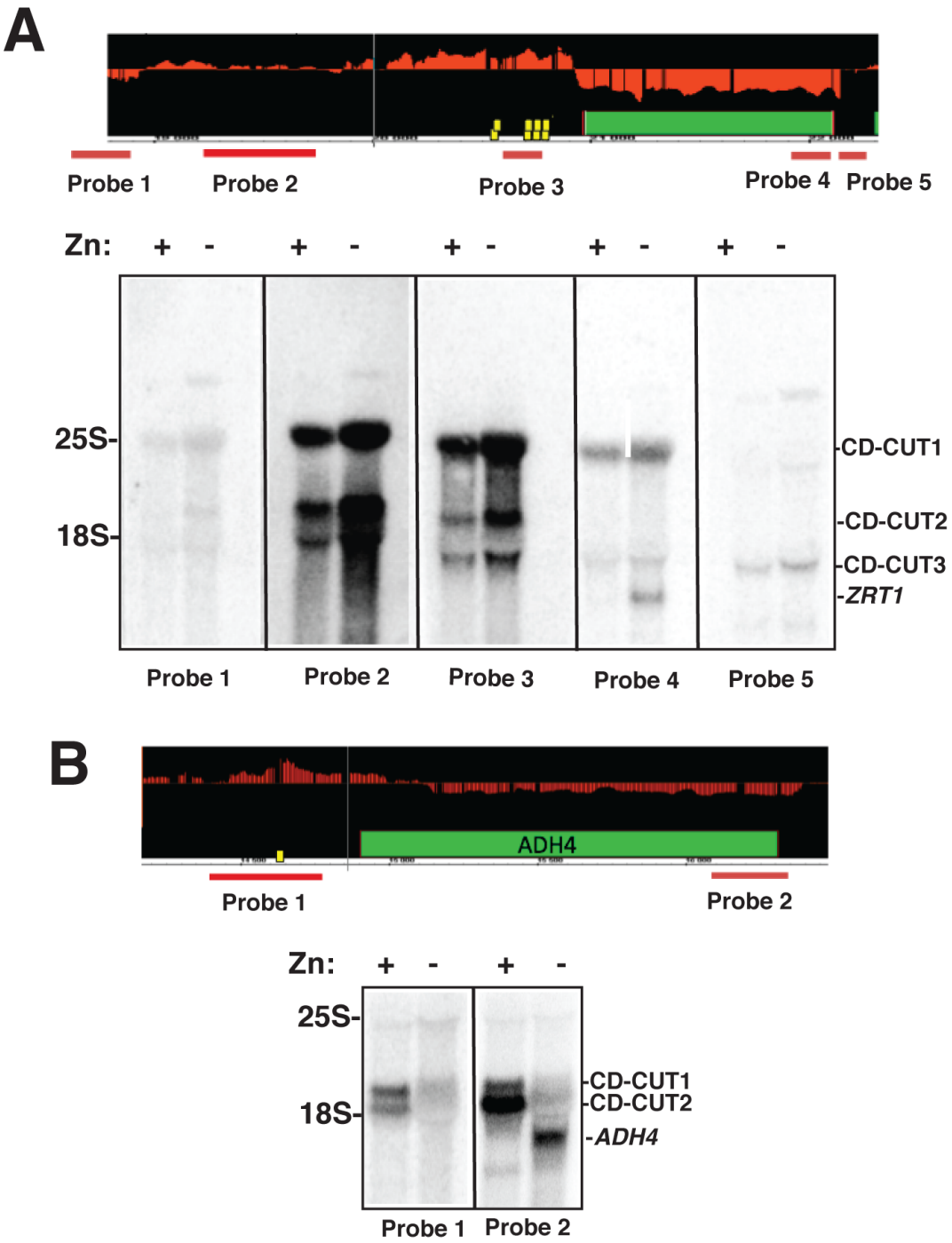


Figure S2. Mapping of the CD-CUTs of ZRT1 (A) and ADH4 (B) genes by northern blot analysis. The ZRT1 probes cover the following nucleotides: Probe 1: −2410 to −2089; Probe 2: −800 to −211; Probe 3: −257 to −84; Probe 4: +931 to +1131; Probe 5: +1141 to +1341 (downstream from the ORF).

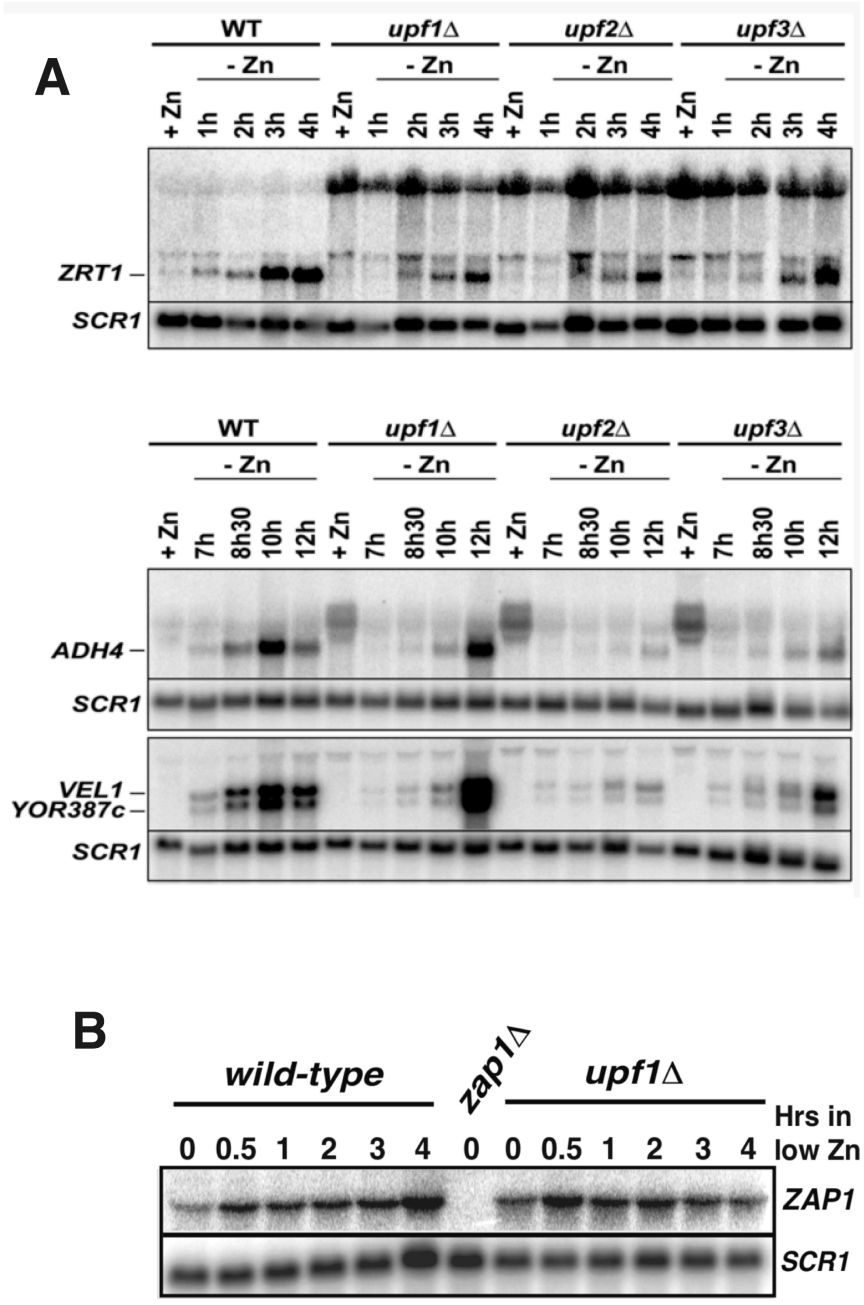


Figure S3. Analysis of zinc regulon genes induction in NMD mutants. A. Kinetics of induction of zinc regulon genes in wild-type, upf2Δ and upf3Δ strains after a shift to a medium lacking zinc. Gene induction was monitored by northern blot using probes hybridizing to the corresponding genes. SCR1 was used as a loading control. B. Analysis of ZAP1 mRNAs levels in wild-type and upf1Δ strains. ZAP1 mRNA levels were analyzed by northern blot from cells grown in SC+2 mM Zn (time zero), or after a shift to SC+EDTA (low Zn). An RNA sample from a zap1Δ strain was included as a negative control for the detection of the ZAP1 mRNA.

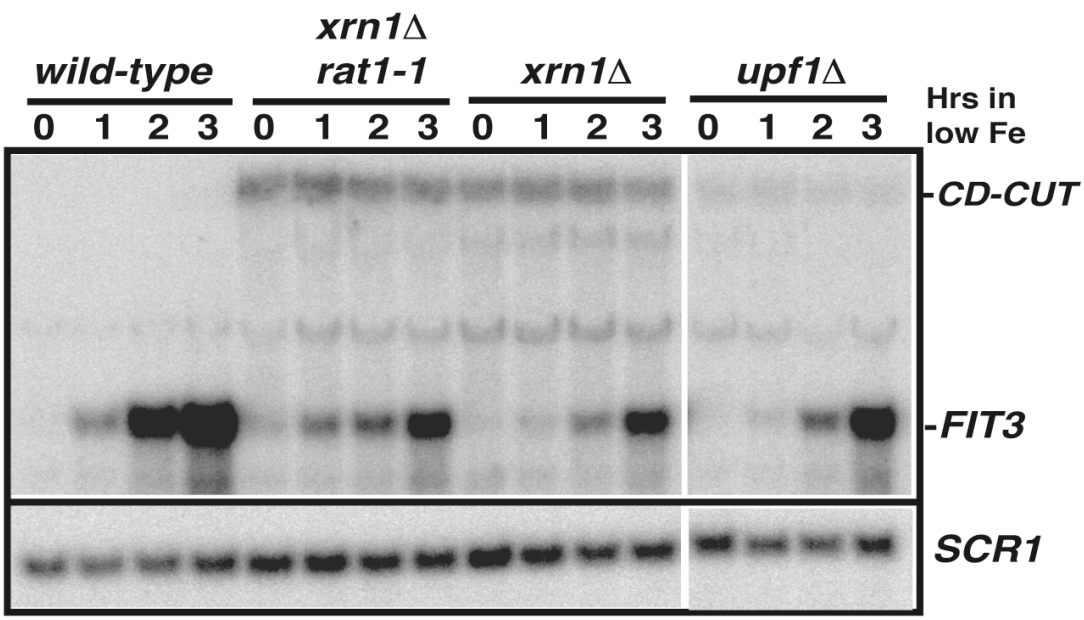


Figure S4. Kinetics of FIT3 induction in strains lacking Xrn1p, Upf1p or in the double mutant xrn1Δrat1-1. Shown is a northern blot analysis of FIT3 expression in the indicated strains using a probe complementary to FIT3.

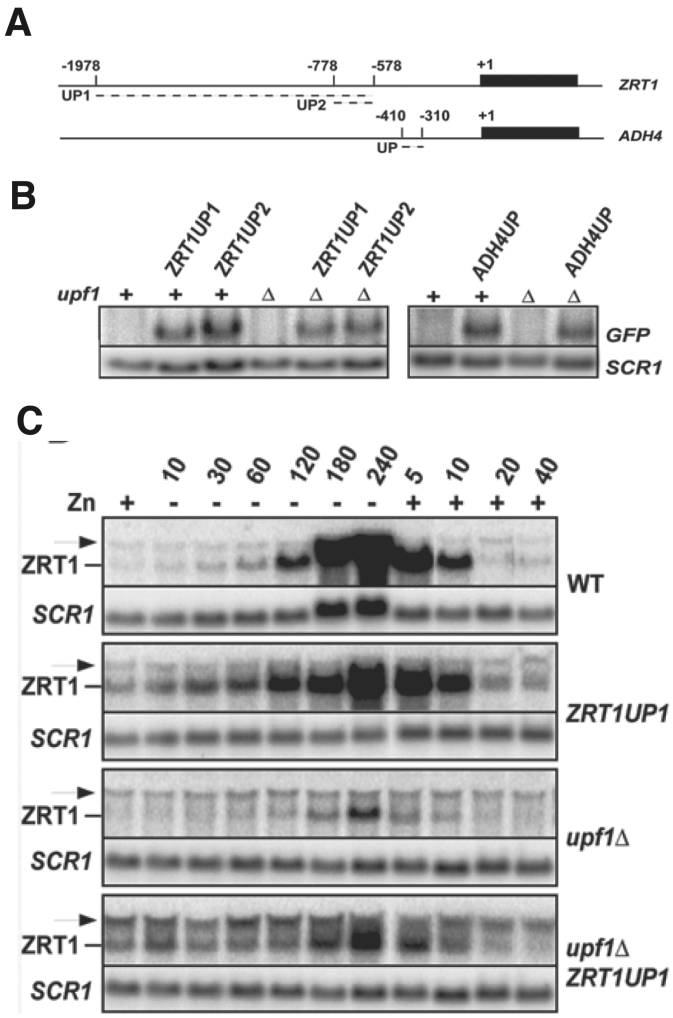


Figure S5. Insertion of GFP cassettes upstream from ZRT1 and ADH4. A. Schematic representation of the ZRT1 and ADH4 genes and location of the GFP-HIS3 cassettes deletions/insertions (UP1 and UP2, UP). The dashed lines represent the regions replaced by the cassettes. B. GFP mRNA levels analyzed by northern blot in the different insertion strains. Levels were normalized to SCR1. A strain without GFP insertion was included as negative control. C. Effects of the deletion of the upstream region and of the insertion of a GFP-HIS3 cassette on the kinetics of induction and shutoff of ZRT1. Insertion of the GFP-HIS3 cassette upstream from ZRT1 (zrt1-up1) results in a three-fold increase in the ZRT1 mRNA peak in the upf1Δ strain during zinc deficiency. ZRT1 induction was faster in the strain carrying this insertion compared to the wild-type, as shown by the amount of the ZRT1 mRNA expressed after 30 to 120 minutes. After 4 hours of induction, the kinetics of disappearance of ZRT1 upon shifting back to zinc-containing medium was also monitored in these strains (+zinc), and samples were harvested at the indicated times after addition of zinc to the medium. RNAs extracted from all four strains were loaded on the same gel and analyzed on the same membranes exposed to the same times, but each strain is shown as a separate panel for clarity and space purposes.

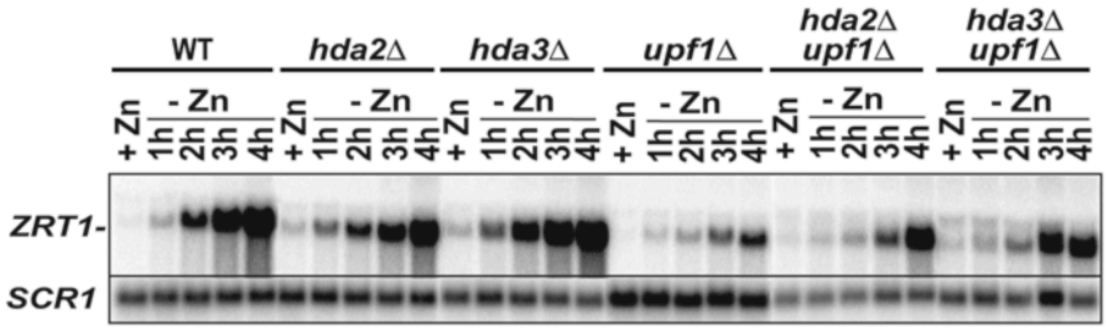


Figure S6. Kinetics of ZRT1 induction in wild-type, hda2Δ hda3Δ, upf1Δ, hda2Δupf1Δ and hda3Δupf1Δ strains.

Table S1. List of S.cerevisiae ORFs for which 5′ extended species were observed by tiling microarrays in the upf1 Δ and/or xrn1 Δ strains.
doi:10.1371/journal.pgen.1002163.s007
(XLS)

References

Anderson, J.S., and Parker, R.P. (1998). The 3' to 5' degradation of yeast mRNAs is a general mechanism for mRNA turnover that requires the SKI2 DEVH box protein and 3' to 5' exonucleases of the exosome complex. The EMBO journal *17*, 1497-1506.

Askwith, C., Eide, D., Van Ho, A., Bernard, P.S., Li, L., Davis-Kaplan, S., Sipe, D.M., and Kaplan, J. (1994). The FET3 gene of S. cerevisiae encodes a multicopper oxidase required for ferrous iron uptake. Cell *76*, 403-410.

Balci, K., Utku, U., Asil, T., and Buyukkoyuncu, N. (2007). Deep cerebral vein thrombosis associated with iron deficiency anaemia in adults. Journal of clinical neuroscience : official journal of the Neurosurgical Society of Australasia *14*, 181-184.

Bird, A., Evans-Galea, M.V., Blankman, E., Zhao, H., Luo, H., Winge, D.R., and Eide, D.J. (2000a). Mapping the DNA binding domain of the Zap1 zinc-responsive transcriptional activator. The Journal of biological chemistry *275*, 16160-16166.

Bird, A.J., Zhao, H., Luo, H., Jensen, L.T., Srinivasan, C., Evans-Galea, M., Winge, D.R., and Eide, D.J. (2000b). A dual role for zinc fingers in both DNA binding and zinc sensing by the Zap1 transcriptional activator. The EMBO journal *19*, 3704-3713.

Blaiseau, P.L., Lesuisse, E., and Camadro, J.M. (2001). Aft2p, a novel iron-regulated transcription activator that modulates, with Aft1p, intracellular iron use and resistance to oxidative stress in yeast. The Journal of biological chemistry *276*, 34221-34226.

Camblong, J., Iglesias, N., Fickentscher, C., Dieppois, G., and Stutz, F. (2007). Antisense RNA stabilization induces transcriptional gene silencing via histone deacetylation in S. cerevisiae. Cell *131*, 706-717.

Carneiro, T., Carvalho, C., Braga, J., Rino, J., Milligan, L., Tollervey, D., and Carmo-Fonseca, M. (2007). Depletion of the yeast nuclear exosome subunit Rrp6 results in accumulation of polyadenylated RNAs in a discrete domain within the nucleolus. Molecular and cellular biology *27*, 4157-4165.

Chang, Y.F., Imam, J.S., and Wilkinson, M.F. (2007). The nonsense-mediated decay RNA surveillance pathway. Annual review of biochemistry *76*, 51-74.

Daugeron, M.C., Mauxion, F., and Seraphin, B. (2001). The yeast POP2 gene encodes a nuclease involved in mRNA deadenylation. Nucleic acids research *29*, 2448-2455.

Davis, C.A., and Ares, M., Jr. (2006). Accumulation of unstable promoter-associated transcripts upon loss of the nuclear exosome subunit Rrp6p in Saccharomyces cerevisiae. Proceedings of the National Academy of Sciences of the United States of America *103*, 3262-3267.

Dix, D., Bridgham, J., Broderius, M., and Eide, D. (1997). Characterization of the FET4 protein of yeast. Evidence for a direct role in the transport of iron. The Journal of biological chemistry *272*, 11770-11777.

Dix, D.R., Bridgham, J.T., Broderius, M.A., Byersdorfer, C.A., and Eide, D.J. (1994). The FET4 gene encodes the low affinity Fe(II) transport protein of Saccharomyces cerevisiae. The Journal of biological chemistry *269*, 26092-26099.

Doma, M.K., and Parker, R. (2006). Endonucleolytic cleavage of eukaryotic mRNAs with stalls in translation elongation. Nature *440*, 561-564.

Eide, D., Davis-Kaplan, S., Jordan, I., Sipe, D., and Kaplan, J. (1992). Regulation of iron uptake in Saccharomyces cerevisiae. The ferrireductase and Fe(II) transporter are regulated independently. The Journal of biological chemistry *267*, 20774-20781.

Frey, A.G., Bird, A.J., Evans-Galea, M.V., Blankman, E., Winge, D.R., and Eide, D.J. (2011). Zinc-regulated DNA binding of the yeast Zap1 zinc-responsive activator. PloS one *6*, e22535.

Frischmeyer, P.A., van Hoof, A., O'Donnell, K., Guerrerio, A.L., Parker, R., and Dietz, H.C. (2002). An mRNA surveillance mechanism that eliminates transcripts lacking termination codons. Science (New York, NY) *295*, 2258-2261.

Georgatsou, E., and Alexandraki, D. (1994). Two distinctly regulated genes are required for ferric reduction, the first step of iron uptake in Saccharomyces cerevisiae. Molecular and cellular biology *14*, 3065-3073.

Hassett, R., Dix, D.R., Eide, D.J., and Kosman, D.J. (2000). The Fe(II) permease Fet4p functions as a low affinity copper transporter and supports normal copper trafficking in Saccharomyces cerevisiae. The Biochemical journal *351 Pt 2*, 477-484.

Heymann, P., Ernst, J.F., and Winkelmann, G. (2000). Identification and substrate specificity of a ferrichrome-type siderophore transporter (Arn1p) in Saccharomyces cerevisiae. FEMS microbiology letters *186*, 221-227.

Hongay, C.F., Grisafi, P.L., Galitski, T., and Fink, G.R. (2006). Antisense transcription controls cell fate in Saccharomyces cerevisiae. Cell *127*, 735-745.

Houseley, J., and Tollervey, D. (2009). The many pathways of RNA degradation. Cell *136*, 763-776.

Hsu, C.L., and Stevens, A. (1993). Yeast cells lacking 5'-->3' exoribonuclease 1 contain mRNA species that are poly(A) deficient and partially lack the 5' cap structure. Molecular and cellular biology *13*, 4826-4835.

Jacquier, A. (2009). The complex eukaryotic transcriptome: unexpected pervasive transcription and novel small RNAs. Nature reviews Genetics *10*, 833-844.

Johnson, A.W. (1997). Rat1p and Xrn1p are functionally interchangeable exoribonucleases that are restricted to and required in the nucleus and cytoplasm, respectively. Molecular and cellular biology *17*, 6122-6130.

Kamizono, A., Nishizawa, M., Teranishi, Y., Murata, K., and Kimura, A. (1989). Identification of a gene conferring resistance to zinc and cadmium ions in the yeast Saccharomyces cerevisiae. Molecular & general genetics : MGG *219*, 161-167.

Kornienko, A.E., Guenzl, P.M., Barlow, D.P., and Pauler, F.M. (2013). Gene regulation by the act of long non-coding RNA transcription. BMC biology *11*, 59.

Lee, A., Henras, A.K., and Chanfreau, G. (2005). Multiple RNA surveillance pathways limit aberrant expression of iron uptake mRNAs and prevent iron toxicity in S. cerevisiae. Molecular cell *19*, 39-51.

Lee, W., Tillo, D., Bray, N., Morse, R.H., Davis, R.W., Hughes, T.R., and Nislow, C. (2007). A high-resolution atlas of nucleosome occupancy in yeast. Nature genetics *39*, 1235-1244.

Leeds, P., Peltz, S.W., Jacobson, A., and Culbertson, M.R. (1991). The product of the yeast UPF1 gene is required for rapid turnover of mRNAs containing a premature translational termination codon. Genes & development *5*, 2303-2314.

Leeds, P., Wood, J.M., Lee, B.S., and Culbertson, M.R. (1992). Gene products that promote mRNA turnover in Saccharomyces cerevisiae. Molecular and cellular biology *12*, 2165-2177.

MacDiarmid, C.W., Gaither, L.A., and Eide, D. (2000). Zinc transporters that regulate vacuolar zinc storage in Saccharomyces cerevisiae. The EMBO journal *19*, 2845-2855.

Marquardt, S., Hazelbaker, D.Z., and Buratowski, S. (2011). Distinct RNA degradation pathways and 3' extensions of yeast non-coding RNA species. Transcription *2*, 145-154.

Martens, J.A., Laprade, L., and Winston, F. (2004). Intergenic transcription is required to repress the Saccharomyces cerevisiae SER3 gene. Nature *429*, 571-574.

Neil, H., Malabat, C., d'Aubenton-Carafa, Y., Xu, Z., Steinmetz, L.M., and Jacquier, A. (2009). Widespread bidirectional promoters are the major source of cryptic transcripts in yeast. Nature *457*, 1038-1042.

Parker, R. (2012). RNA degradation in Saccharomyces cerevisae. Genetics *191*, 671-702.

Passos, D.O., Doma, M.K., Shoemaker, C.J., Muhlrad, D., Green, R., Weissman, J., Hollien, J., and Parker, R. (2009). Analysis of Dom34 and its function in no-go decay. Molecular biology of the cell *20*, 3025-3032.

Peltz, S.W., Brown, A.H., and Jacobson, A. (1993). mRNA destabilization triggered by premature translational termination depends on at least three cis-acting sequence elements and one trans-acting factor. Genes & development *7*, 1737-1754.

Peltz, S.W., He, F., Welch, E., and Jacobson, A. (1994). Nonsense-mediated mRNA decay in yeast. Progress in nucleic acid research and molecular biology *47*, 271-298.

Philpott, C.C., Protchenko, O., Kim, Y.W., Boretsky, Y., and Shakoury-Elizeh, M. (2002). The response to iron deprivation in Saccharomyces cerevisiae: expression of

siderophore-based systems of iron uptake. Biochemical Society transactions *30*, 698-702.

Protchenko, O., Ferea, T., Rashford, J., Tiedeman, J., Brown, P.O., Botstein, D., and Philpott, C.C. (2001). Three cell wall mannoproteins facilitate the uptake of iron in Saccharomyces cerevisiae. The Journal of biological chemistry *276*, 49244-49250.

Rouault, T., and Klausner, R. (1997). Regulation of iron metabolism in eukaryotes. Current topics in cellular regulation *35*, 1-19.

Rouault, T.A., and Klausner, R.D. (1996). The impact of oxidative stress on eukaryotic iron metabolism. Exs *77*, 183-197.

Rutherford, J.C., and Bird, A.J. (2004). Metal-responsive transcription factors that regulate iron, zinc, and copper homeostasis in eukaryotic cells. Eukaryotic cell *3*, 1-13.

Rutherford, J.C., Jaron, S., Ray, E., Brown, P.O., and Winge, D.R. (2001). A second iron-regulatory system in yeast independent of Aft1p. Proceedings of the National Academy of Sciences of the United States of America *98*, 14322-14327.

Sayani, S., Janis, M., Lee, C.Y., Toesca, I., and Chanfreau, G.F. (2008). Widespread impact of nonsense-mediated mRNA decay on the yeast intronome. Molecular cell *31*, 360-370.

Shoemaker, C.J., and Green, R. (2012). Translation drives mRNA quality control. Nature structural & molecular biology *19*, 594-601.

Stearman, R., Yuan, D.S., Yamaguchi-Iwai, Y., Klausner, R.D., and Dancis, A. (1996). A permease-oxidase complex involved in high-affinity iron uptake in yeast. Science (New York, NY) *271*, 1552-1557.

Steiger, M., Carr-Schmid, A., Schwartz, D.C., Kiledjian, M., and Parker, R. (2003). Analysis of recombinant yeast decapping enzyme. RNA (New York, NY) *9*, 231-238.
Thompson, D.M., and Parker, R. (2007). Cytoplasmic decay of intergenic transcripts in Saccharomyces cerevisiae. Molecular and cellular biology *27*, 92-101.

Tucker, M., Valencia-Sanchez, M.A., Staples, R.R., Chen, J., Denis, C.L., and Parker, R. (2001). The Transcription Factor Associated Ccr4 and Caf1 Proteins Are Components of the Major Cytoplasmic mRNA Deadenylase in Saccharomyces cerevisiae. Cell *104*, 377-386.

van Dijk, E.L., Chen, C.L., d'Aubenton-Carafa, Y., Gourvennec, S., Kwapisz, M., Roche, V., Bertrand, C., Silvain, M., Legoix-Ne, P., Loeillet, S.*, et al.* (2011). XUTs are a class of Xrn1-sensitive antisense regulatory non-coding RNA in yeast. Nature *475*, 114-117.

Van Ho, A., Ward, D.M., and Kaplan, J. (2002). Transition metal transport in yeast. Annual review of microbiology *56*, 237-261.

van Hoof, A., Lennertz, P., and Parker, R. (2000). Yeast exosome mutants accumulate 3'-extended polyadenylated forms of U4 small nuclear RNA and small nucleolar RNAs. Molecular and cellular biology *20*, 441-452.

Wyers, F., Rougemaille, M., Badis, G., Rousselle, J.C., Dufour, M.E., Boulay, J., Regnault, B., Devaux, F., Namane, A., Seraphin, B.*, et al.* (2005). Cryptic pol II transcripts are degraded by a nuclear quality control pathway involving a new poly(A) polymerase. Cell *121*, 725-737.

Xu, Z., Wei, W., Gagneur, J., Perocchi, F., Clauder-Munster, S., Camblong, J., Guffanti, E., Stutz, F., Huber, W., and Steinmetz, L.M. (2009). Bidirectional promoters generate pervasive transcription in yeast. Nature *457*, 1033-1037.

Yamaguchi-Iwai, Y., Stearman, R., Dancis, A., and Klausner, R.D. (1996). Iron-regulated DNA binding by the AFT1 protein controls the iron regulon in yeast. The EMBO journal *15*, 3377-3384.

Yamaguchi-Iwai, Y., Ueta, R., Fukunaka, A., and Sasaki, R. (2002). Subcellular localization of Aft1 transcription factor responds to iron status in Saccharomyces cerevisiae. The Journal of biological chemistry *277*, 18914-18918.

Yun, C.W., Bauler, M., Moore, R.E., Klebba, P.E., and Philpott, C.C. (2001). The role of the FRE family of plasma membrane reductases in the uptake of siderophore-iron in Saccharomyces cerevisiae. The Journal of biological chemistry *276*, 10218-10223.

Yun, C.W., Ferea, T., Rashford, J., Ardon, O., Brown, P.O., Botstein, D., Kaplan, J., and Philpott, C.C. (2000a). Desferrioxamine-mediated iron uptake in Saccharomyces cerevisiae. Evidence for two pathways of iron uptake. The Journal of biological chemistry *275*, 10709-10715.

Yun, C.W., Tiedeman, J.S., Moore, R.E., and Philpott, C.C. (2000b). Siderophore-iron uptake in saccharomyces cerevisiae. Identification of ferrichrome and fusarinine transporters. The Journal of biological chemistry *275*, 16354-16359.

Zhao, H., Butler, E., Rodgers, J., Spizzo, T., Duesterhoeft, S., and Eide, D. (1998). Regulation of zinc homeostasis in yeast by binding of the ZAP1 transcriptional activator to zinc-responsive promoter elements. The Journal of biological chemistry *273*, 28713-28720.

Zhao, H., and Eide, D. (1996a). The yeast ZRT1 gene encodes the zinc transporter protein of a high-affinity uptake system induced by zinc limitation. Proceedings of the National Academy of Sciences of the United States of America *93*, 2454-2458.

Zhao, H., and Eide, D. (1996b). The ZRT2 gene encodes the low affinity zinc transporter in Saccharomyces cerevisiae. The Journal of biological chemistry *271*, 23203-23210.

Zhao, H., and Eide, D.J. (1997). Zap1p, a metalloregulatory protein involved in zinc-responsive transcriptional regulation in Saccharomyces cerevisiae. Molecular and cellular biology *17*, 5044-5052.

Chapter 2: Possible Mechanisms for the Cytoplasmic Trafficking of Cytoplasmically Degraded Cryptic Unstable Transcripts (CD-CUTs) in Saccharomyces cerevisiae

From our studies discussed in Chapter 1 (Toesca et al., 2011), a major unanswered question remained; namely the mechanistic actions of these cytoplasmically degraded cryptic unstable transcripts (CD-CUTs). We have shown that these CD-CUTs are degraded by the cytoplasmic Non-Sense Mediated Decay (NMD) Pathway yet mediate the repression of the subtelomeric genes *ZRT1* and *FIT3*. These CD-CUTs must therefore be localized to the nucleus if involved in the transcriptional repression of *ZRT1* and *FIT3*. As discussed in Toesca et al., 2011, we proposed a possible retrograde transport of these CD-CUTs from the cytoplasm to the nucleus, which would allow for the regulation of subtelomeric transcription by the CD-CUTs. A few lines of evidence support this proposal: 1) many subtelomeric genes in *S. cerevisiae* exhibit perinuclear localization (Grund et al., 2008); 2) nuclear activation of genes have been shown to be linked to localization to the nuclear periphery near the nuclear pores (Dieppois and Stutz, 2010); and 3) a component of the NMD system Upf1p has been shown to interact with the Nucleoporins Nup100p and Nup116p, which both localize to the nuclear side of the nuclear pore complex (Nazarenus et al., 2005). Also it could be possible that these CD-CUTs are degraded by NMD as they are translocated out of the nuclear pore complex and failure to degrade would result in increased concentrations of CD-CUTs in the nucleus. In effort to elucidate the mechanistic mode of these CD-CUTs, we sought to study the cytoplasmic trafficking of these species. We hypothesized that the export of the CD-CUTs could be mediated by an mRNA export factor through the nuclear pore complex for cytoplasmic degradation by the NMD system.

In *S. cerevisiae*, mRNA biogenesis in the nucleus and protein translation in the cytoplasm is physically separated by the nuclear envelope. The controlled exchange of material between the two compartments occurs through the nuclear pore complex (NPC), a highly specialized and evolutionarily conserved structure (Nino et al., 2013). mRNA export to the nucleus is a facilitated and energy dependent process, requiring

specific factors to mediate the export of certain RNAs (Lee et al., 1996). Export competent mRNA ribonucleoparticles (mRNPs) are released from their transcription sites and transported to the cytoplasm via the mRNA export receptor complex Mex67p-Mtr2p (Nino et al., 2013; Stewart, 2007). Mex67p promotes the translocation of the mRNP through the NPC by specific interactions with NPC proteins that line the central channel of the pore (Segref et al., 1997). At the cytoplasmic side of the NPC, the mRNP undergoes conformational changes which results in the release of the mRNA into the cytoplasm as the export factors are recycled and shuttled back to the nucleus for the next round of mRNA export.

In yeast, the serine-arginine (SR)-type family of mRNA binding proteins comprised of Npl3p, Hrb1p, and Gbp2p has been shown to be important mediators of mRNA export. All three proteins contain RNA recognition motifs (RRMs) and a serine-arginine (SR) rich domain. Npl3p has been shown to be essential for the export of poly(A)+ RNA with its shuttling capability dependent on the synthesis of poly(A)+ RNA (Lee et al., 1996). Genetic interactions between the mRNA export receptor complex Mex67p-Mtr2p and Npl3p have been identified and along with the export of poly(A)+ RNA, the export of large ribosomal subunits is also dependent on Npl3p (Hackmann et al., 2011). Phosphorylation by the SR-specific protein kinase Sky1p mediates dissociation of Npl3p from mRNPs, while dephosphorylation by the Glc7p phosphatase promotes its interaction with mRNPs and Mex67p (Gilbert and Guthrie, 2004; Gilbert et al., 2001). In addition to being an important mediator for mRNA export, Npl3p has been implicated in the link between chromatin modification and mRNA processing (Moehle et al., 2012), transcription elongation (Nino et al., 2013), and recruitment of splicing factors to pre-mRNAs (Kress et al., 2008).

Homologous to Npl3p, Gbp2p and Hrb1p have also been identified as novel mRNA export factors that shuttle between the nucleus and cytoplasm (Windgassen and

Krebber, 2003; Windgassen et al., 2004). Gbp2p has been shown to bind poly(A)+ RNA and nuclear export of Gpb2p is dependent on active RNA polymerase II transcription and other mRNA export factors (Windgassen and Krebber, 2003). Dissociation of Gpb2p from mRNPs and nuclear import is dependent on the SR-specific protein kinase Sky1p and the nuclear import receptor Mtr10p. Inactivation of either or both Sky1p and Mtr10p results in cytoplasmic mislocalization of the nuclear Gbp2p as well as increased poly(A)+ RNA binding (Windgassen and Krebber, 2003). The last of the SR-type mRNA export factors, Hrb1p, has also been shown to bind poly(A)+ RNA (Hacker and Krebber, 2004). Like Gbp2p, nuclear import of Hrb1p is dependent on the nuclear import receptor Mtr10p as well as phosphorylation by the SR-specific protein kinase Sky1p (Hacker and Krebber, 2004). While all three SR-type proteins share similar import requirements, they display differences in export requirements. Export of both Gbp2p and Hrb1p are dependent on two components of the THO complex, Mft1p and Hpr1p (Hacker and Krebber, 2004), while Npl3p export is mediated by the arginine methyltransferase Hmt1p (Shen et al., 1998). The heterotetrameric THO complex comprised of Tho2p, Hpr1p, Mft1p, and Thp2p along with the mRNA export factors Sub2p and Yra1p make up the TREX complex (Transcription/Export) which has been shown to couple transcription and mRNA export (Strasser et al., 2002). Npl3p has been suggested to be recruited to the mRNA via RNA polymerase II (Lei et al., 2001), while recruitment of Gbp2p and Hrb1p to the mRNA is dependent on the components of the THO complex Mft1p and Hpr1p (Hacker and Krebber, 2004). This association with the export competent mRNP allows for the SR-like shuttling proteins to follow the mRNP to the cytoplasm where they undergo dissociation from the mRNP and are reimported to the nucleus for the next round of mRNA export.

As mentioned above, export competent mRNPs are translocated through the nuclear pore complex via the mRNA export receptor complex Mex67p-Mtr2p. This

heterodimeric shuttling transporter requires other shuttling SR-type mRNA binding and adaptor proteins for proper cytoplasmic export of the mRNP. Mex67p mediates the export of poly(A)+ RNA, including a variety of RNA polymerase II transcripts involved in the heat shock response, transcriptional repression, and glycolytic enzymes (Hurt et al., 2000; Segref et al., 1997). At permissive temperature this essential protein predominately localizes to the nuclear pore. However a Mex67p mutant shifted to restrictive temperatures dissociates from the nuclear pores into the cytoplasm (Segref et al., 1997). Mex67p has also been genetically linked to Nup85p, a member of the Nup84p complex which has important roles in NPC biogenesis and mRNA export (Nino et al., 2013; Segref et al., 1997). The other half of the heterodimeric transporter complex, Mtr2p, is essential for Mex67p binding to the nuclear pores. Impaired function of Mtr2p results in dissociation of the Mex67p-Mtr2p complex as well as dissociation of Mex67p from the nuclear pores. A nuclear accumulation of poly(A)+ RNA is also evident in mutants of Mtr2p, indicating a role for poly(A)+ RNA export (Santos-Rosa et al., 1998). Like Mex67p, Mtr2p has also been shown to interact with Nup85p, a member of the Nup84p nucleoporin complex involved in NPC biogenesis and mRNA export (Santos-Rosa et al., 1998; Segref et al., 1997; Siniossoglou et al., 2000).

While Mex67p plays a major essential role in mRNA export, it requires adaptor proteins for stable interaction with mRNPs. These adaptor proteins include the RNA binding protein Yra1p, the SR-type shuttling export factor Npl3p, and the hnRNP shuttling protein Nab2p (Anderson et al., 1993; Gilbert and Guthrie, 2004; Segref et al., 1997). RNA binding of Mex67p is mediated by Yra1p, facilitating recruitment of Mex67p to the mRNP. Prior to nuclear exit of the mRNP, ubiquitination by the E3 ligase Tom1p results in dissociation of Yra1p from the mRNP, where it is recycled in the nucleus for the next round of mRNP export complex assembly (Iglesias et al., 2010; Strasser and Hurt, 2000). The hnRNP protein Nab2p forms a tripartite complex with Mex67p and

Yralp (Iglesias et al., 2010). Nab2p has been shown to interact with most RNA transcripts and acts as a global mRNA export factor (Batisse et al., 2009). Unlike Yra1p, Nab2p is exported out of the nucleus with Mex67p and the mRNP during export. Nab2p dissociation from the mRNP and Mex67p is dependent on the activity of the DEAD-Box protein Dbp5p with subsequent nuclear import by the karyopherin Kap104p (Tran et al., 2007). Dbp5p also has been shown to be responsible for removing Mex67p from the exported mRNP to terminate export (Lund and Guthrie, 2005).

In the following studies, we explore the possible roles of the SR-type family of mRNA export factors Npl3p, Gbp2p, and Hrb1p in the cytoplasmic trafficking of *ZRT1* and *FIT3* CD-CUTs. We also sought to elucidate the involvement of Mex67p in the export of *ZRT1* and *FIT3* CD-CUTs, as proper export of these species becomes necessary for efficient degradation by the cytoplasmic turnover machinery. We hypothesized that export of *ZRT1* and *FIT3* CD-CUTs may be mediated by the SR-type export factors (Npl3p, Gbp2p, and Hrb1p) and Mex67p. As these species exit the nuclear pore complex, association with the nucleoporins Nup100p/Nup116p may then target these species for cytoplasmic degradation by the Non-Sense Mediated Decay (NMD) Pathway. By assessing the cytoplasmic trafficking of these CD-CUTs in mutant strains of these SR-type proteins, we hoped it would provide insight into the mechanistic action of how these species mediate subtelomeric gene transcription.

The role of SR-type proteins in the cytoplasmic trafficking of ZRT1 and FIT3 CD-CUTs

To assess whether the *ZRT1* and *FIT3* CD-CUTs were targets of the SR-type mRNA export factors, the expression levels of *ZRT1*/*FIT3* mRNA and CD-CUTs were profiled in deletion mutants of each SR-type export factor (*npl3Δ*, *gpb2Δ*, *hrb1Δ*) as well as mutations coupled to inactivation of the NMD system (*npl3Δupf1Δ, gbp2Δupf1Δ*, *hrb1Δupf1Δ*). Inactivation of the NMD system is required for stabilization of the CD-

CUTs as they are degraded by the NMD pathway (Toesca et al., 2011). mRNA and CD-CUT levels were assessed during conditions of metal replete and deplete conditions.

As shown in Figure 2.1, deletion of Npl3p does not stabilize the expression of the *ZRT1* CD-CUT in normal and low zinc conditions (lane 2,7). The *ZRT1* CD-CUT is only stabilized upon inactivation of Upf1p, a key component of the NMD Pathway (lane 2,4,6,8), but no additive effect occurs in the stabilization of these species when coupled to deletion of Npl3p. The reduction in *ZRT1* mRNA expression in the single *npl3Δ* mutant when compared to the wild type strain during low zinc conditions may be attributed to decreased *ZRT1* transcription resulting from defective transcriptional elongation as Npl3p has also been shown to mediate transcriptional elongation (Nino et al., 2013). In the *npl3Δupf1Δ* double mutant, the stabilization of the *ZRT1* CD-CUT results in exacerbation of decreased *ZRT1* mRNA expression in conditions of low zinc when compared to wild type (lane 8). This exacerbation could result from the combined stabilization of the *ZRT1* CD-CUT prevents that proper *ZRT1* induction and the loss of Npl3p attenuates proper and efficient transcription elongation.

ZRT1 mRNA and CD-CUT levels were also assessed in single *gbp2Δ* mutant as well as the double *gbp2Δupf1Δ* mutant during low zinc conditions. As shown in Figure 2.2, deletion of Gbp2p has no effect on the stabilization of the *ZRT1* CD-CUT (lanes 9-12). Similar to the expression profile in the Npl3p mutant strain, NMD inactivation coupled to the deletion of Gbp2p does not result in increased stabilization of the *ZRT1* CD-CUT during a zinc starvation time course (lanes 13-16). *ZRT1* mRNA expression is however reduced and a delay of induction is evident in the in *gbp2Δupf1Δ* mutant during the zinc starvation time course when compared to the wild type strain (compare lanes 13-16 to lanes 1-4). As Gbp2p functions in the export of poly(A)+ RNA, the loss of Gbp2p may result in an overall block of efficient mRNA export. Proper nuclear processing and recruitment of export factors to the mRNA is required for efficient export.

In the event of improper processing, the transcript can be recognized by the nuclear surveillance machinery where nuclear retention triggers degradation by the nuclear exosome (Carmody and Wente, 2009). This could very well be the case for *ZRT1* mRNA in the *gbp2Δ* and *gbp2Δupf1Δ* mutant strains, where improper processing and export results in nuclear retention and degradation by the nuclear exosome.

Unlike the *ZRT1* mRNA/CD-CUT expression profiles observed in the *npl3Δ* and *gbp2Δ* mutants, loss of Hrb1p results in stabilization of the *ZRT1* CD-CUT as well as a delayed and reduced expression of *ZRT1* mRNA (Figure 2.3 lanes 9-12). When coupled to inactivation of NMD, the delayed and reduced expression of *ZRT1* mRNA is further exacerbated (Figure 2.3 lanes, 13-16). However, loss of Hrb1p does not seem to increase CD-CUT levels even in the absence of functional NMD (Figure 2.3 lanes 13-16). While deletion of individual SR-type export factors (*npl3Δ, gbp2Δ, hrb1Δ*) result in a general decrease in *ZRT1* mRNA levels during a zinc starvation time course, the stabilization of the *ZRT1* CD-CUT in the absence of Hrb1p indicates that the three SR-type proteins have different mRNA targets. This stabilization of CD-CUTs in the absence of Hrb1p is also applicable to the *FIT3* CD-CUT (Figure 2.4, lanes 9-12). Although we were unable to observe a concomitant decrease in *FIT3* mRNA expression in low iron conditions in the *hrb1Δ* and *hrb1Δupf1Δ* mutant strains (Figure 2.4, lanes 9-16) as evident in the *npl3Δ* and *gbp2Δ* mutant strains, we believe that the *ZRT1* and *FIT3* CD-CUT are substrates for Hrb1p mediated export.

To corroborate the *ZRT1* mRNA expression results observed in our Northern analysis, we studied RNA polymerase II occupancy at the *ZRT1* promoter using chromatin immunoprecipitation of the Rpb3p subunit. In the wild-type strain, Rpb3p occupancy at the *ZRT1* promoter in normal zinc conditions is slightly above background levels. As expected, switch to low zinc conditions resulted in ~2 fold Rpb3p occupancy enrichment, indicating increased *ZRT1* transcription. Pol II occupancy is decreased to

slightly above background levels in the *upf1Δ, hrb1Δ,* and *npl3Δ* mutant strains in low zinc conditions (compare to wild type, Figure 2.5). This decrease in pol II occupancy is in agreement with our Northern analysis of the *ZRT1* mRNA in the *upf1Δ*, *hrb1Δ*, and *npl3Δ* mutants. We also studied Hrb1p association with the upstream promoter region of the major *ZRT1* CD-CUT (Toesca et al., 2011) using chromatin immunoprecipitation of Hrb1-MYC. Hrb1p occupancy levels at the upstream promoter were detectable only to background levels (data not shown) in both normal and low zinc conditions. This could be due to inefficient immunoprecipitation of the crosslinked Hrb1p or possibly that this upstream promoter region is not actively transcribed. Chromatin immunoprecipitation studies show that Hrb1p associates with coding regions of actively transcribed genes such as the *PMA1* gene. Together with the TREX complex, Hrb1p moves with elongating RNA pol II along activated genes (Hurt et al., 2004). As the *ZRT1* CD-CUT is transcribed from an upstream intergenic promoter ~2.2Kb upstream of the *ZRT1* ORF (Toesca et al., 2011), Hrb1p occupancy would not be expected in this upstream region.

We also tested whether loss of Hrb1p results in stabilization of other RNA transcripts other than *FIT3*/*ZRT1* CD-CUTs. Northern analysis of the transcript encoding the protein of the large ribosomal subunit Rpl122bp, exhibits a stabilization of unspliced species similar to that of the *upf1Δ* mutant (Figure 2.6, compare lanes 4-8 and 9-12). Unspliced Rpl22b, an intron-containing gene, has been shown to be a substrate of NMD (Sayani et al., 2008). As shown in Figure 2.6, the use of intronic riboprobes allows specific detection of the *RPL22B* unspliced transcript that accumulates in both the *hrb1Δ* and *upf1Δ* mutant strains when compared to the wild type strain. These results indicate that Hrb1p may mediate the export of NMD substrates such as the unspliced *RPL22B* and the *ZRT1*/*FIT3* CD-CUTs.

In attempt to study the localization of the *ZRT1* CD-CUTs in the absence of Hrb1p, we made use of the MS2-MCP system (Weil et al., 2010) for endogenously

tagging the major *ZRT1* CD-CUT (CD-CUT 1, (Toesca et al., 2011)). This system is comprised of two components: a reporter mRNA and a GFP-MS2 fusion protein. The GFP-MS2 was expressed under the control of the constitutive GPD promoter, while the reporter mRNA was under the control of the GAL promoter. The reporter mRNA contains six binding sites for the coat protein of the bacterial phage MS2. Detection of *ZRT1* CD-CUT localization was achieved using a CY3 labeled fluorescent probe complementary to the stem loop region inserted in the upstream promoter region of the major *ZRT1* CD-CUT. This strain was then utilized to detect the *ZRT1*255UP-MS2 transcript in both the wild type and *hrb1Δ* strains. Strains were grown in normal and low zinc conditions to assess localization of these species in the absence of Hrb1p (data not shown). We were unable to discern exact localization of these species, as repeated FISH studies exhibited diffuse nuclear and cytoplasmic signal. The technical constraints with our detection method prevent us from definitely localizing the *ZRT1* CD-CUT in the absence of Hrb1p.

Inactivation of the mRNA export factor Mex67p alters degradation of ZRT1 and FIT3 CD-CUTs

Recent studies from our laboratory identified a cytoplasmic to nuclear shift in transcript turnover upon induction of an export defect after a temperature shift to non-permissive temperatures (37°C). This shift in transcript turnover was evident in the unspliced *RPS17B* and *RPS22B* NMD targets (Sayani and Chanfreau, 2012). Their findings showed that inhibition of mRNA export at non-permissive temperatures in the *mex67-5* strain results in retention of transcripts normally degraded by NMD and targeted for degradation by the nuclear exosome (*RPS17B*/*RPS22B*). Since *ZRT1*/*FIT3* CD-CUTs are degraded by NMD (Toesca et al., 2011), we hypothesized that these CD-CUTs may undergo the same fate in degradation turnover when faced in conditions of blocked export. Since Mex67p is an essential RNA export factor, we utilized strains harboring deletion of Mex67p at the genomic locus and a plasmid expressing a wild-type

version or the thermosensitive point mutant *mex67-5* (Segref et al., 1997). Inactivation of NMD (*upf1Δ*) and the nuclear exosome component (*rrp6Δ)* were coupled to this Mex67p strain. Strains were grown in normal zinc (SD+2mM $ZnCl_2$) and normal iron (YPD) media at the permissive temperature of 25°C and shifted to non-permissive temperature 37°C. We then analyzed the expression of the *ZRT1* mRNA/CD-CUT and the *FIT3* mRNA/CD-CUT to investigate the possible cytoplasmic to nuclear shift of degradation upon defects in mRNA export.

As expected, we observed an accumulation of the *ZRT1* CD-CUT in the strain expressing *mex67-5* in the *upf1Δ* background (Figure 2.7, lane 2) at the permissive temperature of 25°C. Accumulation of the *ZRT1* CD-CUT is not expected in the *mex67-5 rrp6Δ* strain (Figure 2.7, lane 3) as these transcripts are primarily degraded by the cytoplasmic NMD system. Upon shift to restrictive temperature of 37°C, we are able to observe accumulation of the *ZRT1* CD-CUT in the both the *mex67-5upf1Δ* and *mex67-5rrp6Δ* strains (Figure 2.7, lane 5-6). This accumulation of the *ZRT1* CD-CUT is slightly higher in the *mex67-5rrp6Δ* strain (Figure 2.7, lane 6). Analysis of expression of the *FIT3* CD-CUT utilizing the *mex67-5upf1Δ* and *mex67-5rrp6Δ* strains also show a similar pattern of accumulation (Figure 2.7B). At the permissive temperature of 25°C, accumulation of the *FIT3* CD-CUT is observed in the *mex67-5upf1Δ* strain. Upon shift to restrictive temperature of 37°C to induce defective export, we now observe an increase in the accumulation of the CD-CUT in the *mex67-5rrp6Δ* strain (Figure 2.7B, compare lanes 5-6 vs. 2-3). These results indicate that when mRNA export is blocked in the *mex67-5* strain at the restrictive temperature, *ZRT1*/*FIT3* CD-CUTs that are normally degraded by NMD are now subjected to nuclear retention and degradation by nuclear exosome (Figure 2.7A,B). In addition, export of these *ZRT1*/*FIT3* CD-CUTs are also dependent on the mRNA export factor Mex67p.

The nucleoporins Nup100p and Nup116p do not mediate export of ZRT1 and FIT3 CD-CUTs

We hypothesized that as the *ZRT1*/*FIT3* CD-CUTs exit the nuclear pore complex, association with the nucleoporins Nup100p and Nup116p may target these species for cytoplasmic degradation by NMD. Nup100p and its paralog Nup116p, comprise the central core of the nuclear pore complex and predominately localize to the cytoplasmic side of the nuclear pore. Nup100p/Nup116p participate in mRNA export and its GLFG regions serve as critical binding sites for Mex67p at the nuclear pore (Strawn et al., 2001; Suntharalingam and Wente, 2003). We chose to study the possible role of these nucleoporins in the export of the *ZRT1*/*FIT3* CD-CUTs as a genetic interaction between the NMD component Upf1p has been established with Nup100p and Nup116p (Nazarenus et al., 2005). We hypothesized that loss of Nup100p or Nup116p could result in the increased stabilization of the *ZRT1* or *FIT3* CD-CUT.

To study the possible role of Nup100p/Nup116p in the export of these CD-CUTs, we utilized yeast strains lacking Nup100p/Nup116p (*nup100Δ*/*nup116Δ)* as well as mutant Nup100p/Nup116p coupled to inactivation of NMD (*nup100Δpupf1Δ*/*nup116Δpupf1Δ)*. Inactivation of NMD is critical to observe the stabilization of the *ZRT1*/*FIT3* CD-CUTs. These strains were then subjected to a low zinc shift and *ZRT1* mRNA/CD-CUT levels were analyzed. As our northern analysis indicates, loss of Nup100p or Nup116p does not result in stabilization of the *ZRT1* CD-CUT (Figure 2.8 A,B lanes 9-12). Accumulation of the *ZRT1* CD-CUT is only evident in strains with the inactive NMD (*upf1Δ)* and loss of Nup100p/Nup116p coupled to NMD inactivation does not display an additive effect on the stabilization of these species (Figure 2.8, lanes 13-16). We also observe a delayed and decreased induction expression of *ZRT1* mRNA in the single *nup100Δ* and *nup116Δ* (Figure 2.8 A, B lanes 9-12) strains. This delayed and reduced *ZRT1* mRNA expression could be an artifact of a

general block of mRNA export, which could result in nuclear retention of the transcript and turnover by the nuclear exosome. We believe that the exacerbated reduction of *ZRT1* mRNA in the *nup100Δupf1Δ* and the *nup116Δupf1Δ* (Figure 2.8 A,B, lanes 13-16) strains is also due to a combination of a general defect of mRNA export and the presence of the ZRT1 CD-CUT stabilized due to the inactivation of NMD, and not due to the absence of Nup100p/Nup116p.

Discussion

In these studies we sought to understand the mechanistic mode of action of Cytoplasmically Degraded Cryptic Unstable Transcripts (CD-CUTs) in mediation of *ZRT1* and *FIT3* transcriptional repression. We chose to study trafficking of these species, as nuclear export is critical for cytoplasmic Non-Sense Mediated Decay (NMD) degradation. A possible retrograde transport of these CD-CUTs from the nucleus to the cytoplasm may occur which could allow for the regulation of *ZRT1*/*FIT3* by these CD-CUTs. Export of these CD-CUTs may be mediated by specific mRNA export factors that ensure proper export through the nuclear pore and subsequent cytoplasmic degradation. We hypothesized that export of CD-CUTs could be mediated by the SR-type mRNA export factors (Npl3p, Gbp2p, and Npl3p) and Mex67p. As these species are translocated through the nuclear pore complex, association with the nucleoporins Nup100p and Nup116p allow interaction and subsequent degradation by NMD.

Our findings show that *ZRT1* CD-CUTs are not substrates for Npl3p or Gbp2p mediated export (Figure 2.1, 2.2) Loss of either Npl3p or Gbp2p does not result in the stabilization of the *ZRT1* CD-CUTs. A delayed and decreased expression of *ZRT1* mRNA is observed in the absence of Npl3p or Gbp2p. This decreased *ZRT1* expression could be attributed to inefficient transcriptional elongation, as Npl3p has been shown to be required for efficient transcriptional elongation (Nino et al., 2013); and a general block

of mRNA export. Both Npl3p and Gbp2p play essential roles in mRNA export and inefficient export could result in nuclear retention of *ZRT1* mRNA/CD-CUTs and targeted degradation by the nuclear exosome. When loss of Npl3p/Gbp2 function is coupled to the inactivation of NMD, a drastic reduction of *ZRT1* mRNA is observed (Figure 2.1, 2.2). We believe that this drastic reduction is due to the stabilization of the *ZRT1* CD-CUT by the loss of NMD which prevents the proper activation of *ZRT1*; as well as the general block of mRNA export by the loss of Npl3p/Gbp2p and not due to increased stabilization of *ZRT1* CD-CUTs in the mutant strains.

The loss of Hrb1p resulted in the stabilization of both the *ZRT1* and *FIT3* CD-CUT (Figure 2.3, 2.4). However, an increase in the stabilization of CD-CUTs was not observed when deletion of Hrb1p was coupled to inactivation of NMD. Consistent with Npl3p and Gbp2p results, a dramatic decrease in *ZRT1* mRNA expression was observed in both the hrb1Δ and *hrb1Δupf1Δ* mutant strains. This decrease in *ZRT1* mRNA expression observed in the *hrb1Δupf1Δ* strain is consistent with our model of Hrb1p mediated export of CD-CUTs. In the absence of Hrb1p, the accumulation of the CD-CUT (Figure 2.3, 2.4 lanes 9-12) would prevent proper induction of *ZRT1* and result in dramatically reduced *ZRT1* mRNA expression. In addition, we show that loss of Hrb1p resulted in the stabilization of the unspliced *RPL22B* transcript indicating that Hrb1p may mediate the export of NMD substrates (unspliced *RPL22B*, *ZRT1*/*FIT3* CD-CUTs)

We have also identified a role for the essential mRNA export factor Mex67p in the export of *ZRT1* and *FIT3* CD-CUTs. Proper Mex67p mediated export is critical for cytoplasmic turnover of *ZRT1*/*FIT3* CD-CUTs (Figure 2.7A,B). Inhibition of mRNA export results in a cytoplasmic to nuclear shift in degradation routes, allowing for nuclear retention of these transcripts and degradation by the nuclear exosome. Although it was attractive to propose that association of CD-CUTs with the Nucleoporins Nup100p/Nup116p, which would target these species for NMD degradation, our results

indicate that this is not the case. We were unable to observe an increased accumulation of the *ZRT1* CD-CUT in the absence of Nup100p/Nup116p (Figure 2.8A,B) and also in the absence of a functional NMD. As in the case of the SR-type mutants (Npl3p, Gbp2p), decreased *ZRT1* mRNA expression in the Nucleoporin mutants could be a consequence of the lack of degradation of CD-CUTs, which prevents proper induction of *ZRT1* and a general block of mRNA export.

We have yet to establish the localization of *ZRT1*/*FIT3* CD-CUTs in the absence of Hrb1p. Repeated FISH experiments to detect the tagged main *ZRT1* CD-CUT in the *hrb1Δ* background displayed both nuclear and cytoplasmic signal. As our results indicate that *ZRT1*/*FIT3* CD-CUTs accumulate in the absence of Hrb1p, it could be possible that export of these species are mediated by other uncharacterized mRNA export factors not addressed in these studies. In addition, it would be beneficial to address whether Hrb1p associates with *ZRT1*/*FIT3* CD-CUTs through RNA immunoprecipitation studies as shown for *PMA1* and *HYP1* transcripts (Hurt et al., 2004). While it has been shown that Hrb1p mediates RNA export, its role in active mRNP assembly in the nucleus remains unknown (Hurt et al., 2004), thus it is possible that Hrb1p passively associates with these transcripts to follow them out of the nucleus where they are then subjected to degradation by NMD.

In conclusion, our results have identified a likely role for the SR-type mRNA binding protein Hrb1p in the cytoplasmic trafficking of the *ZRT1* and *FIT3* CD-CUTs (Figure 2.9). We sought to study the cytoplasmic trafficking of these CD-CUTs to understand how these transcripts can mediate transcriptional repression of the subtelomeric genes *ZRT1* and *FIT3*. We found that loss of Hrb1p results in stabilization of both *ZRT1* and *FIT3* mRNA as well as a concomitant decrease in *ZRT1/FIT3* mRNA expression during low metal conditions. In addition we show that loss of Hrb1p results in accumulation of the unspliced *RPL22B* transcript, indicating that Hrb1p mediates export

of other NMD substrates (unspliced *RPL22B*, *ZRT1/FIT3* CD-CUTs). We show that export of *ZRT1/FIT3* CD-CUTs is also dependent on the essential mRNA export factor Mex67p as inactivation of Mex67p results in nuclear retention and degradation by the nuclear exosome.

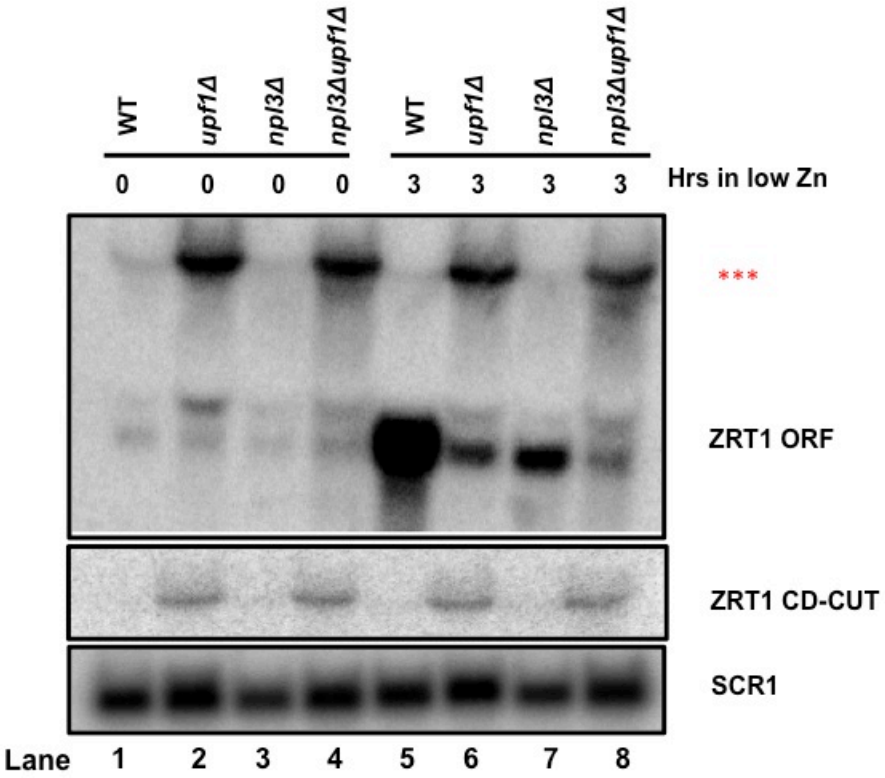


Figure 2.1. **Decreased levels of ZRT1 mRNA upon loss of Npl3p.** Northern Blot analysis of *ZRT1* mRNA and *ZRT1* CD-CUT expression in NMD and SR-type mRNA export factors (Npl3p) grown in normal and low zinc conditions. Strains with indicated genotypes were grown in normal (SD+2mM $ZnCl_2$) and low zinc medium for indicated times. Low zinc conditions achieved by addition of EDTA to SD media for final EDTA concentration of 1mM EDTA. *** =*ZRT1* CD-CUT detected with *ZRT1* ORF probe.

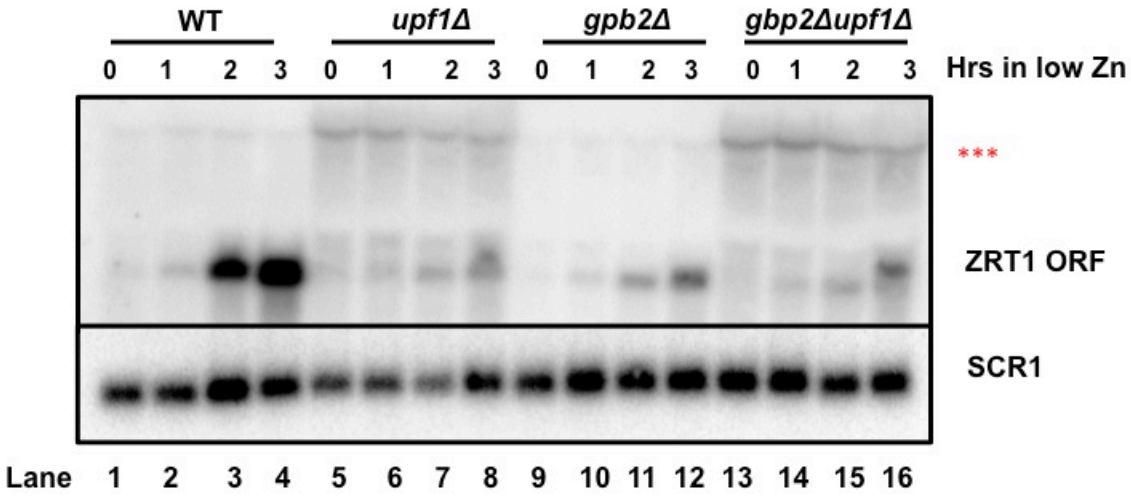


Figure 2.2. Loss of Gbp2p does not affect stabilization of *ZRT1* CD-CUT. Northern Blot analysis of *ZRT1* mRNA and *ZRT1* CD-CUT expression in NMD and SR-type mRNA export factors (Gbp2p) grown in normal and low zinc conditions. Strains with indicated genotypes were grown in normal (SD+2mM $ZnCl_2$) and low zinc medium for indicated times. Low zinc conditions achieved by addition of EDTA to SD media for final EDTA concentration of 1mM EDTA. *** indicates *ZRT1* CD-CUT detected with *ZRT1* ORF probe.

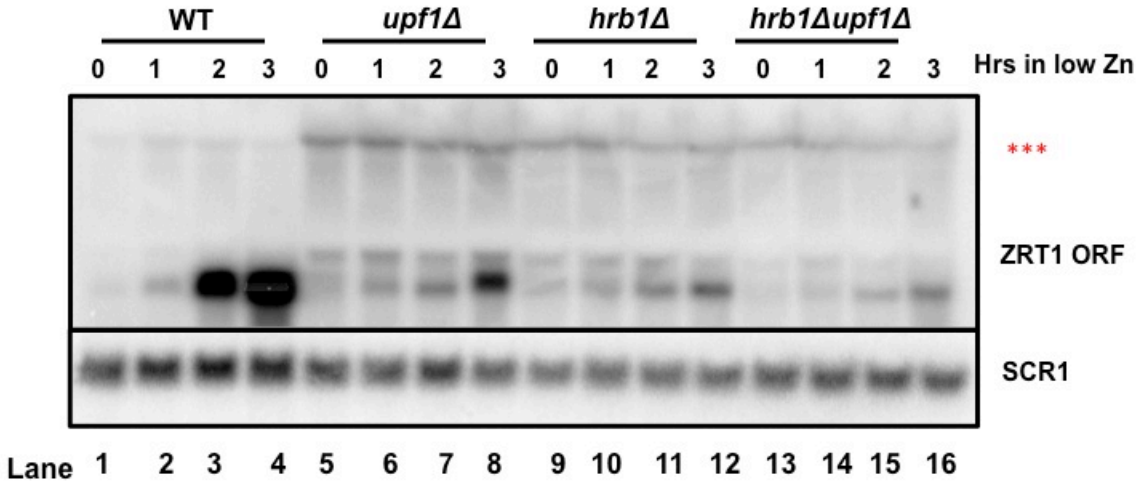


Figure 2.3 *ZRT1* CD-CUTs are stabilized by loss of Hrb1p. Northern Blot analysis of *ZRT1* mRNA and *ZRT1* CD-CUT expression in NMD and SR-type mRNA export factors (Hrb1p) grown in normal and low zinc conditions. Strains with indicated genotypes were grown in normal (SD+2mM $ZnCl_2$) and low zinc medium for indicated times. Low zinc conditions achieved by addition of EDTA to SD media for final EDTA concentration of 1mM EDTA. *** indicates *ZRT1* CD-CUT detected with *ZRT1* ORF probe.

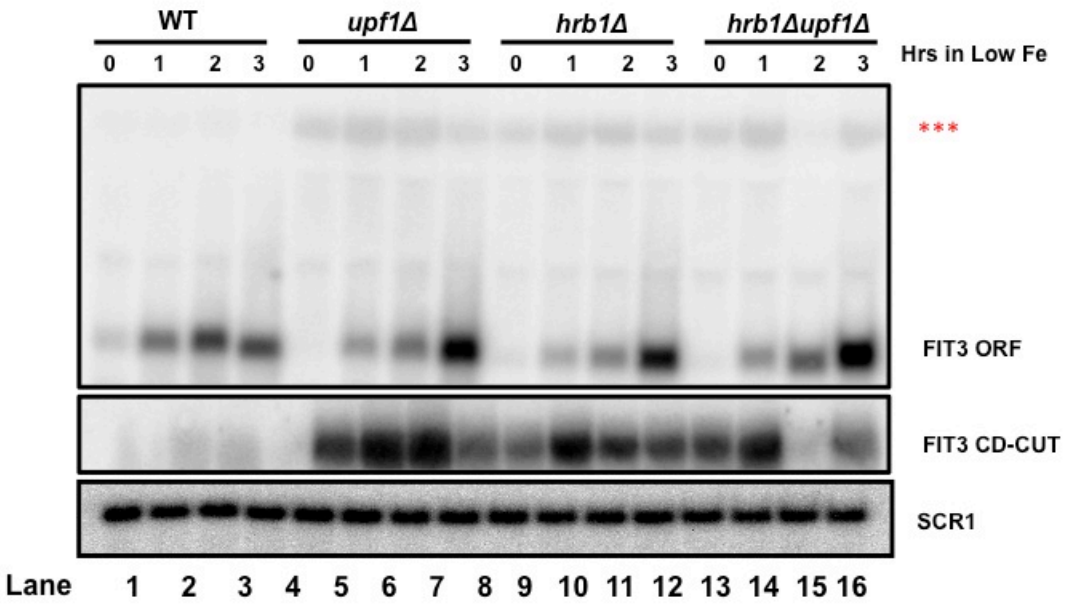


Figure 2.4. *FIT3* CD-CUTs are stabilized upon loss of Hrb1p. Northern blot analysis of *FIT3* mRNA and *FIT3* CD-CUT expression in NMD and SR-type mRNA export factor mutants (Hrb1p) grown in normal and low iron conditions. Strains with indicated genotypes were grown in normal (YPD) and low iron medium for indicated times. Low iron conditions achieved by addition of the iron chelator, Bathophenanthroline disulfonic acid (BPS) to YPD for final BPS concentration of 300mM BPS. *** indicates *FIT3* CD-CUT detected with *FIT3* ORF probe.

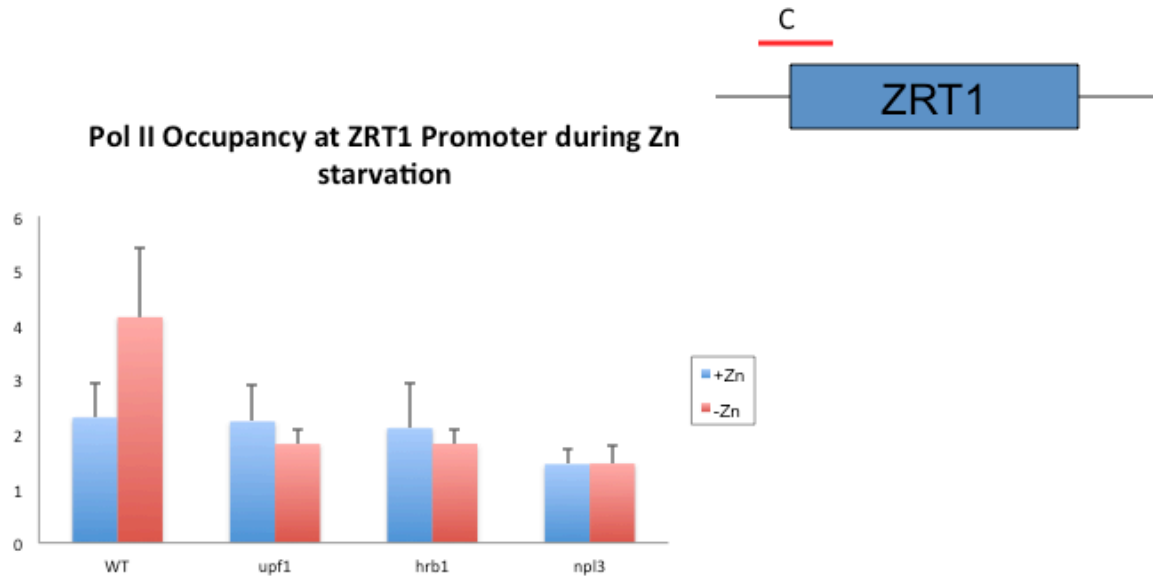


Figure 2.5. RNA pol II occupancy is decreased in NMD and SR-type mRNA export factor mutants. Analysis of RNA pol II occupancy in wild type, *upf1Δ*, *hrb1Δ*, and *npl3Δ* strains grown in normal zinc (+Zn) media and after 3 hour shift to low zinc media (-Zn). Shown are normalized qPCR analysis of the *ZRT1* promoter region from ChIP samples using anti-Rpb3 normalized to input DNA and to a qPCR product for a control non-transcribed subtelomeric region.

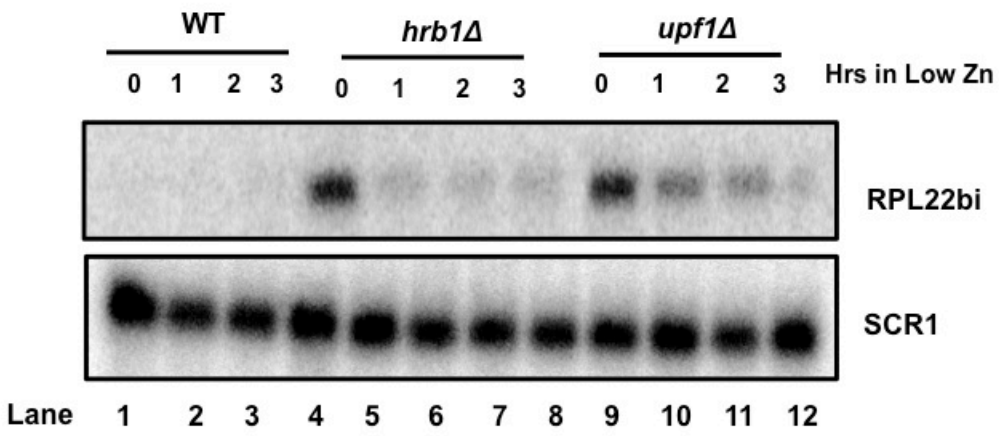


Figure 2.6. Non-sense Mediated Decay Pathway targets are also substrates for Hrb1p mediated export. Northern blot analysis of the NMD sensitive transcript *RPL22B* in NMD (*upf1Δ*) and SR-type export factor (*hrb1Δ*) mutants grown in normal (SD+2mM $ZnCl_2$) and low zinc medium. Low zinc conditions achieved by addition of EDTA to SD media for final EDTA concentration of 1mM EDTA. Riboprobe specific to *RPL22B* intron detects unspliced transcript accumulation.

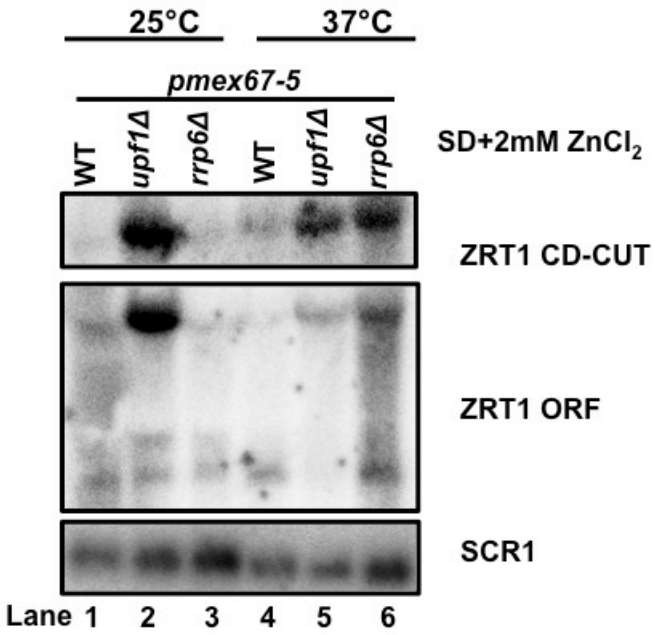


Figure 2.7A. Inhibition of mRNA export results in higher fraction of ZRT1 CD-CUTs degraded by the nuclear exosome. Northern blot analysis of *ZRT1* CD-CUT and *ZRT1* mRNA in strains with inactive NMD/nuclear exosome coupled to blocked export. Strains with indicated genotypes were grown in normal zinc medium (SD+2mM $ZnCl_2$) at the permissive temperature 25°C until logarithmic phase and shifted to restrictive temperature 37°C for 3 hours.

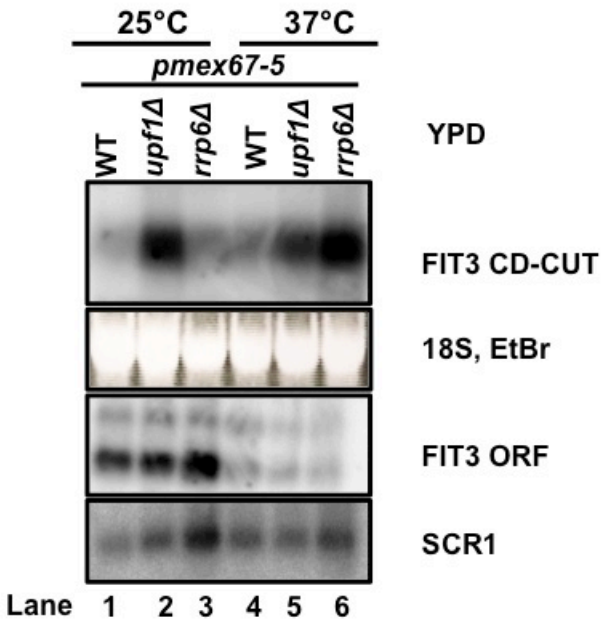


Figure 2.7B. Inhibition of mRNA export results in higher fractions of *FIT3* CD-CUTs degraded by the nuclear exosome. Northern blot analysis of *FIT3* CD-CUT and *FIT3* mRNA in strains with inactive NMD/nuclear exosome coupled to blocked export. Strains with indicated genotypes were grown in normal iron medium (YPD) at the permissive temperature 25°C until logarithmic phase and shifted to restrictive temperature 37C for 3 hours.

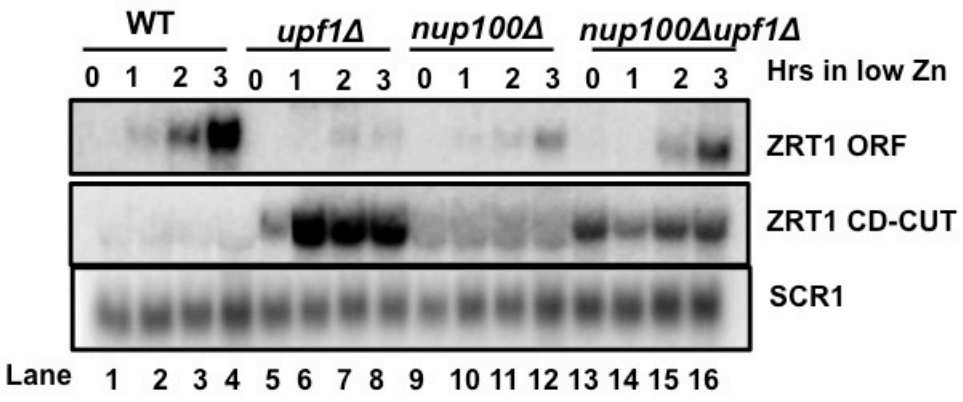


Figure 2.8 A. Nup100p does not mediate export of ZRT1 CD-CUT. Northern analysis of *ZRT1* CD-CUT and *ZRT1* mRNA in NMD and Nucleoporin (*nup100Δ*) mutants. Strains with indicated genotypes were grown in normal (SD+2mM $ZnCl_2$) and low zinc medium. Low zinc conditions achieved by addition of EDTA to SD media for final EDTA concentration of 1mM EDTA.

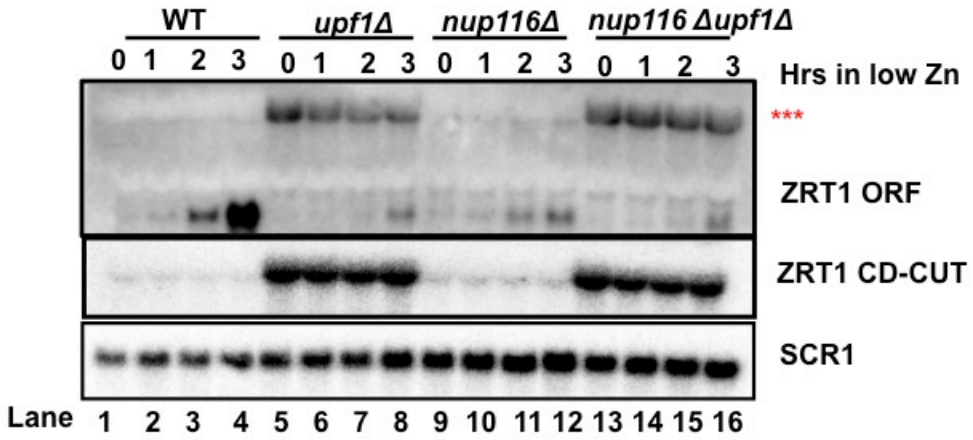


Figure 2.8 B. Nup116p does not mediate export of *ZRT1* CD-CUT. Northern analysis of *ZRT1* CD-CUT and *ZRT1* mRNA in NMD and Nucleoporin (*nup116Δ)* mutants. Strains with indicated genotypes were grown in normal (SD+2mM $ZnCl_2$) and low zinc medium. Low zinc conditions achieved by addition of EDTA to SD media for final EDTA concentration of 1mM EDTA. *** indicates *ZRT1* CD-CUTs detected with *ZRT1* ORF probe.

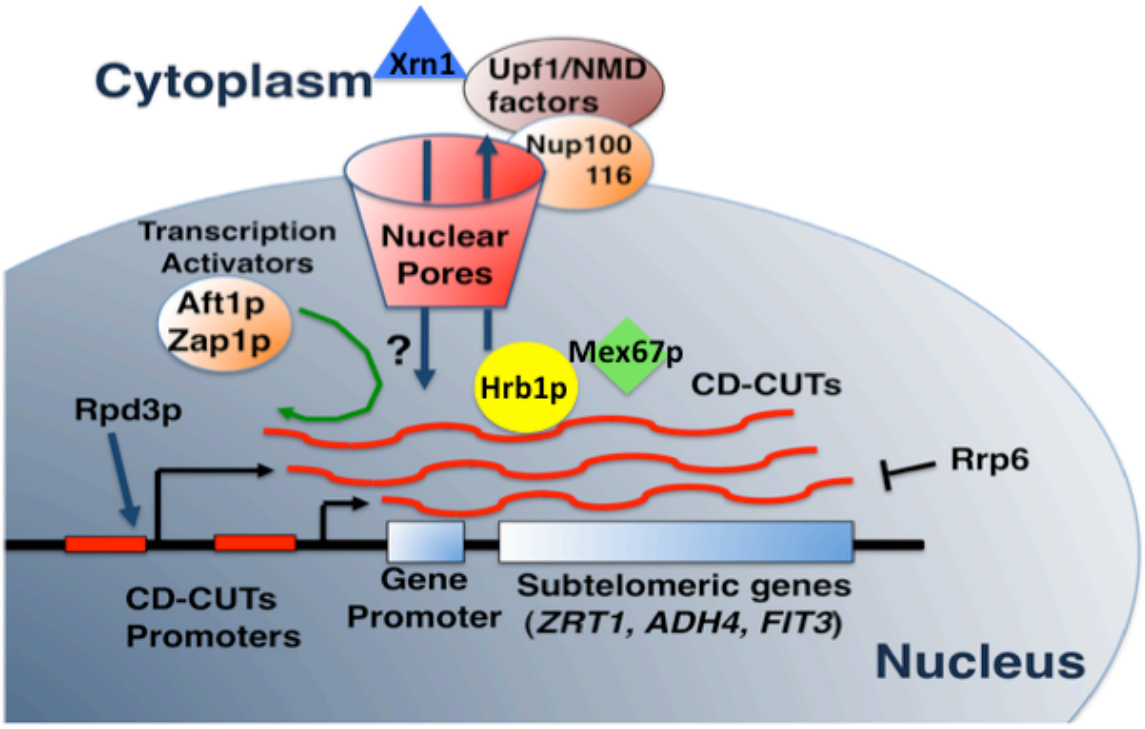


Figure 2.9. *ZRT1* and *FIT3* CD-CUTs are likely exported by the SR-like protein Hrb1p and dependent on the essential export factor Mex67p. Model for cytoplasmic trafficking of *ZRT1* and *FIT3* CD-CUTs.

References

Anderson, J.T., Wilson, S.M., Datar, K.V., and Swanson, M.S. (1993). NAB2: a yeast nuclear polyadenylated RNA-binding protein essential for cell viability. Molecular and cellular biology 13, 2730-2741.

Batisse, J., Batisse, C., Budd, A., Bottcher, B., and Hurt, E. (2009). Purification of nuclear poly(A)-binding protein Nab2 reveals association with the yeast transcriptome and a messenger ribonucleoprotein core structure. The Journal of biological chemistry 284, 34911-34917.

Carmody, S.R., and Wente, S.R. (2009). mRNA nuclear export at a glance. Journal of cell science 122, 1933-1937.

Dieppois, G., and Stutz, F. (2010). Connecting the transcription site to the nuclear pore: a multi-tether process that regulates gene expression. Journal of cell science 123, 1989-1999.

Gilbert, W., and Guthrie, C. (2004). The Glc7p nuclear phosphatase promotes mRNA export by facilitating association of Mex67p with mRNA. Molecular cell 13, 201-212.

Gilbert, W., Siebel, C.W., and Guthrie, C. (2001). Phosphorylation by Sky1p promotes Npl3p shuttling and mRNA dissociation. RNA (New York, NY) 7, 302-313.

Grund, S.E., Fischer, T., Cabal, G.G., Antunez, O., Perez-Ortin, J.E., and Hurt, E. (2008). The inner nuclear membrane protein Src1 associates with subtelomeric genes and alters their regulated gene expression. The Journal of cell biology 182, 897-910.

Hacker, S., and Krebber, H. (2004). Differential export requirements for shuttling serine/arginine-type mRNA-binding proteins. The Journal of biological chemistry 279, 5049-5052.

Hackmann, A., Gross, T., Baierlein, C., and Krebber, H. (2011). The mRNA export factor Npl3 mediates the nuclear export of large ribosomal subunits. EMBO reports 12, 1024-1031.

Hurt, E., Luo, M.J., Rother, S., Reed, R., and Strasser, K. (2004). Cotranscriptional recruitment of the serine-arginine-rich (SR)-like proteins Gbp2 and Hrb1 to nascent mRNA via the TREX complex. Proceedings of the National Academy of Sciences of the United States of America 101, 1858-1862.

Hurt, E., Strasser, K., Segref, A., Bailer, S., Schlaich, N., Presutti, C., Tollervey, D., and Jansen, R. (2000). Mex67p mediates nuclear export of a variety of RNA polymerase II transcripts. The Journal of biological chemistry 275, 8361-8368.

Iglesias, N., Tutucci, E., Gwizdek, C., Vinciguerra, P., Von Dach, E., Corbett, A.H., Dargemont, C., and Stutz, F. (2010). Ubiquitin-mediated mRNP dynamics and surveillance prior to budding yeast mRNA export. Genes & development 24, 1927-1938.

Kress, T.L., Krogan, N.J., and Guthrie, C. (2008). A single SR-like protein, Npl3, promotes pre-mRNA splicing in budding yeast. Molecular cell 32, 727-734.

Lee, M.S., Henry, M., and Silver, P.A. (1996). A protein that shuttles between the nucleus and the cytoplasm is an important mediator of RNA export. Genes & development 10, 1233-1246.

Lei, E.P., Krebber, H., and Silver, P.A. (2001). Messenger RNAs are recruited for nuclear export during transcription. Genes & development 15, 1771-1782.

Lund, M.K., and Guthrie, C. (2005). The DEAD-box protein Dbp5p is required to dissociate Mex67p from exported mRNPs at the nuclear rim. Molecular cell 20, 645-651.
Moehle, E.A., Ryan, C.J., Krogan, N.J., Kress, T.L., and Guthrie, C. (2012). The yeast SR-like protein Npl3 links chromatin modification to mRNA processing. PLoS genetics 8, e1003101.

Nazarenus, T., Cedarberg, R., Bell, R., Cheatle, J., Forch, A., Haifley, A., Hou, A., Wanja Kebaara, B., Shields, C., Stoysich, K., et al. (2005). Upf1p, a highly conserved protein required for nonsense-mediated mRNA decay, interacts with the nuclear pore proteins Nup100p and Nup116p. Gene 345, 199-212.

Nino, C.A., Herissant, L., Babour, A., and Dargemont, C. (2013). mRNA Nuclear Export in Yeast. Chemical reviews.

Santos-Rosa, H., Moreno, H., Simos, G., Segref, A., Fahrenkrog, B., Pante, N., and Hurt, E. (1998). Nuclear mRNA export requires complex formation between Mex67p and Mtr2p at the nuclear pores. Molecular and cellular biology 18, 6826-6838.

Sayani, S., and Chanfreau, G.F. (2012). Sequential RNA degradation pathways provide a fail-safe mechanism to limit the accumulation of unspliced transcripts in Saccharomyces cerevisiae. RNA (New York, NY) 18, 1563-1572.

Sayani, S., Janis, M., Lee, C.Y., Toesca, I., and Chanfreau, G.F. (2008). Widespread impact of nonsense-mediated mRNA decay on the yeast intronome. Molecular cell 31, 360-370.

Segref, A., Sharma, K., Doye, V., Hellwig, A., Huber, J., Luhrmann, R., and Hurt, E. (1997). Mex67p, a novel factor for nuclear mRNA export, binds to both poly(A)+ RNA and nuclear pores. The EMBO journal 16, 3256-3271.

Shen, E.C., Henry, M.F., Weiss, V.H., Valentini, S.R., Silver, P.A., and Lee, M.S. (1998). Arginine methylation facilitates the nuclear export of hnRNP proteins. Genes & development 12, 679-691.

Siniossoglou, S., Lutzmann, M., Santos-Rosa, H., Leonard, K., Mueller, S., Aebi, U., and Hurt, E. (2000). Structure and assembly of the Nup84p complex. The Journal of cell biology 149, 41-54.

Stewart, M. (2007). Ratcheting mRNA out of the nucleus. Molecular cell 25, 327-330.
Strasser, K., and Hurt, E. (2000). Yra1p, a conserved nuclear RNA-binding protein, interacts directly with Mex67p and is required for mRNA export. The EMBO journal 19, 410-420.

Strasser, K., Masuda, S., Mason, P., Pfannstiel, J., Oppizzi, M., Rodriguez-Navarro, S., Rondon, A.G., Aguilera, A., Struhl, K., Reed, R., et al. (2002). TREX is a conserved complex coupling transcription with messenger RNA export. Nature 417, 304-308.

Strawn, L.A., Shen, T., and Wente, S.R. (2001). The GLFG regions of Nup116p and Nup100p serve as binding sites for both Kap95p and Mex67p at the nuclear pore complex. The Journal of biological chemistry 276, 6445-6452.

Suntharalingam, M., and Wente, S.R. (2003). Peering through the pore: nuclear pore complex structure, assembly, and function. Developmental cell 4, 775-789.

Toesca, I., Nery, C.R., Fernandez, C.F., Sayani, S., and Chanfreau, G.F. (2011). Cryptic transcription mediates repression of subtelomeric metal homeostasis genes. PLoS genetics 7, e1002163.

Tran, E.J., Zhou, Y., Corbett, A.H., and Wente, S.R. (2007). The DEAD-box protein Dbp5 controls mRNA export by triggering specific RNA:protein remodeling events. Molecular cell 28, 850-859.

Weil, T.T., Parton, R.M., and Davis, I. (2010). Making the message clear: visualizing mRNA localization. Trends in Cell Biology 20, 380-390.

Windgassen, M., and Krebber, H. (2003). Identification of Gbp2 as a novel poly(A)+ RNA-binding protein involved in the cytoplasmic delivery of messenger RNAs in yeast. EMBO reports 4, 278-283.

Windgassen, M., Sturm, D., Cajigas, I.J., Gonzalez, C.I., Seedorf, M., Bastians, H., and Krebber, H. (2004). Yeast shuttling SR proteins Npl3p, Gbp2p, and Hrb1p are part of the translating mRNPs, and Npl3p can function as a translational repressor. Molecular and cellular biology 24, 10479-10491.

Chapter 3: A Novel Role for the Glucose Repressor Mig1p in the Repression of FIT3

Although iron is an essential nutrient for every living organism, excess amounts of iron can have potentially toxic effects to cells; therefore iron uptake and utilization are tightly regulated. While iron is abundantly present in the earth's crust, it remains largely bio-unavailable to many organisms due to its insolubility. The budding yeast *Saccharomyces cerevisiae* respond to fluctuating levels of iron by increasing or repressing expression of genes involved in iron uptake and utilization. In iron starvation conditions, *S. cerevisiae* respond by transcriptional activation of genes that express proteins that facilitate the import of free iron or the mobilization of siderophore-bound iron (Philpott et al., 2002). Iron import into *S. cerevisiae* is mediated by a number of import proteins whose transcriptional activation is dependent on Aft1p/Aft2p, a transcriptional activator in low iron conditions (Yamaguchi-Iwai et al., 1996). Aft1p/Aft2p target genes include *FRE1-FRE3* (Dancis et al., 1990), components of the reductive system of elemental iron uptake; the high affinity iron transporters *FET3* and *FTR1* (Askwith et al., 1994; Stearman et al., 1996); and *FIT1-FIT3*, cell wall mannoproteins that facilitate the uptake of siderophore bound iron (Protchenko et al., 2001). In the absence of Aft1p, Aft2p functions to activate genes involved in intracellular iron use. The direct transcriptional activation of iron homeostasis genes mediated by Aft1p or Aft2p is gene specific and iron dependent (Blaiseau et al., 2001). While the mechanism of induction and transcriptional targets of Aft1p and Aft2p are well characterized, other regulatory mechanisms that control these genes and their expression in normal and low iron conditions remains unknown. Elucidating these mechanisms of transcriptional control is important because the abnormal expression of these genes may lead to iron deficiency or toxicity in iron deplete and replete condition, respectively.

We have identified a novel role for the glucose repressor Mig1p in the regulation of *FIT3*. *FIT3* encodes the cell wall mannoprotein involved in the transport of siderophore bound iron through the cell wall. The *FIT3* gene is repressed during normal iron

conditions, but activated during iron deprivation to facilitate iron import (Protchenko et al., 2001). While *FIT3* is a known target of the transcription factor Aft1p, the repression of *FIT3* in normal iron conditions must be mediated by a separate regulatory mechanism. While we have shown that upstream cryptic transcription is used as means for regulatory control of *FIT3* (Toesca et al., 2011), we have identified an additional mode of regulation through the action of the glucose repressor Mig1p. As Mig1p has been extensively studied as a repressor for glucose repressed genes, we show that its repressive effect can be applied to iron regulation. We believe that Mig1p regulates the repression of *FIT3* during conditions of normal iron and/or after switch back to normal iron conditions after iron starvation to prevent deleterious expression of *FIT3*, thereby preventing the potentially harmful effects of iron toxicity.

Regulation of Glucose Repression by Mig1p in Saccharomyces cerevisiae

The role of Mig1p in the regulation of glucose repression has been extensively characterized. Glucose repression is a conserved and widely spread mechanism regulating carbon metabolism and results in the inactivation of many genes in *S. cerevisiae* (Klein et al., 1998). A key component of the glucose repression mechanism is the Mig1p transcriptional repressor. In high glucose conditions, binding of Mig1p to GC-rich sequences upstream of target promoters recruits the general transcriptional repressors Ssn6p(Cyc8p)-Tup1p, resulting in the repression of the target genes (Lutfiyya and Johnston, 1996; Papamichos-Chronakis et al., 2004). The Ssn6p-Tup1p general repressor complex is recruited to these promoters by Mig1p and mediates repression by interacting with chromatin remodeling factors and/or general transcriptional machinery. This complex represses transcription of genes regulated by glucose, cell type, DNA damage, and oxygen availability (Malave and Dent, 2006). Low glucose conditions activate the Snf1p kinase, resulting in phosphorylation of Mig1p at serine 311. This

phosphorylation event weakens the repressor complex formed between Mig1p and Ssn6p-Tup1p resulting in both cytoplasmic export of Mig1p as well as the derepression of Mig1p target genes (Papamichos-Chronakis et al., 2004; Treitel and Carlson, 1995; Treitel et al., 1998). Mig1p has been shown to mediate the repression of glucose-repressed genes such as *SUC2*, *HXK1*, *TPS1*, and *HXT2* (Lutfiyya and Johnston, 1996; Sarma et al., 2007; Treitel et al., 1998).

In yeast, Mig1p shares high homology to Mig2p and Mig3p (Lutfiyya et al., 1998; Westholm et al., 2008). All three proteins have been shown to bind similar recognition sequences; a GC-rich box flanked by a 5' AT-rich region but with different affinities (Lundin et al., 1994). While Mig1p, Mig2p, and Mig3p are highly homologous, only Mig1p and Mig2p have been shown to be redundant glucose repressors on many glucose repressed genes involved in metabolic pathways, the heat shock and stress response, and mitochondrial functions (Lutfiyya et al., 1998). *SIR2* is the only known gene target of Mig3p, as this repressor does not regulate the same set of genes as Mig1p and Mig2p in high glucose conditions (Westholm et al., 2008). Localization of these repressor proteins is also regulated differently; Mig1p localization is mediated by glucose concentration as Mig1p is predominately nuclear in high glucose and cytoplasmic as glucose concentration decreases. Mig2p and Mig3p localization is not affected by glucose concentration, both repressors exhibit nuclear localization in the presence or absence of glucose (Lutfiyya et al., 1998). In addition, these repressor proteins display different activation requirements; Snf1-dependent phosphorylation inactivates only Mig1p and not Mig2p or Mig3p. (Papamichos-Chronakis et al., 2004; Treitel et al., 1998). The mechanism of Mig2p/Mig3p activation remains unknown.

Mig1p Mediated Regulation of the Iron Import Gene FIT3

Previous microarray studies conducted to determine the effect of deletion of the Migp repressor proteins on the entire yeast transcriptome identified genes exclusively repressed by Mig1p and Mig3p and genes redundantly repressed by both Mig1p and Mig2p (Westholm et al., 2008). Of these genes detailed in this study, the siderophore transport gene *FIT3* was identified as an exclusive Mig1p target gene. Analysis of the *FIT3* promoter region identified two Mig1p-like binding sites located ~172 and ~116 base pairs upstream of the FIT3 ATG. While we have previously shown regulation of *FIT3* through the actions of Cytoplasmically Degraded Cryptic Unstable Transcripts (CD-CUTS) (Toesca et al., 2011), these observations raised the possibility that repression of *FIT3* during non-inducing (normal iron) conditions could be also mediated by a separate repressor protein like Mig1p. We previously observed that wild-type strains grown in galactose (YPGAL) experience a slight derepression of *FIT3* when compared to a wild type strain grown in normal glucose (YPD; Figure 3.1 compare lanes 1 vs. 2). These results were consistent with previous array analysis showing higher *FIT3* mRNA expression levels in wild type strains grown in galactose (YPGAL) versus wild type strains grown in glucose (YPD; (Xu et al., 2009)). We also observed a more robust expression of *FIT3* mRNA in a wild type strain subjected to iron starvation in galactose media when compared to low iron conditions in glucose (Figure 3.1, compare lanes 3 vs. 4). The derepression of the *FIT3* mRNA in a wild-type strain grown in galactose, along with the two Mig1p-like binding sites in the *FIT3* promoter region led us to hypothesize a possible role for Mig1p-mediated repression of *FIT3*. We reasoned that under non-inducing conditions (normal iron) and/or in return to normal iron conditions following iron starvation, *FIT3* transcription is repressed through the actions of the Mig1p-repressor complex. Mig1p binds to the Mig1p-like binding sequences upstream of the *FIT3* promoter in normal iron conditions where it recruits the Ssn6p-Tup1p repressor complex

to mediate repression of *FIT3*. In the event of lowered glucose concentration or a change of a sugar source such as galactose, the Snf1-dependednt phosphorylation of Mig1p results in nuclear exclusion of Mig1p and the depression of *FIT3* (Figure 3.1, (Xu et al., 2009)). Mig1p mediated repression would prevent the deleterious activation of *FIT3* during normal iron conditions, thereby precluding the potentially toxic effects of premature activation.

To determine the differential effects of the Migp repressor proteins on the expression of *FIT3* mRNA, *FIT3* northern analysis were conducted on strains harboring deletion of the individual Migp repressor proteins (*mig1Δ*, *mig2Δ*, *mig3Δ*). Deletion strains were grown in normal iron media (YPD) and subjected to iron starvation (YPD+BPS) for three hours. As shown in Figure 3.2, *FIT3* mRNA expression in normal iron conditions show differential profiles for the different Migp mutants when compared to the wild type strains (lanes 1,5,9,13). A depression of *FIT3* mRNA is evident in the *mig1Δ* mutant, however the *mig2Δ* and *mig3Δ* mutants do not exhibit this observed *FIT3* mRNA derepression. *FIT3* mRNA expression during iron starvation in the *mig1Δ* mutant also displays a slightly faster induction when compared to the wild type strain (Figure 3.2, compare lanes 5-8 vs. 1-4). This faster induction could be as a result of the contribution of the derepression of *FIT3* already present in the *mig1Δ* mutant. We also assessed the mRNA expression patterns of other members of the *FIT* family iron transporters in the Migp repressor mutants (Figure 3.3). Along with *FIT3*, the *FIT* family of iron transporters is comprised of *FIT1* and *FIT2*, all mediate the import of siderophore bound iron through the yeast cell wall and are activated during low iron conditions (Protchenko et al., 2001). Unlike its *FIT3* counterpart, loss of Mig1p does not result in the derepression of *FIT1* and *FIT2* (Figure 3.3 lane 2). Consistent with previous results, we are able to observe *FIT3* derepression in absence of Mig1p (Figure 3.3 lane 2, Figure 3.2). Loss of Mig2p and Mig3p also do not result in derepression of *FIT1*, *FIT2*, and *FIT3*

mRNA during normal iron conditions (Figure 3.3, lane 3,4 t=0). These results indicate that the Migp repressor proteins (Mig1p, Mig2p, Mig3p) do not have repressor functions in the regulation of *FIT1* and *FIT2* mRNA during normal iron conditions. *FIT3* mRNA repression is predominantly mediated by Mig1p. We did observe a higher expression of *FIT2* mRNA in the absence of Mig1p (Figure 3.3, lane 10) when compared to the wild type strain. Our results also showcase the different expression patterns of the *FIT* family proteins, as they display different induction times but are all robustly expressed by three hours of iron starvation (Figure 3.3, compare induction times of *FIT1* vs. *FIT2*, *FIT3*).

We also asked if Mig1p-mediated repression of *FIT3* in normal iron conditions could be applied to other iron genes in the Aft1p iron regulon. We chose to assess the expression profiles of the *ARN* and *FRE* family of proteins. The *ARN*-family of proteins mediates the transport of siderophore bound iron through the plasma membrane during conditions of iron starvation (Heymann et al., 2000; Yun et al., 2000). *FRE1* is a member of the *FRE* family of plasma membrane reductases and encodes a ferric reductase activated during low iron conditions (Yun et al., 2001). As shown in Figure 3.4, loss of the Migp repressor proteins (*mig1Δ*, *mig2Δ*, *mig3Δ*) does not affect the mRNA expression profiles for *ARN2*, *ARN4*, and *FRE1* in normal iron conditions. These results indicate that Mig1p mediated repression during normal iron condition is specific to *FIT3*. Our results also show case the induction profiles for the different members of the Aft1p iron regulon, as some genes are induced earlier in the iron starvation time course (Figure 3.4, compare *FRE1* vs. *ARN2*). We also observed less induction of *ARN2*, *ARN4*, and *FRE1* in the Migp mutants (Figure 3.4 lanes 13-16, *mig1Δ*, *mig2Δ*, *mig3Δ*) when compared to wild type during the later time stages of iron starvation (3hrs). These results further validate previous observations of the different kinetics and expression profiles of the different proteins of the Aft1p/Aft2p iron regulon.

As we have observed that the strongest *FIT3* mRNA derepression during normal iron conditions occurs in the absence of Mig1p, we assayed all possible deletion combinations of the Migp repressor proteins and their effect on the expression of *FIT3* mRNA during normal and now iron conditions (Figure 3.5-Figure 3.8). We hypothesized that a greater derepression of *FIT3* mRNA would be evident in double deletion mutants harboring a deletion of Mig1p due to the dominant repression exerted by Mig1p over Mig2p/Mig3p As shown in Figure 3.5, derepression of *FIT3* mRNA is observed in the *mig1Δ* mutant (lane 2) with even greater derepression observed in double mutants harboring a deletion of Mig1p (lanes 5,6). Consistent with our previous results, *FIT3* mRNA derepression occurs in the absence of Mig1p (Figure 3.6, lane 2) when compared to wild type in normal iron conditions. This derepression does not occur in the absence of Mig2p (Figure 3.6, lane 3), indicating that *FIT3* is not redundantly regulated by both Mig1p and Mig2p. An increased level of *FIT3* mRNA is evident in the double *mig1Δmig2Δ* mutant (Figure 3.6, lane 4). Previous studies have shown that the repressive function of Mig2p is always in conjunction with Mig1p (Lutfiyya and Johnston, 1996), so absence of both repressors could result in a higher level of derepression. *FIT3* mRNA is also more expressed in the Migp repressor mutants (*mig1Δ*, *mig1Δmig2Δ*) during the early time points of the low iron shift (Figure 3.6, lanes 6,8). This increased *FIT3* expression could be attributed to the contribution of *FIT3* derepression during normal iron conditions that occurs in the absence of Mig1p and Mig2p, so already activated *FIT3* can result in higher expression during inducing (low iron) conditions. We did not observe the same mRNA expression profiles observed for *FIT3* in northern analysis for *FRE1* and *ARN3* in the single *mig1Δ*, *mig2Δ* mutants and the double *mig1Δmig2Δ* mutant (Figure 3.6 *FRE1*, *ARN3* panel). Once again these results show the specificity of Mig1p and Mig2p mediated repression for *FIT3*.

A similar *FIT3* mRNA expression profile was observed in the *mig1Δmig3Δ* double mutant grown in normal iron conditions. As shown in Figure 3.7, *FIT3* mRNA derepression is observed in the *mig1Δ* and the *mig1Δmig3Δ* strains (lane 1,4). Increased *FIT3* mRNA expression is also observed in all strains lacking Mig1p during the low iron shift, as well as full induction of *FIT3* mRNA during the early time points of the low iron shift. This pattern of induction and expression of *FIT3* is specific, as we do not observe the same profile for other genes assayed (Figure 3.7, *FRE1*, *FIT2*, *ARN4* panels). Further evidence for *FIT3* specificity of Mig1p mediated repression is exemplified when *FIT3* expression during normal iron conditions is assayed in the single *mig2Δ* and *mig3Δ* strains and the double *mig2Δmig3Δ* strain. Consistent with our previous Northern analysis (Figure 3.2, Figure 3.3), loss of Mig2p, Mig3p or in combination of each other has no effect on the derepression of *FIT3* during normal iron conditions (Figure 3.8, *FIT3* panel). Northern analysis of *ARN2* mRNA for the single *mig2Δ* and *mig3Δ* mutants as well as the double *mig2Δmig3Δ* show indicate that loss of Mig2p/Mig3p has no effect on the expression patterns of *ARN2* (Figure 3.7, *ARN2* panel). Collectively our results indicate *FIT3* mRNA repression under normal iron conditions is primarily mediated by the Mig1p repressor and Northern analysis of individual and double mutant combinations of the Migp repressor proteins indicate Mig1p is the dominant repressor of *FIT3* in normal iron conditions (Figure 3.8). In the absence of Mig1p, Mig2p can contribute to a lower level of repression of *FIT3* which is represented by the higher level of *FIT3* expression in the *mig1Δmig2Δ* (Figure 3.6), however our data suggest that Mig1p plays a more dominant repressor role in *FIT3* mRNA regulation.

We have identified that Mig1p plays a dominant role in *FIT3* repression among the Migp repressor proteins in normal iron conditions, we then asked if Mig1p also mediates repression of *FIT3* after growth conditions are switched back to normal iron following iron starvation. To monitor *FIT3* expression after switch back to normal iron

conditions, combinations mutants of the Migp repressor proteins (*mig1Δmig2Δ*, *mig1Δmig3Δ*, *mig2Δmig3Δ*) were subjected to iron starvation then switched back to normal iron media. Our results indicate that loss of Mig1p results in increased *FIT3* mRNA expression during normal iron conditions following iron starvation (Figure 3.9A). As observed in the *mig1Δmig2Δ* and *mig1Δmig3Δ* double mutants, loss of Mig1p in combination with Mig2p/Mig3p results in increased *FIT3* expression in normal iron conditions after growth in low iron when compared to wild type (Figure 3.9A, compare lanes 9-12, 15-18 to lanes 3-6). We do not observe the same *FIT3* expression profile in the *mig2Δmig3Δ* strain subjected to the same backshift experiment (Figure 3.9B), which exhibits a *FIT3* expression profile similar to wild type in normal iron conditions following iron starvation. These results strengthen our belief that Mig1p plays the major repressor role in *FIT3* repression in conditions of normal iron as well as after switch back to normal iron following a period of iron starvation.

Analysis of the *FIT3* promoter region identified two Mig1p-like binding sites located ~172 and ~116 base pairs upstream of the *FIT3* promoter region. We hypothesized that deletion of these binding sites should abolish Mig1p binding and result in loss of Mig1p-mediated repression of *FIT3* during normal iron conditions. Consistent with our hypothesis, deletion of the first Mig1p-like binding site ~172 base pairs upstream of the *FIT3* promoter region resulted in a slight derepression of *FIT3* mRNA in normal iron conditions (Figure 3.10A). We also tested whether deletion of this first upstream Mig1p-like binding (~172 position) site would have any effect on the repression of *FIT3* after switch back to normal iron following iron starvation. As shown in Figure 3.10B, a slight increase in *FIT3* mRNA expression is observed in the binding mutant grown in normal iron conditions following iron starvation (compares lanes 8-10 vs. 3-5). We cannot rule out the contribution of the second Mig1p-like binding site at position ~117 upstream of the *FIT3* ATG in the repression of *FIT3* in this mutant strain. It could

be possible that a low level of repression still occurs through this remaining binding site and that deletion of both binding sites is necessary to confer noticeable derepression of *FIT3* in normal iron conditions. Due to technical constraints, we were unable to generate the double Mig1p-like binding site (positions ~172 an ~117) mutant required for this study.

Discussion

We have previously shown that cryptic transcription can be used as a means for regulatory control of the subtelomeric iron transport gene *FIT3* (Toesca et al., 2011). However, we cannot rule out the possibility that *FIT3* regulation during normal iron conditions may also be regulated through the actions of a repressor protein. Regulation of *FIT3* maybe mediated through the dual actions of cryptic transcription (CD-CUTs) and a DNA binding repressor protein. In these studies we have identified an additional mode of regulation of FIT3 through the action of the glucose repressor Mig1p. Mig1p has been extensively studied as repressor for glucose repressed genes such as *SUC2* and *HXT2* (Ahuatzi et al., 2004; Lutfiyya and Johnston, 1996) and here we show that its repressive effect can also be applied to iron regulation. We hypothesized that Mig1p-mediated repression of *FIT3* occurs during conditions of normal iron, as well as after switch back to growth in normal iron conditions following iron starvation. This *FIT3* repression is critical to prevent deleterious expression of *FIT3* during normal iron conditions, thereby preventing the potentially harmful effects of iron toxicity.

Our findings show that Mig1p mediated repression during normal iron conditions is specific to *FIT3*; Northern analysis of other Aft1p iron regulon genes (ARN-family, *FRE1*, *FET3*, *FIT1*, *FIT2*) did not exhibit the same mRNA expression profile as that observed for *FIT3* (Figure 3.3-3.8). In the absence of Mig1p, a derepression of *FIT3* during normal iron conditions was observed. Derepression of *FIT3* during normal iron

conditions was also specific to Mig1p, as deletion of Mig2p or Mig3p did not alter *FIT3* mRNA expression. Deletion of Mig2p or Mig3p only altered *FIT3* mRNA expression when coupled to the loss of Mig1p, indicating that Mig1 was the major repressor amongst the Migp repressor proteins (Figure 3.5), however Mig2p and Mig3p can also contribute to a lower level of repression. Our northern analysis results of *FIT3* derepression during normal iron conditions is in agreement with previous microarray studies showing around a four-fold increase in expression of *FIT3* in the *mig1Δ* strain (Westholm et al., 2008).

As discussed above, deletion of Mig2p/Mig3p only alters *FIT3* mRNA expression during normal iron conditions when coupled to the absence of Mig1p. The effects of the Migp double mutants (*mig1Δmig2Δ*, *mig1Δmig3Δ*) on *FIT3* mRNA expression is exemplified in our backshift experiments where increased *FIT3* expression is observed in normal iron conditions following iron starvation when compared to a wild type strain (Figure 3.9A). Increased *FIT3* expression is not observed in the *mig2Δmig3Δ* mutant post iron starvation (Figure 3.9B) further supporting our belief that the repressive effects on *FIT3* is primarily due to the action of Mig1p. Deletion of the first Mig1p-like binding site ~172 upstream of the *FIT3* promoter region resulted in a slight depression of *FIT3* mRNA during normal iron conditions (Figure 3.10A). We reasoned that deletion of this Mig1p-like binding site would abolish Mig1p-mediated repression of *FIT3* during normal iron conditions and our initial results from this binding site mutant is in agreement with our hypothesis. However, we are unable to discount the repressive effects on the second Mig1p-like binding site located at ~117 upstream of the FIT3 promoter region. Technical issues have prevented us from generating the double Mig1p-like binding site mutant; where both sites at positions are ~172 and ~117 are deleted. Deletion of both binding sites could be necessary to observe a complete loss of Mig1p mediated repression of *FIT3* during normal iron conditions.

In addition, we attempted to use Mig1-HA Chromatin Immunoprecipitation (ChIP) to observe Mig1p association at the Mig1p binding sites upstream of the *FIT3* ATG. We hoped to detect Mig1p binding at the binding sites located ~172 and ~117 upstream of the *FIT3* promoter region during conditions of normal iron as well as normal iron conditions following iron starvation. We were able to detect Mig1p association at the upstream binding sites (data not shown) during normal iron conditions as well as in normal iron conditions post iron starvation. Mig1p association at the upstream binding sites was also detected during low iron conditions. This association with the Mig1p-binding sites during low iron conditions is expected as the glucose concentration in the YPD media (2%) is considered to be of normal glucose concentration. As we were able to detect Mig1p association at the upstream Mig1p-binding sites during normal iron, low iron, and normal iron conditions following iron starvation, we have observed great variability within individual experiments. This variability is due to technical issues within the individual experiments, but can resolved with trouble shooting of data analysis and normalization to wild type controls.

In conclusion, we have identified an additional mode of regulation of *FIT3* during normal iron conditions by the glucose repressor Mig1p (Figure 3.11). As Mig1p has been classically studied as an important mediator for glucose regulation, we show that its repressive effects can be applied to iron regulation. While we were unable to rule out loss of full repression in the Mig1p binding site mutants and variability among our Mig1p ChIP studies due to technical constraints, our initial evidence of Mig1p mediated repression of *FIT3* is in agreement with previous microarray studies indicating a role of Mig1p in the regulation of *FIT3* (Westholm et al., 2008). Future studies to address localization of Mig1p during iron stress would be useful in determining whether Mig1p nuclear exclusion results in activation of *FIT3* or if Mig1p remains bound at the *FIT3* promoter regardless of cellular iron concentration.

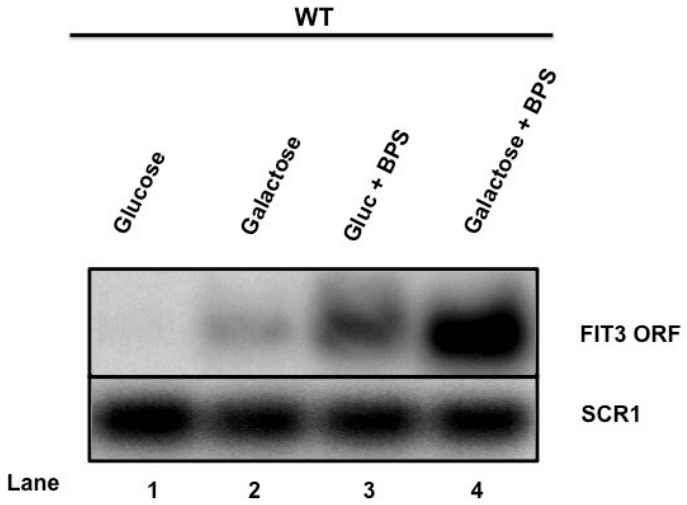


Figure 3.1 *FIT3* depression in wild-type strain grown in galactose. Northern blot analysis of *FIT3* mRNA in wild type strain (OB 4741) grown in glucose (YPD) and galactose (YPGAL) with iron depletion for each condition. Wild type strain grown in YPD/YPG to logarithmic phase then switched to growth in low iron conditions for 3 hours. Low iron conditions achieved by addition of the iron chelator Bathophenanthroline disulfonic acid (BPS) to medium for final BPS concentration of 300mM BPS.

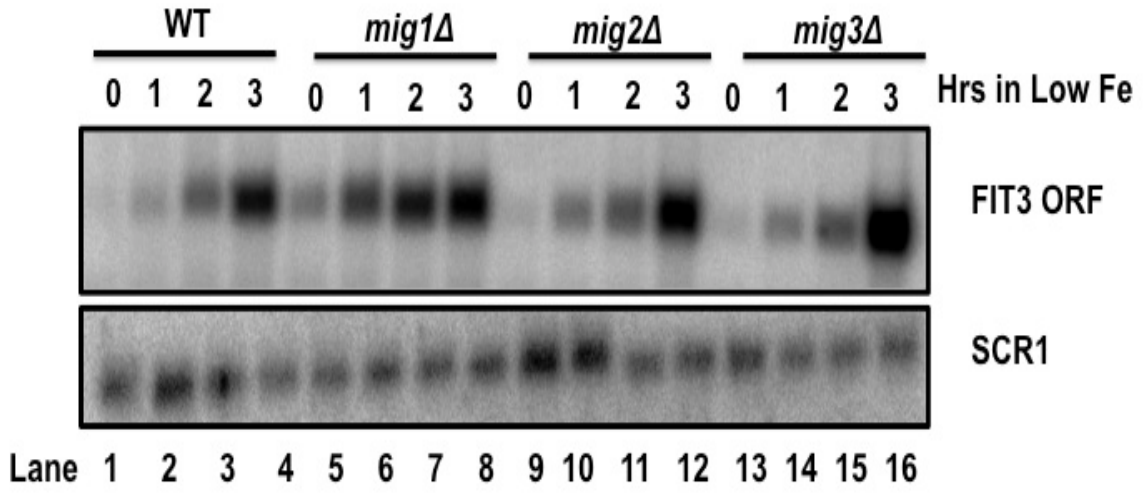


Figure 3.2 Migp mutants exhibit differential *FIT3* mRNA expression profiles. Northern blot analysis of *FIT3* mRNA in wild type strain (OB 4741) and Migp repressor mutants grown in normal iron, (YPD) and low iron conditions (YPD+BPS). Strains with indicated genotypes grown in normal iron (YPD) to logarithmic phase then switched to growth in low iron conditions for three hours. Low iron conditions achieved by addition of the iron chelator Bathophenanthroline disulfonic acid (BPS) to medium for final concentration of 300mM BPS.

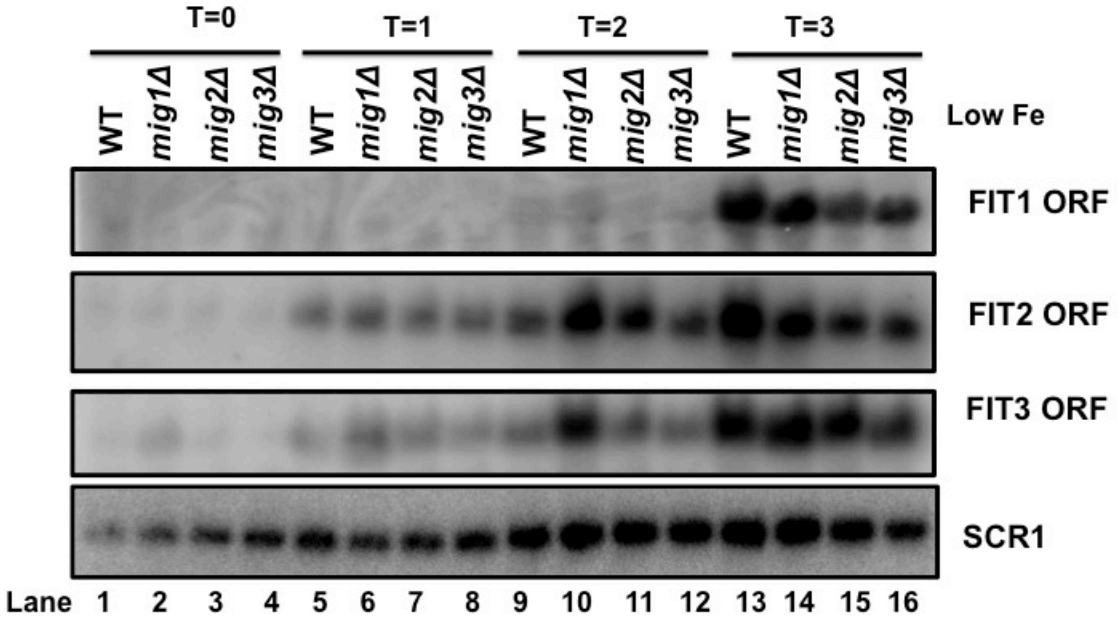


Figure 3.3. Migp mutants display differential *FIT*-family expression profiles. Northern blot analysis of *FIT1*, *FIT2*, and *FIT3* mRNA expression in Migp repressor mutants grown in normal (YPD) and low iron conditions (YPD+BPS). Strains with indicated genotypes grown in normal iron (YPD) to logarithmic phase then switched to growth in low iron conditions for three hours. Low iron conditions achieved by addition of the iron chelator Bathophenanthroline disulfonic acid (BPS) to medium for final BPS concentration of 300mM BPS.

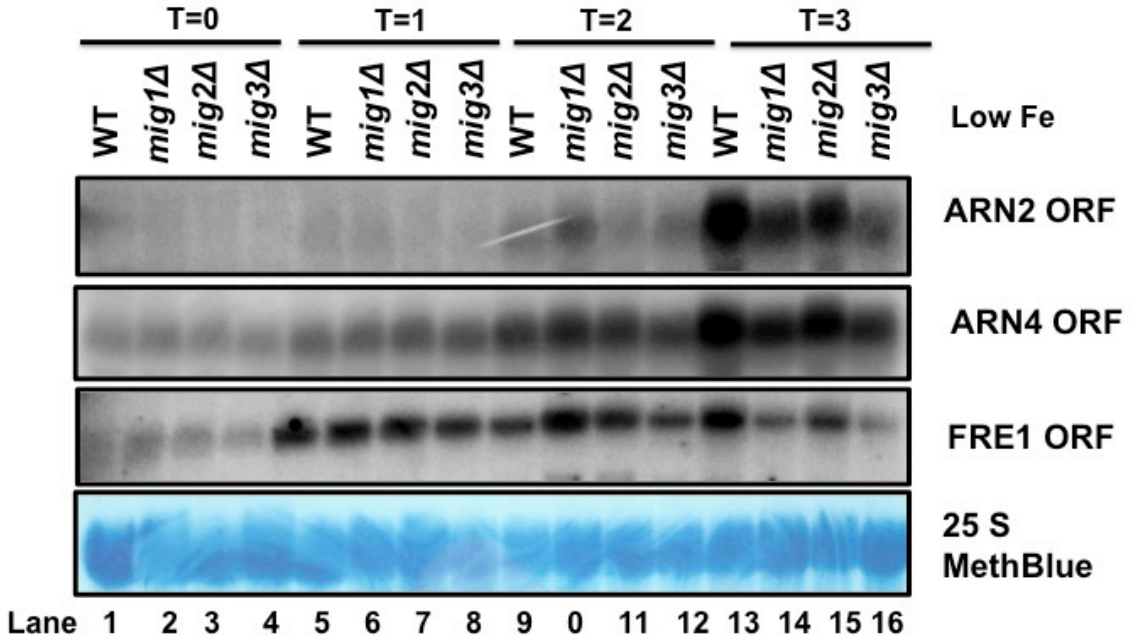


Figure 3.4. Mig1p mediated repression is not observed for other genes (*ARN, FRE)* in the Aft1p iron regulon. Northern blot analysis of *ARN2*, *ARN4*, and *FRE1* mRNA expression in Migp repressor mutants grown in normal and low iron conditions. Strains with indicated genotypes grown in normal iron (YPD) to logarithmic phase and switched to growth in low iron conditions (YPD+BPS) for three hours. Low iron conditions achieved by addition of the iron chelator Bathophenanthroline disulfonic acid (BPS) to medium for final BPS concentration of 300mm BPS.

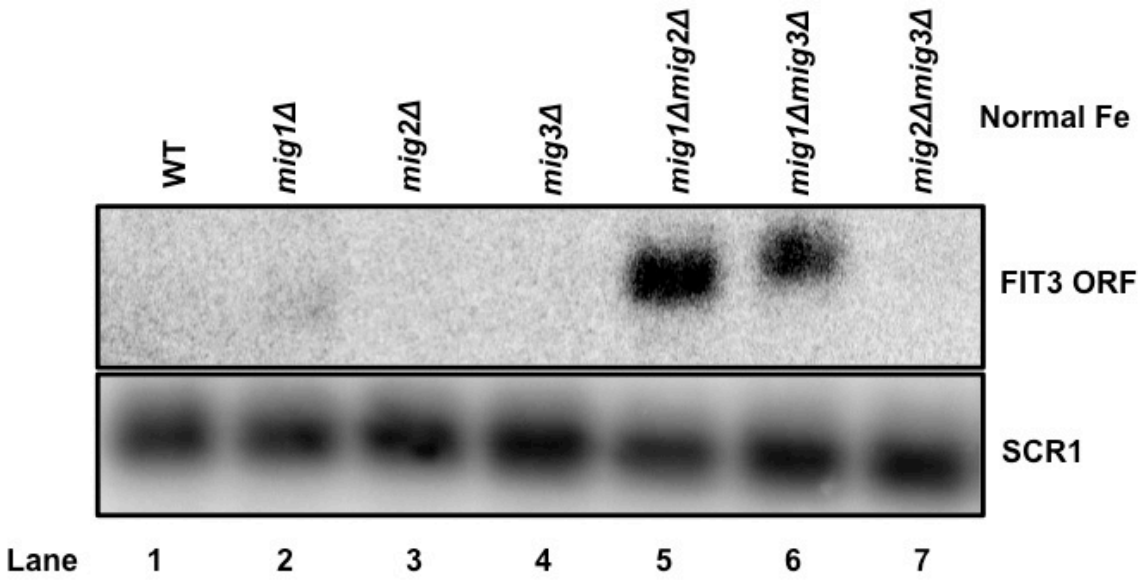


Figure 3.5. Mig1p mediates *FIT3* mRNA repression in normal iron conditions. Northern blot analysis of *FIT3* mRNA in Migp repressor single (*mig1Δ, mig2Δ, mig3Δ*) and double (*mig1Δmig2Δ*, *mig1Δmig3Δ*, and *mig2Δmig3Δ*) strains grown to logarithmic phase in normal iron (YPD) conditions.

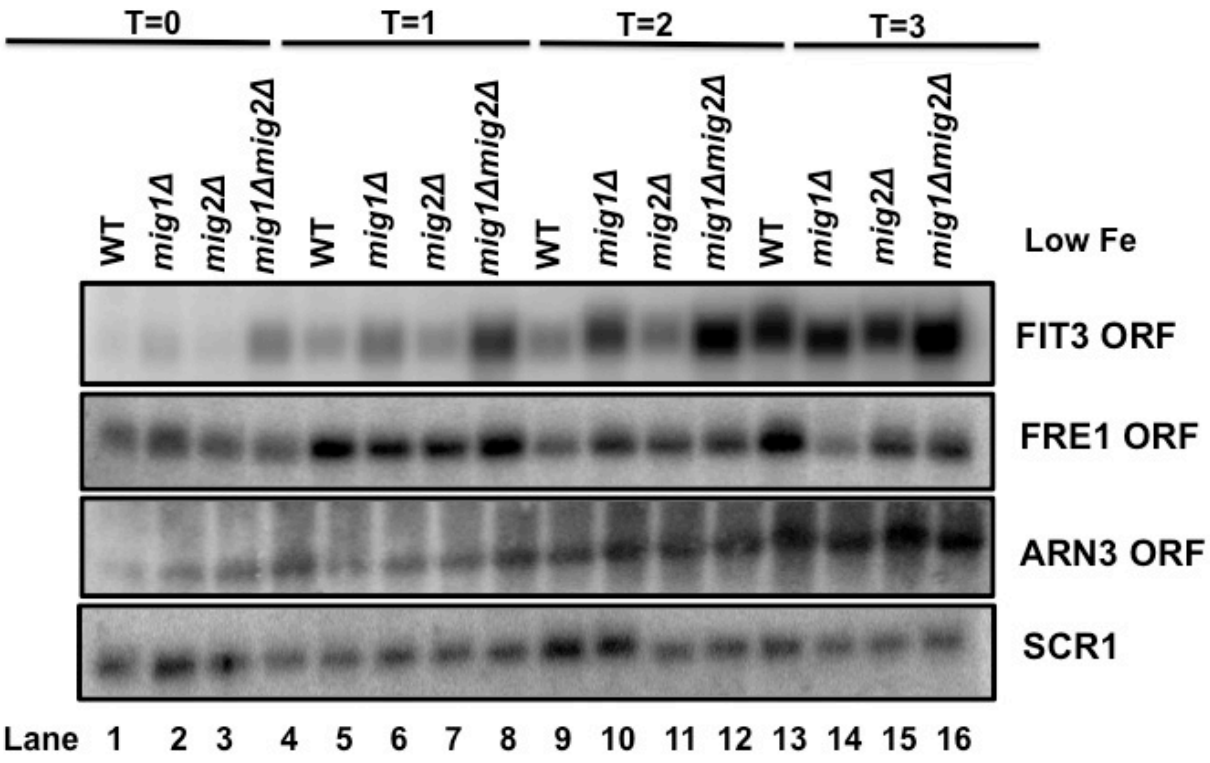


Figure 3.6. Mig1p mediated repression is specific to *FIT3*. Northern blot analysis of *FIT3*, *FRE1*, and *ARN3* mRNA in Migp repressor single (*mig1Δ*, *mig2Δ*) and double (*mig1Δmig2Δ*) grown in normal and low iron conditions. Strains with indicated genotypes grown in normal iron (YPD) to logarithmic phase and switched to growth in low iron conditions (YPD+BPS). Low iron conditions achieved by addition of the iron chelator Bathophenanthroline disulfonic acid (BPS) to medium for final BPS concentration of 300mm BPS.

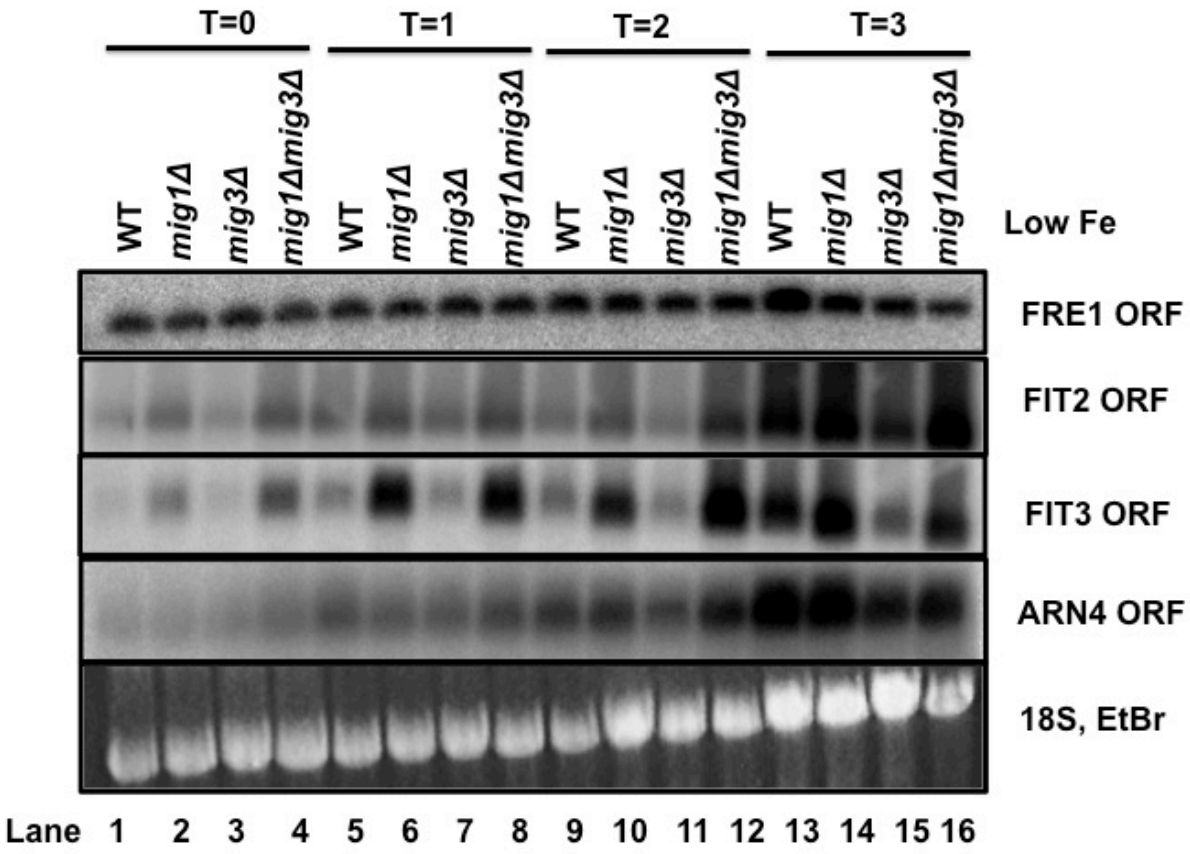


Figure 3.7. Mig1p mediated repression is specific to *FIT3*. Northern blot analysis of *FRE1*, *FIT2*, *FIT3*, *FIT3*, and *ARN4* mRNA in the Migp repressor single (*mig1Δ*, *mig3Δ*) and double (*mig1Δmig3Δ*) mutants grown in normal (YPD) and low iron (YPD+BPS) conditions. Strains with indicated genotypes grown in normal iron (YPD) to logarithmic phase and switched to growth in low iron conditions (YPD+BPS). Low iron conditions achieved by addition of the iron chelator Bathophenanthroline disulfonic acid (BPS) to medium for final BPS concentration of 300mm BPS.

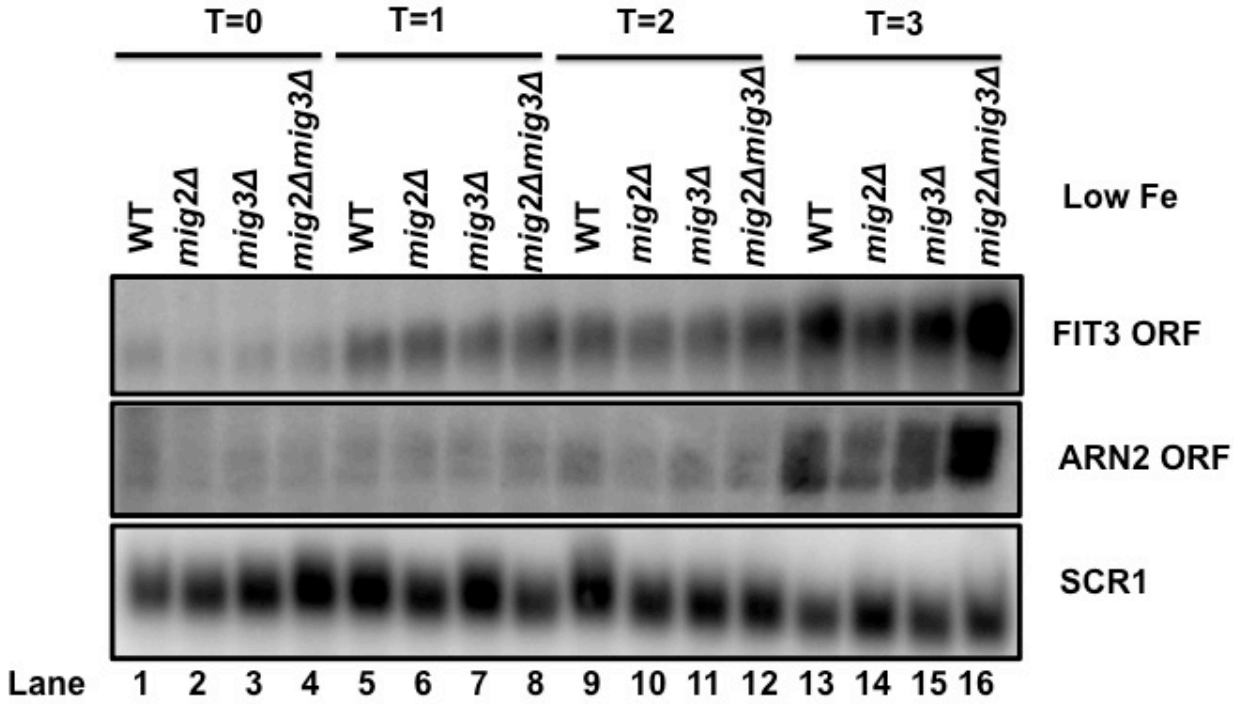


Figure 3.8. Mig1p mediated repression is specific to *FIT3.* Northern blot analysis of *FIT3* and *ARN2* mRNA in Migp repressor single (*mig2Δ*, *mig3Δ*) and double (*mig2Δmig3Δ*) mutants grown in normal (YPD) and low iron (YPD+BPS) conditions. Strains with indicated genotypes grown in normal iron (YPD) to logarithmic phase and switched to growth in low iron conditions (YPD+BPS). Low iron conditions achieved by addition of the iron chelator Bathophenanthroline disulfonic acid (BPS) to medium for final BPS concentration of 300mm BPS.

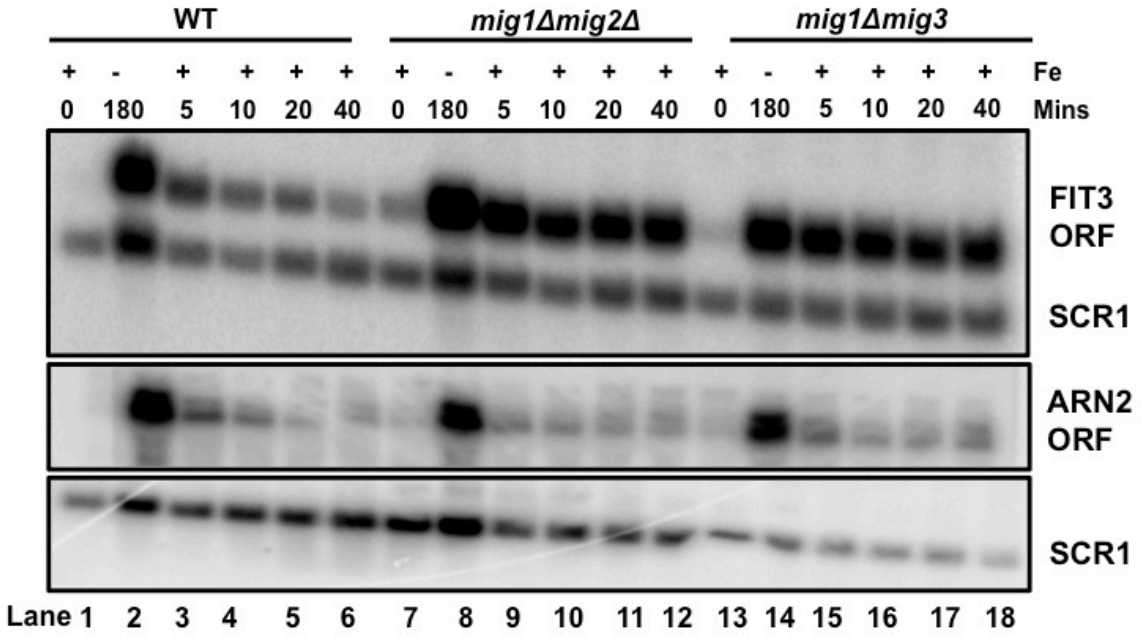


Figure 3.9A. Mig1p mediates repression of *FIT3* after switch to normal iron conditions following iron starvation. Northern blot analysis of *FIT3* and *ARN2* mRNA in Migp repressor double mutants (*mig1Δmig2Δ*, *mig1Δmig3Δ*) subjected to backshift growth conditions. Strains with indicated genotypes grown in normal iron conditions (YPD) to logarithmic phase, switched to growth in low iron conditions (YPD+BPS) for three hours, then grown in normal iron (YPD) conditions. Time points taken 5,10,20, and 40 mins following low iron shift. Low iron conditions achieved by addition of the iron chelator Bathophenanthroline disulfonic acid (BPS) to medium for final BPS concentration of 300mm BPS.

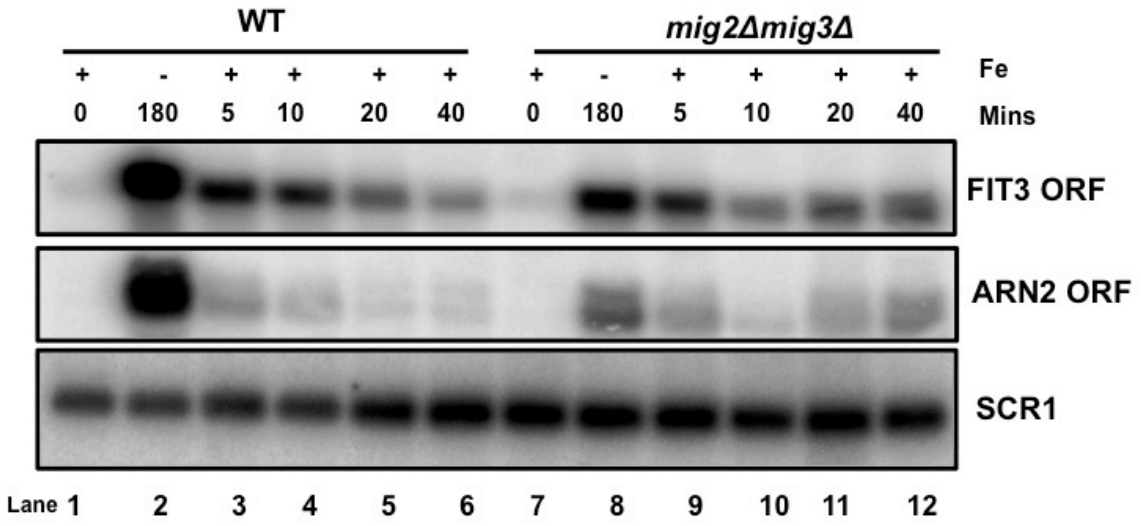


Figure 3.9B. Mig1p mediates repression of *FIT3* after switch to normal iron conditions following iron starvation. Northern blot analysis of *FIT3* and *ARN2* mRNA in Migp repressor double mutants (*mig2Δmig3Δ*) subjected to backshift growth conditions. Strains with indicated genotypes grown in normal iron conditions (YPD) to logarithmic phase, switched to growth in low iron conditions (YPD+BPS) for three hours, then grown in normal iron (YPD) conditions. Time points taken 5,10,20, and 40 mins following low iron shift. Low iron conditions achieved by addition of the iron chelator Bathophenanthroline disulfonic acid (BPS) to medium for final BPS concentration of 300mm BPS.

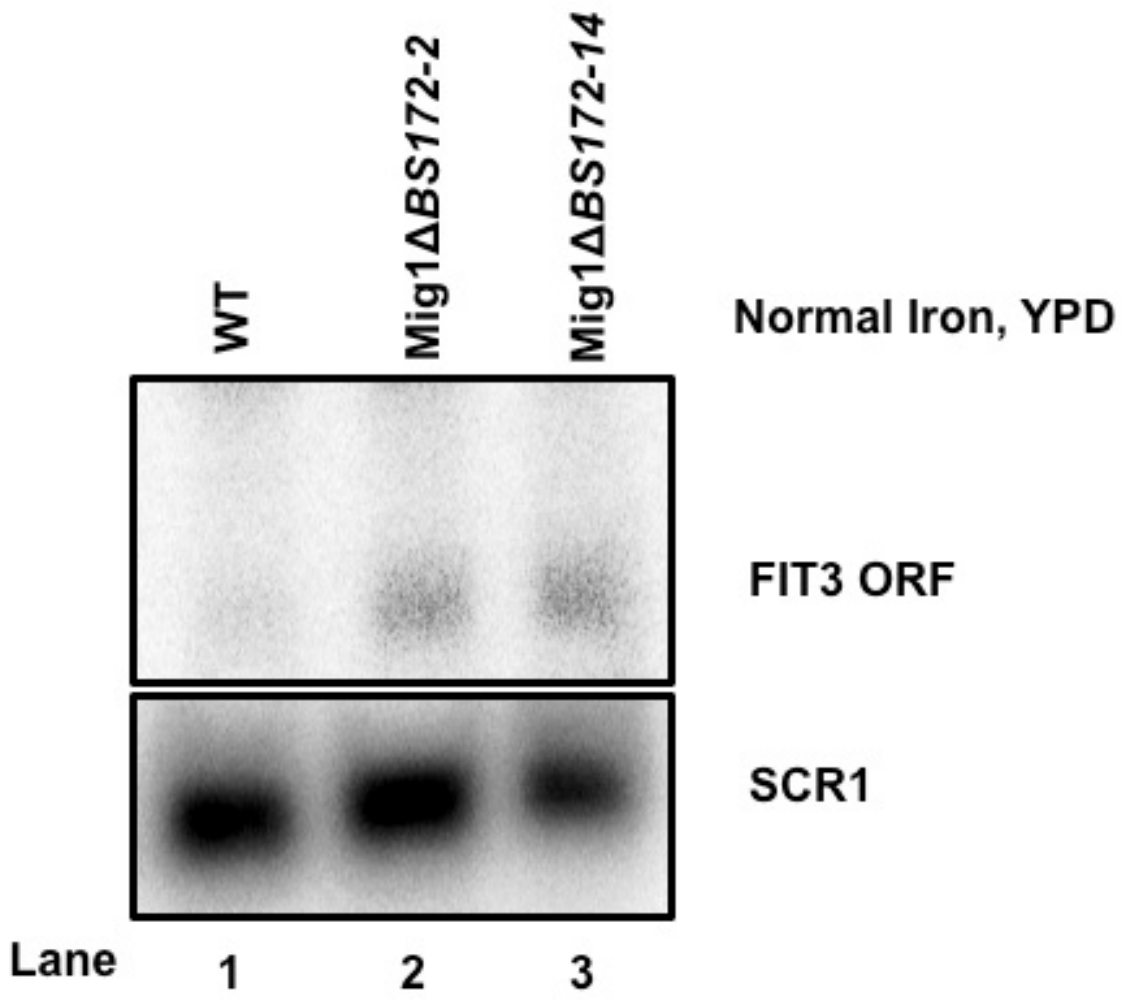


Figure 3.10A. Deletion of upstream Mig1p-like binding confers partial derepression of *FIT3*. Northern analysis of *FIT3* mRNA in wild type background strain lacking first Mig1p-like binding site ~172 base pairs upstream of *FIT3* promoter region. Mig1p-like binding site mutants (independent clones 2,4) generated using *delitto* perfetto (Storici et al., 2001). Strains with indicated genotypes grown in normal iron conditions (YPD) to logarithmic phase.

Storici, F., Lewis, L.K., and Resnick, M.A. (2001). In vivo site-directed mutagenesis using oligonucleotides. Nature biotechnology *19*, 773-776.

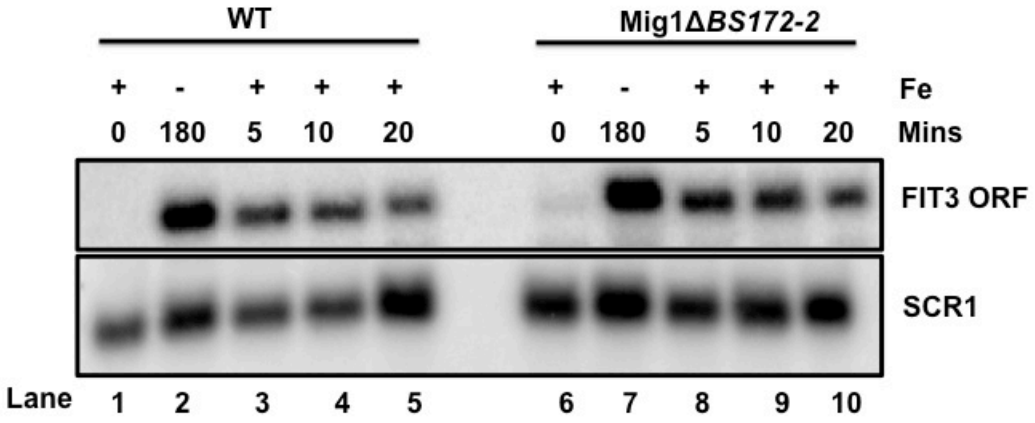


Figure 3.10B. Deletion of upstream Mig1p-like binding site increases *FIT3* mRNA expression after shift to normal iron conditions following iron starvation. Northern analysis of *FIT3* mRNA in wild type background strain lacking first Mig1p-like binding site ~172 base pairs upstream of *FIT3* promoter region subjected to backshift growth conditions. Mig1p-like binding site mutant (independent clone 2) generated using *delitto* perfetto (Storici et al., 2001). Strains with indicated genotypes grown in normal iron conditions (YPD) to logarithmic phase, switched to growth in low iron conditions (YPD+BPS) for three hours, then grown in normal iron (YPD) conditions. Time points taken 5,10,20, and 40 mins following low iron shift. Low iron conditions achieved by addition of the iron chelator Bathophenanthroline disulfonic acid (BPS) to medium for final BPS concentration of 300mm BPS.

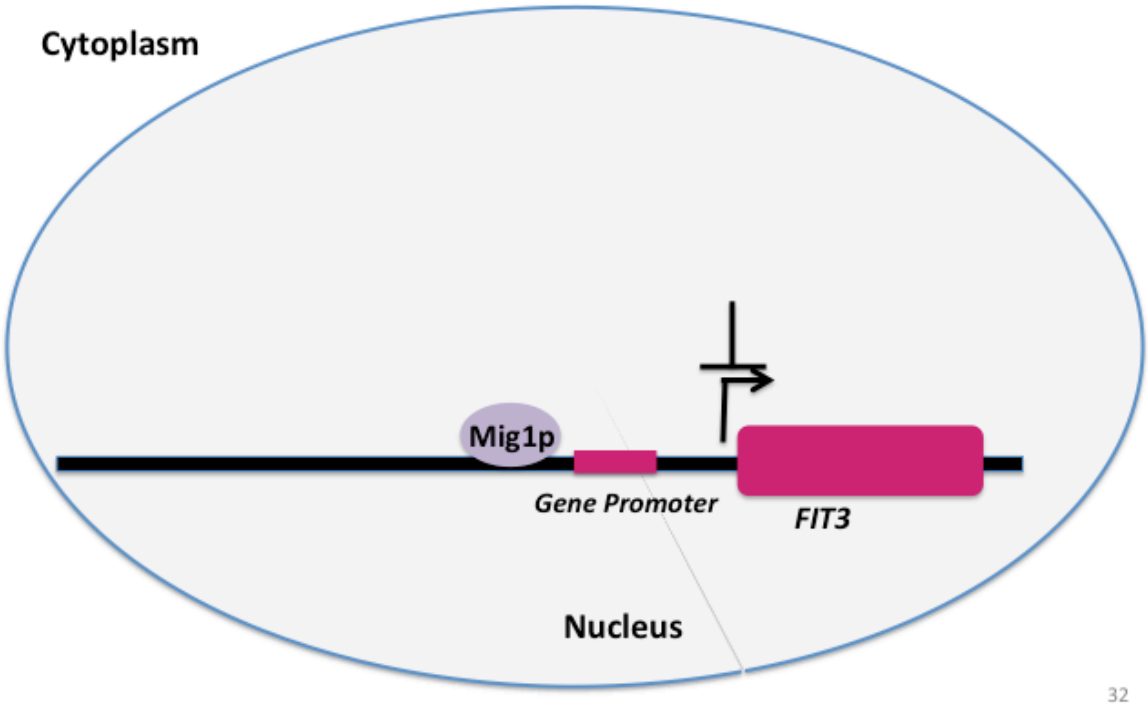


Figure 3.11. Model for Mig1p mediated repression for *FIT3* in normal iron conditions. In normal iron conditions and after cells are switched back to normal iron following iron starvation, Mig1p binds to recognition sequences upstream of *FIT3* to mediate repression of *FIT3.*

References

Ahuatzi, D., Herrero, P., de la Cera, T., and Moreno, F. (2004). The glucose-regulated nuclear localization of hexokinase 2 in Saccharomyces cerevisiae is Mig1-dependent. The Journal of biological chemistry 279, 14440-14446.

Askwith, C., Eide, D., Van Ho, A., Bernard, P.S., Li, L., Davis-Kaplan, S., Sipe, D.M., and Kaplan, J. (1994). The FET3 gene of S. cerevisiae encodes a multicopper oxidase required for ferrous iron uptake. Cell 76, 403-410.

Blaiseau, P.L., Lesuisse, E., and Camadro, J.M. (2001). Aft2p, a novel iron-regulated transcription activator that modulates, with Aft1p, intracellular iron use and resistance to oxidative stress in yeast. The Journal of biological chemistry 276, 34221-34226.

Dancis, A., Klausner, R.D., Hinnebusch, A.G., and Barriocanal, J.G. (1990). Genetic evidence that ferric reductase is required for iron uptake in Saccharomyces cerevisiae. Molecular and cellular biology 10, 2294-2301.

Heymann, P., Ernst, J.F., and Winkelmann, G. (2000). Identification and substrate specificity of a ferrichrome-type siderophore transporter (Arn1p) in Saccharomyces cerevisiae. FEMS microbiology letters 186, 221-227.

Klein, C.J., Olsson, L., and Nielsen, J. (1998). Glucose control in Saccharomyces cerevisiae: the role of Mig1 in metabolic functions. Microbiology (Reading, England) 144 (Pt. 1), 13-24.

Lundin, M., Nehlin, J.O., and Ronne, H. (1994). Importance of a flanking AT-rich region in target site recognition by the GC box-binding zinc finger protein MIG1. Molecular and cellular biology 14, 1979-1985.

Lutfiyya, L.L., Iyer, V.R., DeRisi, J., DeVit, M.J., Brown, P.O., and Johnston, M. (1998). Characterization of three related glucose repressors and genes they regulate in Saccharomyces cerevisiae. Genetics 150, 1377-1391.

Lutfiyya, L.L., and Johnston, M. (1996). Two zinc-finger-containing repressors are responsible for glucose repression of SUC2 expression. Molecular and cellular biology 16, 4790-4797.

Malave, T.M., and Dent, S.Y. (2006). Transcriptional repression by Tup1-Ssn6. Biochemistry and cell biology = Biochimie et biologie cellulaire 84, 437-443.

Papamichos-Chronakis, M., Gligoris, T., and Tzamarias, D. (2004). The Snf1 kinase controls glucose repression in yeast by modulating interactions between the Mig1 repressor and the Cyc8-Tup1 co-repressor. EMBO reports 5, 368-372.

Philpott, C.C., Protchenko, O., Kim, Y.W., Boretsky, Y., and Shakoury-Elizeh, M. (2002). The response to iron deprivation in Saccharomyces cerevisiae: expression of siderophore-based systems of iron uptake. Biochemical Society transactions 30, 698-702.

Protchenko, O., Ferea, T., Rashford, J., Tiedeman, J., Brown, P.O., Botstein, D., and Philpott, C.C. (2001). Three cell wall mannoproteins facilitate the uptake of iron in Saccharomyces cerevisiae. The Journal of biological chemistry 276, 49244-49250.

Sarma, N.J., Haley, T.M., Barbara, K.E., Buford, T.D., Willis, K.A., and Santangelo, G.M. (2007). Glucose-responsive regulators of gene expression in Saccharomyces cerevisiae function at the nuclear periphery via a reverse recruitment mechanism. Genetics 175, 1127-1135.

Stearman, R., Yuan, D.S., Yamaguchi-Iwai, Y., Klausner, R.D., and Dancis, A. (1996). A permease-oxidase complex involved in high-affinity iron uptake in yeast. Science (New York, NY) 271, 1552-1557.

Toesca, I., Nery, C.R., Fernandez, C.F., Sayani, S., and Chanfreau, G.F. (2011). Cryptic transcription mediates repression of subtelomeric metal homeostasis genes. PLoS genetics 7, e1002163.

Treitel, M.A., and Carlson, M. (1995). Repression by SSN6-TUP1 is directed by MIG1, a repressor/activator protein. Proceedings of the National Academy of Sciences of the United States of America 92, 3132-3136.

Treitel, M.A., Kuchin, S., and Carlson, M. (1998). Snf1 protein kinase regulates phosphorylation of the Mig1 repressor in Saccharomyces cerevisiae. Molecular and cellular biology 18, 6273-6280.

Westholm, J.O., Nordberg, N., Muren, E., Ameur, A., Komorowski, J., and Ronne, H. (2008). Combinatorial control of gene expression by the three yeast repressors Mig1, Mig2 and Mig3. BMC genomics 9, 601.

Xu, Z., Wei, W., Gagneur, J., Perocchi, F., Clauder-Munster, S., Camblong, J., Guffanti, E., Stutz, F., Huber, W., and Steinmetz, L.M. (2009). Bidirectional promoters generate pervasive transcription in yeast. Nature 457, 1033-1037.

Yamaguchi-Iwai, Y., Stearman, R., Dancis, A., and Klausner, R.D. (1996). Iron-regulated DNA binding by the AFT1 protein controls the iron regulon in yeast. The EMBO journal 15, 3377-3384.

Yun, C.W., Bauler, M., Moore, R.E., Klebba, P.E., and Philpott, C.C. (2001). The role of the FRE family of plasma membrane reductases in the uptake of siderophore-iron in Saccharomyces cerevisiae. The Journal of biological chemistry 276, 10218-10223.

Yun, C.W., Tiedeman, J.S., Moore, R.E., and Philpott, C.C. (2000). Siderophore-iron uptake in saccharomyces cerevisiae. Identification of ferrichrome and fusarinine transporters. The Journal of biological chemistry 275, 16354-16359.